Exploring Wind Ramping as a Determinant of Pesticide Drift

Yoni Rodriguez

A thesis

submitted in partial fulfillment of the
requirements of

Master of Science

University of Washington

2022

Committee:
Edward J. Kasner
Michael G. Yost
Von P. Walden
Chris Zuidema

Program Authorized to Offer Degree:
Department of Environmental and Occupational Health Sciences

University of Washington

Abstract

Exploring Wind Ramping as a Determinant of Pesticide Drift

Yoni Rodriguez

Chair of Supervisory Committee:
Clinical Assistant Professor Edward J. Kasner
Department of Environmental & Occupational Health Sciences

The Washington State Department of Health investigates hundreds of pesticide illness reports each year, many of which are related to pesticide spray drift. Drift is the movement of pesticide aerosols through the air from an area of application to any unintended site and accounts for up to half of the pesticide-related illnesses among agricultural workers in the United States. Unfavorable wind conditions are a leading contributing factor for illnesses resulting in the off-target movement of pesticides from sprayer sources to human receptors. Meteorological conditions such as wind speed and wind direction directly impact the environmental fate and transport of pesticide aerosols. Washington state requires pesticide applicators to record wind direction and wind speed, usually with a handheld anemometer, at the beginning of a spray. However, the state does not specify a standardized method for measuring these variables, disregarding rapid changes in meteorological conditions throughout a spray period. This project will explore the concept of "wind ramping" as a tool for predicting drift-prone conditions. Wind ramping is defined as large shifts in wind speed and direction at a given location over a period of time of at least 30 minutes. We were primarily interested in sudden positive changes in windspeed. Washington State University's AgWeatherNet system captures weather data at several hundred different meteorological weather stations positioned throughout agricultural regions of eastern Washington. Weather data from five locations that involved human drift cases in Yakima and Benton counties were the primary dataset for this study. Time series-based prediction methods based on autoregressive integrated moving average (ARIMA) models also known as the Box-Jenkins approach, were explored to forecast wind changes 2.5-hours ahead in a local area. The end goal was to develop a tool with that alerts applicators about drift-prone wind conditions to minimize pesticide exposure and improve the practice of pesticide application.

Acknowledgements

Foremost, I would like to thank my advisor and Committee Chair, Dr. Edward J. Kasner, for his generous time, constructive feedback, mentorship, patience, practical advice, accessibility, genuine interest in the success of this project, and a few meals here and there. Dr. Michael G. Yost for his immense knowledge of time series analysis, pesticide drift, exposure science, and, most importantly, his ability to blend science principles with practical field application. Dr. Chris Zuidema for his extensive knowledge, mentorship, substantial time with the R software coding, and expertise in environmental health. Dr. Von P. Walden for this continued support and mentorship post-baccalaureate, vast knowledge in atmospheric science, large dataset analysis, weather predictability modeling, and model validation. Dr. Tamre Cardoso for her mentorship and expertise with time series analysis, statistical modeling, and significant patience and time with the R software coding.

Dr. June T. Spector for teaching me about environmental health diseases through public health scenarios and clinical cases, her additional mentorship with heat exposure risks among agricultural workers, and career guidance at Harborview Medical Center. Dr. Scott J. Meschke for his advice on navigating a graduate studies path and expertise in the transport, fate, and detection of heavy metals and pathogens in water. Dr. Peter Rabinowitz for teaching me to have a comprehensive overview of environmental health that considers one health and planetary health models for assessing and managing environmental health risks. Dr. Terrance J. Kavanagh for his instruction on the adverse health effects of pesticides and other environmental toxicants. Drs. Chris Simpson and Marty A. Cohen for their flexible time, mentorship, and education with field research and sampling. Brain High and DEOSH IT for their computing support and introduction to R. Trina Sterry for her genuine interest in my success as a graduate student and for steering me through graduate school and department requirements for graduation. Hayley Leventhal for her resume-building and job interview support and feedback.

Linda Van Hooser, Dawn Duddleson, and Drs. Stephen G. Whittaker, Katie M. Fellows, and Trevor Peckham with the Research Services Team for the Hazardous Waste Management Program in King County for their mentorship during my summer graduate internship focused on investigating lead exposure in Afghan refugee children. Which led to my first peer-reviewed research publication! Dr. Shar Samy, Luke Moser, and Christine Olson for helping me complete the analytical chemistry portion of this summer research project at the UW Environmental Health Laboratory and Trace Organics Analysis Center.

The Palouse Community comprised of April Seehafer and Drs. Raymond Herrera, Shelley N. Pressley, Casey Bartrem, Margrit von Braun, Ian H. von Lindern, Lisa M. Gloss, and John A. Alderete, for always being willing to revise my writing, helping me get accepted to the UW SPH Environmental Health program, and for their continued support throughout my life and career goals.

Dr. Tanya Knickerbocker, for introducing me to environmental health research by inviting me to join her summer research project investigating drinking water as a source of birth anencephaly cases in the Yakima Valley. Faculty and Staff from the Yakima Valley Michael Alamos, George Lopez, Michal Ramos, Carolyn Scut, Jerred Seveyka, Drs. Matthew Loeser, Claire Carpenter, Stephen Rodrigue, Panyada Sullivan, and Sam Mazhari.

Finally, I thank my family and friends for their love and support. My father, Avito Rodriguez, for teaching his sons the meaning of hard work by waking us before the crack of dawn to thin tree fruit and harvest soil and tree crops in the Yakima Valley. My mother, Imelda Rodriguez, for always being there and teaching me how to live independently (e.g., washing clothes, cooking, and cleaning). My Grandparents, for their sacrifice and bravery to immigrate to the U.S. from Ayoquezco, Oaxaca in Mexico, and Manzanillo, Colima in Mexico. My sisters Cynthia Ornelas, Adriana Torres, and Samaria Rodriguez, for their support in all endeavors, their push to make me better, and laughs. My brothers Eddie Diaz, Josue Rodriguez, and Jacob Rodriguez for the companionship in sports, long drives across the state, music, and comedy. Mis tios y tias Jose Rodriguez, Cleofas Rodriguez, Odelia Velasco, Leonel Rodriguez, Aquino Rodriguez, Romeo Rodriguez, Catarino Rodriguez, Pedro Rodriguez, Enedina Santiago, and Carlos Rodriguez.

I would like to thank all my primos and primas for their support. Especially those that joined me on my college journey Moses Rodriguez, Jesse Rodriguez, Ale (Chuparrosa) Rodriguez, Lilibet Rodriguez, Amarilis Santiago, Alleni Velasco, and Alyne Velasco.

A massive shoutout to the YVC Crew, WSU friends and community, friends from the jiujitsu community, and UW friends and cohort members!

This research project was supported by the National Institute for Occupational Safety and Health (NIOSH) under Federal Training Grant T42OH008433 The content is solely the responsibility of the authors and does not necessarily represent the official views of NIOSH. Also, the Pacific Northwest Agricultural Safety and Health Center (PNASH) under a graduate research assistant appointment. Supplementary funding was awarded by the School of Public Health Office Dean Master's Fellowship, the Latino Center for Health Student Scholars Fellowship, the Graduate School's Office of Student Equity and Excellence Latinx Scholars Fellowship, and the American Industrial Hygiene Foundation Student Scholarship.

Table of Contents

List of Figures

List of Tables

Acronyms and Definitions

ACF	Autocorrelation Function
AFA	Axial Fan Airblast
AI	Artificial Intelligence
ANN	Artificial Neural Network
ARIMA	autoregressive (AR) integrated (I) moving average (MA)
AWN	AgWeatherNet
CERCLA	Comprehensive Environmental Response, Compensation, and Liability Act
CDC	Centers of Disease Control and Prevention
DAT	Directed Air Tower
DEOHS	Department of Environmental and Occupational Health Sciences
DRT	Drift Reduction Technology
EPA	United States Environmental Protection Agency
FAO	Food and Agriculture Organization of the United Nations
FIFRA	Federal Insecticide, Fungicide, and Rodenticide Act
GAP	Good Agricultural Practices
hrs.	Hours
IQR	Interquartile Range
mi	miles
min	Minute
MFT	Multi-Headed Fan Tower
ML	Machine Learning

mph	Miles per Hour
m/s	Meters per Second
NN	Neural Network
NIOSH	National Institute for Occupational Safety and Health
OSHA	Occupational Safety and Health Administration
PNASH	Pacific Northwest Agricultural Safety and Health Center
PPE	Personal Protective Equipment
s	Seconds
SD	Standard Deviation
STL	Seasonal and Trend decomposition using Loess
USDA	United States Department of Agriculture
UW	University of Washington
WADOH	Washington State Department of Health
WSDA	Washington State Department of Agriculture
WSU	Washington State University

Introduction

Public Health Relevance

Global Food Demand

By 2100, the human population is projected to increase by approximately 4 billion people (Tilman et al., 2011). As a result, our global food demand will need to increase approximately two-fold (Tilman et al., 2011). Although this thesis focuses on the challenges of predicting pesticide drift, the relationship between food production and pesticide use runs in the same direction. Pesticides are the chosen strategy to increase food production to feed the world 50 years from now because they are an efficient and powerful tool to prevent food degradation in agriculture and provide food security (Field et al., 2020; Xue et al., 2021). However, the spray efficacy of pesticides is inadequate due to wind-caused spray drift during field applications which can alter nutrient cycles, contribute to environmental pollution, biodiversity loss, contaminate drinking water, devastate our food quality, and cause direct toxicity (Springmann et al., 2018; Xue et al., 2021).

Land Use Change and Soil Pollution

In 1700, almost half of the terrestrial biosphere was wild (Ellis et al., 2010). By 2000, humans converted most of the biosphere from prairies to agricultural croplands and cleared forests for pastures or urban areas (Ellis et al., 2010). The distribution of pesticides on farmlands and grasslands from spray applications and wind-enabled spray drift can be taken up by non-target species and ingested by humans and animals (Field et al., 2020). Pesticides and other agrochemicals can persist in the environment, and some are considered possible endocrine disrupters that can also increase the risk of cancers, thyroid disease, neurobehavioral disorders, and reproduction dysfunction (Frumkin et al., 2020; Gore et al., 2015). The wind can pick up particulate pollutants in the soil and transport them over long distances to adjacent farms and homes. These soil-deposited pollutants can also leach into surface water and groundwater, resulting in human exposure and ecosystem damage (Myers et al., 2020).

Water Scarcity and Water Pollution

Between 1960 and 2010, the world increased agricultural production by a factor of 2.5 (FAO, 2020). At the same time, agricultural irrigation accounted for 70% of all freshwater withdrawals (FAO, 2020). Expanding crop production to feed a growing global population implies increased freshwater use and pesticide use for agricultural crops (Maroufpoor et al., 2021). Thus, freshwater scarcity may threaten sustainable social and environmental development (Maroufpoor et al., 2021). Pesticides can contaminate surface water bodies (e.g., lakes, rivers, streams) in various ways: aerial spray application, wind-enabled spray drift, soil leaching, shallow subsurface runoff, heavy rainfall-runoff, and vaporization (Vryzas, 2018; Zaidon et al., 2020). Pesticides with high water solubility persist longer in water bodies and are more likely to move from agricultural soils to surface water via runoff or irrigation. Thus, drinking water surveillance should consider environmental conditions such as high temporal variability and rainfall events before, during, and after pesticide applications (Khan et al., 2020; Zaidon et al., 2020).

Food Quality, Pollinator Loss, and Biodiversity Loss

Soil and water pollution reduce food quality in areas where incompletely treated wastewater containing pesticides (i.e., heavy metals, hazardous chemicals) irrigate crops (Lu et al., 2015; Myers, 2020). Crop pollinators (e.g., bees) are regularly exposed to pesticides and pesticide residues when foraging, which can suppress their immune system and increase parasite and pathogen infections leading to declines in wild and managed pollinators (Sanchez-Bayo et al., 2016; Wilfert et al., 2021). Pollinators are essential for plant and crop biodiversity and are indirect drivers of human health (Wilfert et al., 2021). Crops dependent on pollinators (e.g., fruits, vegetables, nuts, and seeds) provide essential micronutrients such as Vitamin A and folate to the human diet (Chaplin-Kramer et al., 2014; Eilers et al., 2011; Ellis et al., 2015; Wilfert et al., 2021). Researchers have estimated that a 50% global loss of pollinators would cause 700,000 additional deaths worldwide each year due to malnutrition, ischemic heart disease, and stroke (Smith et al., 2015).

Agricultural Communities

Public areas (e.g., playgrounds, schools, worksites) and homes next to intensively managed tree fruit orchards and vineyards are not commonly monitored or assessed for pesticides (Linhart et al., 2019). Recent studies have found pesticide contamination on playgrounds near sprayed fields and playgrounds far from agricultural areas (Linhart et al., 2019; Schwaier et al., 2017). Concerns related to pesticide exposure in adults and occupationally exposed workers are associated with cancer, neurodegenerative diseases, endocrine disruptors, and reproductive and developmental toxicity (Costa, 2021). Children's exposure to pesticides is crucial, given the health risks associated with low-dose exposure from spray drift during sensitive developmental stages (Bassil et al., 2007; Sapcanin et al., 2016). Also, for children, the risk for cancer is associated with parental exposure to pesticides (Bailey et al., 2014; Dai et al., 2021; Van Maele-Fabry et al., 2017).

Pesticide Exposure Routes

Exposure to pesticides can be direct or indirect and can occur via three main exposure routes: ingestion, inhalation, or skin penetration (Phillips et al., 2015; US EPA, 2021a). High-dose ingestion cases leading to severe poisoning and death are commonly associated with suicidal intentions or accidental ingestion due to the improper storage of pesticides (Costa, 2021; Lee et al., 2015). The general population consumes chronic, low oral doses of pesticide residues via food or contaminants in drinking water (US EPA, 2021b). There are regulations to ensure the magnitude of pesticide residues in drinking water and food does not exceed levels of concern (US EPA, 1966; US EPA, 2021b).

Workers involved in the production, transport, mixing and loading, application of pesticides, and harvesting of pesticide-sprayed crops are at the highest risk for pesticide exposure (Fenske, 1993; Marrs et al., 2004; US EPA, 2011). Pesticide poisoning symptoms can be mistaken for symptoms of other illnesses, such as the flu or heat exhaustion (US EPA, 2015). This is especially true when pesticide handlers are working with organophosphate or carbamate insecticides in warm and hot environments (US EPA, 2015). Therefore, effective exposure controls and emergency plans are

imperative in rural agricultural areas where it may be difficult for medical first responders to navigate, establish telecommunications, locate and transport workers suffering from pesticide poisoning, heat exhaustion, ergonomic injuries or other issues.

Chemicals can be absorbed through the skin during normal handling or application of pesticides, accidental spilling over body areas not covered by protective clothing, such as the face or the hands (Fenske, 1993; Lesmes-Fabian et al., 2012; US EPA 2011). Additional oral exposures might result from workers' hand-to-mouth activities when hands are not washed after pesticide handling or before eating. Also, the deposition of pesticides on worker clothing and shoes may lead to chronic, slow penetration, dermal exposures known as the take-home pathway, an important exposure pathway for children (Aicher et al., 2021; Menegaux et al., 2006).

The inhalation of pesticides that leads to human poisoning is associated with wind-enabled spray drift and volatilization (Aicher et al., 2021; Kuster et al., 2021; Lee et al., 2011). Pesticide particles ranging from 5 μm or larger, usually are deposited in the nasopharyngeal region; particles inhaled through the mouth are swallowed within minutes, and if water-soluble, they can dissolve in the mucus and absorb through the nasal epithelium then into the blood (Slitt, 2021). Particles approximately 2.5 μm in diameter are deposited mainly in the tracheobronchial regions of the lungs, while particles 1 μm or smaller penetrate to the alveolar sacs of the lungs where they can cause lung damage characterized by pneumocyte toxicity, inflammation, and interstitial pulmonary fibrosis (Lehman-McKeeman, 2010; Slitt, 2021). Skin contact is also an important route of exposure for the drift exposure pathway (Fenske, 1993; Marrs et al., 2004; US EPA, 2011).

Drift

Pesticide Drift

Pesticide spray drift and its health impacts on agricultural workers, neighboring residents, and bystanders is the focus of this thesis. Drift is divided into two categories: "primary spray drift" and "secondary off-target movement" (US EPA, 2016b). Primary spray drift considers the airborne pesticide particles or particulate matter (PM), a mixture of solid particles and liquid droplets, that deflects away from the target crop by the action of the wind during or shortly after spray application (Matthews et al., 1993; Matthews et al., 2014; US EPA 2014a). Secondary off-target movement or drift deposits are the volatilizations and or the degradation of pesticides by photolysis from surfaces (e.g., plants, soil, water, structures) well after spray application (US EPA 2014a; US EPA 2014b). Both forms of drift can affect human health when traveling outside agricultural fields, but only primary drift is regulated (US EPA 2014a; US EPA 2014b; Goumenou et al. 2021). In this thesis, the term "drift" and prevention strategies discussed are related to the primary form of drift.

Drift Regulations

In the 1950s, pesticide drift was recognized and used as an economic spraying technique to cover large areas of land utilizing wind (Courshee, 1959). From 1960 to the 1980s, environmental movements increased calls for Congress to protect the environment (Moeller, 2019). In response,

Congress passed amendments to the Federal Insecticide, Fungicide, and Rodenticide Act (FIFRA), transforming the labeling law to a comprehensive regulatory statute, and Comprehensive Environmental Response, Compensation, and Liability Act (CERCLA), commonly known as "Superfund," to identify sites where hazardous agents threaten the environment and public health and identify responsible parties (Hope, 2013; Moeller, 2019).

The labels for pesticide products are legal documents that include warnings, ingredients, use classifications, and statements of practical treatments to maximize the beneficial use of pesticides and minimize harm to human health and the environment (Moeller, 2019). In 2009, the EPA issued a draft pesticide registration notice to improve guidance on pesticide drift prevention. An example label reads: "For orchard/vineyard airblast applications, do not directly spray above trees/vines and turn off outward pointing nozzles at row ends and outer rows. Apply only when wind speed is 3-10 mph at the application site as measured by an anemometer outside of the orchard/vineyard on the upwind side (US EPA, 2001)."

To further prevent drift, FIFRA requires pesticide applicators to follow all label directions, complete pesticide application training, and be certified (Centner et al., 2014; US Code, 2006). Despite these regulations, some agricultural growers consider drift unavoidable and a byproduct of crop production. An EPA workgroup acknowledged that some tolerance for diminutive exposure should exist, and crop producers insist that FIFRA's "no unreasonable adverse effect" standard considers drift inherently inevitable (Centner et al., 2014, US EPA, 2007).

Courts and legislatures address claims surrounding drift at the state and federal levels (Moeller, 2019). Even after Congress passed FIFRA and CERCLA, states and localities still need to supplement the federal efforts by providing guidance to local pesticide users and responding to concerns that require enforcement actions against federal and state pesticide laws which vary widely by state (Klass, 2005; US Supreme Court, 1991). Pesticide land use cases involve state law claims for damages by non-pesticide users against pesticide users for pesticide-related damages that require analysis of records, maps, laws, and policies at the local level (Klass, 2005; US EPA, 2021c). Spray drift claims are typically brought under state common law theories of liability, including "trespass, nuisance, negligence, and strict liability for ultrahazardous conditions" (West Group, 2003). If one can prove they suffered harm under one of these theories, they may recover damages (Moeller, 2019; West Group, 2003).

At the federal level, FIFRA has been used for pesticide violation claims under theories of negligence, based on non-compliance with the labeling (Klass, 2005; Moeller, 2019). However, it is important to note that pesticide drift cases are still being raised under state laws, with few extending to FIFRA (Klass, 2005; Moeller, 2019). Federal courts have also struggled to apply CERCLA to drift cases because the act provides an exemption for pesticide use, and farmers are usually considered exempt under the standards for a "covered person (US Court for the District of Puerto Rico, 2000)." Although, the Eleventh Circuit has interpreted these exemptions differently and held that "the pesticide exemption does not absolve the Landowners of liability under

CERCLA (US Court of Appeals, Eleventh Circuit, 1996).” Other courts have struggled with the term “covered person” when applying CERCLA (US Supreme Court, 1984).

Drift Reducing Strategies

The disagreements in the courts about how to interpret and apply laws on drift and its offenders led the EPA to launch drift reduction technology (DRT) programs to reduce exposure to humans, wildlife, and the environment in 2016 (US EPA, 2016). Innovations to reduce drift include new sprayer technologies that minimize the distance between applicator nozzles to target crops, the use of hedgerows as windbreakers or barriers to mitigate indoor pesticide population in neighboring homes, and mathematical models to estimate pesticide exposure (Kasner et al., 2020; Langenbach et al., 2021; Metruccio et al., 2021). Studies assessing new sprayer technologies report drift was reduced by 35-37%, but the lack of adequate incentives does not stimulate grower adoption, who still use conventional airblast sprayers designed in the 1950s (Kasner et al., 2020; Palardy et al., 2017). Windbreaker reports indicate vegetative barriers reduce drift by 60-68%, but research is limited, and quantification is needed to determine ideal size, shape, leaf type, and distances between hedges and sprayed crops to plant hedges practically (Langenbach et al., 2021). Mathematical models are used for regulatory risk assessment but are based on assumptions and defined working conditions such as applicator equipment, application type, number of pesticides applied, stable meteorological conditions, flat terrains, and no vegetative barriers, all of which impact drift exposure and absorption rates for dermal and inhalation routes (Metruccio et al., 2021).

The Food and Agriculture Organization of the United Nations (FAO) has developed Good Agricultural Practices (GAP) toolkits as administrative and personal protective equipment (PPE) guides to prevent drift exposure (FAO, 2021; Mandić-Rajčević et al., 2021). Agricultural workers can be exposed to drift during and after the spray application phase, which is why GAP indicates that reentry after spray application should not take place before a complete drying, given that pesticide deposits on the surface of leaves and branches can be dislodged and resuspended by manual activity and inhaled if windy (Baldi et al., 2014).

Therefore, the rational choice and proper use of PPE for agricultural workers include coveralls, head/face protection, eye protection, and gloves (Mandić-Rajčević et al., 2018; Spaan et al., 2020). However, different types of gloves cause can cause additional exposure. Thick gloves impair hand manipulation, which causes workers to remove them to gain touch and then wear them again without hand washing, leading to hand contamination inside the gloves (Mandić-Rajčević et al., 2021). Multiple-use gloves are lined with textiles that absorb contaminates and release them on the hands if reused. Also, single-use elastomeric gloves worn on contaminated skin can increase dermal absorption rates when the worker is sweating, which may enhance pesticide solubility (Mandić-Rajčević et al., 2021). Half-face respirators with replaceable filters in a canister protect workers against micro-sized droplets that penetrate to the alveolar sacs of the lungs, while hats, common scarves, and knotted handkerchiefs can protect against head dermal exposures (FAO, 2020a). The GAP specifies that correct planning of pesticide application days decreases

unnecessary exposure-related risks by not spraying on windy days and when rain is forecasted to avoid drift and runoff (Mandić-Rajčević et al., 2021).

Determinants of Drift

Several factors can influence drift in agriculture. These factors range from agricultural machinery, operator's skill, terrain characteristics, terrain architecture, meteorology, and planning of spray application. The characteristics of the terrain (e.g., plain versus mountainous) and the architecture of the terrain (i.e., plant height, tree canopy size, and density) will determine tractor type, spray treatment type, spray pressure, duration of the application, and local wind characteristics that are important parameters for drift (Mandić-Rajčević et al., 2019; Mandić-Rajčević et al., 2021). Tractor and spray technology type significantly influence drift exposure. Studies report that the widespread use of axial fan airblast (AFA) sprayers, a 1950s model, coupled with reduced tree height and canopy density, lead to a 45% or more loss of pesticides applied to the ground or drift (Herrington et al., 1981; Kasner et al., 2020; Raisigl, 1991; Steiner, 1969; Vercruysse, 1999). Our previous work showed that 89% of drift events involved axial fan airblast sprayers in tree fruit (Kasner et al., 2020, Kasner et al., 2021). New DRT sprayers, the directed air tower (DAT) and multi-headed fan tower (MFT) models, had 4-15% and 35-37% less drift measured by volume than the conventional axial fan airblast (AFA) but did not eliminate drift (Kasner et al., 2020). Variable wind speed and directions are leading contributors to drift and related illnesses (Kasner et al., 2021; Lee et al., 2011).

Drift and Wind

Researchers have considered the influence of wind speed and direction on pesticide drift by developing agricultural, biological, and environmental assessment and prediction models (Butler Ellis et al., 2018; Desmarteau et al., 2020; Kasner et al., 2021; Teysseire et al., 2021). The addition of meteorological data significantly improved these models (Butler Ellis et al., 2018; Desmarteau et al., 2020; Teysseire et al., 2021). However, general weather assumptions are made in these models; for example, high wind speeds of 4.47 m/s or 10 mph in a specific direction with constant temperature and relative humidity (Butler Ellis et al., 2018; Desmarteau et al., 2020). These conservative assumptions underestimate drift and disregard the multiple spray applications in a growing season spaced days apart with variable meteorological conditions and other determinants of drift (Butler Ellis et al., 2018; Desmarteau et al., 2020; Mandić-Rajčević et al., 2021). Wind velocity and direction change more frequently in comparison to temperature and humidity over the course of minutes to hours (Butler Ellis et al., 2018; Kasner et al., 2021). Fluctuations in wind speed and direction also result from turbulence across diverse terrain and microclimates (Butler Ellis et al., 2018; Kasner et al., 2021). Additionally, mathematical modeling, spray records, and pesticide illness cases can be severely limited in situations lacking reliable meteorological data (Calvert et al., 2015; Kasner et al., 2021; Venäläinen et al., 2002). Dense networks of weather stations are required to accurately capture the spatio-temporal extent of drift events, illness reports, and prediction models across all terrains (Desmarteau et al., 2020; Kasner et al., 2021; Luo et al., 2008; Venäläinen et al., 2002).

Wind Ramping

The wind energy industry faces enormous challenges like grid integration, reserve management, power quality, and accurate wind forecasting (Dhiman et al., 2020; Mammedov et al., 2021). Wind power must be able to handle sudden changes in wind speed and direction, a phenomenon called a wind ramp event or wind ramping (Dhiman et al., 2020; Mammedov et al., 2021). A wind ramp differs from a wind gust in three primary ways. The first is that a wind gust does not consider changes in wind direction (Graphical.weather.gov). The second is that a wind gust is reported when wind speeds reach at least 16 knots (~18 mph) and the variation in wind speed between peaks and lulls is at least 9 knots (~10 mph) (Graphical.weather.gov). Thirdly, a wind gust duration is usually less than 20 seconds (Graphical.weather.gov). Therefore, it is our goal to find wind metrics to best define a wind ramp event as it relates to agricultural pesticide drift.

Wind Forecasting

In the early 1980s, wind forecasting methods started as time series models (Brown et al., 1984). The wind energy industry has studied time series models to simulate wind speed and power ranging from very short-term (seconds to 30 minutes) to very long-term (3 days to 1 week or more) time scales (Brown et al., 1984). Ramp events have been applied to wind power, reservoir walls, forest fires, air quality, and other events that are significantly impacted by rapid changes in wind speed and direction (Chen et al., 2016; Finnigan et al., 1995; Greaves et al., 2009; Hannah et al., 1995; Jiao-jun et al., 2004; Peña et al., 2008; Simpson et al., 1990).

Stationary and Non-Stationary Time Series

A time series is a collection of observations made sequentially through time and can fall into one of two categories: stationary or non-stationary. Conceptually, a time series is stationary if there is no systematic change in mean (no trend), variance, and or if periodic variations have been removed (Chatfield et al., 2004; Haslett., 1997; Priestley., 1988; Yaglom., 1962). A non-stationary time series contains seasonal variations, cyclic trends, and other irregular fluctuations (Chatfield et al., 2004; Haslett., 1997; Priestley., 1988; Yaglom., 1962). Wind speed is a known as a non-stationary time series with a cyclic seasonal and diurnal trend (Chatfield et al., 2004; Dhiman et al., 2020). For this thesis, we were interested in decoupling the predictive seasonal trend from the irregular fluctuations (ramp events) to determine if they can be forecasted using probability theory (Chatfield et al., 2004; Dhiman et al., 2020). For this reason, our time series analysis required a transformation of a non-stationary series into a stationary series using statistical time series analysis.

Deterministic and Stochastic Time Series

The purpose of this statistical time series analysis was to develop a short-term wind forecasting (30 minutes to 6 hours ahead) model that could alert growers of short-term changes in wind speed that might lead to pesticide drift. It is important to note that many statistical time series authors use the terms ‘prediction’ and ‘forecasting’ interchangeably, but some do not. For the purposes of this thesis, we used ‘prediction’ and ‘forecasting’ interchangeably. If a time series can be predicted exactly, it was considered deterministic. However, most time series are stochastic, where future

values are partly determined by historical values. Forecasting of stochastic time series is difficult and based on the idea that future values have a probability distribution and prediction trained on historical data.

Weather-Based versus Time Series Based Models

Wind forecasting methods are categorized into weather-based and statistically-based (time series) prediction methods (Dhiman et al., 2020). Weather-based prediction models require multiple input factors such as the topology of the land, wind measuring instruments and their respective heights from the ground, ambient temperature, ambient pressure, and other factors to predict future values (Dhiman et al., 2020; Mammedov et al., 2021). Statistical prediction models require only a single input factor (i.e. historical wind data) (Dhiman et al., 2020; Mammedov et al., 2021). Our work explored the application of a statistical prediction model known as ARIMA: autoregressive (AR or p) integrated (I) moving average (MA or q). ARIMA modeling is often used in wind forecasting and classified by their timescales (Chatfield et al., 2004). Statistical prediction models can be used to forecast wind speeds on short-term (30-minutes to 6 hours ahead) and medium-term (6 hours to 1 day) timescales (Dhiman et al., 2020).

Forecasting literature shows that ARIMA models are often coupled with machine learning (ML) methods to improve short-term forecast accuracy of non-stationary time series data (Dhiman et al., 2020). Machine learning is the development of artificial intelligence (AI). Neural networks (NNs) are a different non-linear approach compared to statistical models in this thesis (Chatfield et al., 2004). The NNs are a result of mathematical attempts to model how the brain works and are often referred to as artificial neural networks (ANN) to emphasize that it is a mathematical model. Artificial Neural Networks that use ML to train a model how to classify, predict, and recognize specific wind events are categorized as supervised ML (Dhiman et al., 2020). Unsupervised ML is when an ANN analyzes and classifies the data on its own to develop a forecast (Dhiman et al., 2020). Accurate wind speed forecasting depends on the availability of a large historical dataset to train an ANN model or hybrid ANN and ARIMA model (Dhiman et al., 2020).

Hybrid wind forecasting models are a result of accurate wind forecasting needs from the wind energy sector (Zhang et al., 2018; Zhang et al., 2020). Precise short-term wind forecasting methods have been developed and applied on wind farms to harness renewable energy (Hu et al., 2020; Natarajan et al., 2021; Snoun et al., 2019). This thesis explored the first known application of these methods to build a short-term wind forecasting model that could alert growers, pesticide applicators and surrounding communities about future (3-6 hours ahead) wind ramping events that could lead to drift-prone conditions.

Study Area

The Yakima Fold Belt in the Columbia Basin

The Columbia Basin (Figure 1) results from flood basalts that erupted in the Miocene period and flooded a basin centered around the Tri-Cities of Pasco, Kennewick, and Richland (Carson et al., 1987; Miller et al., 2017; Reidel et al., 2013). Most of the Columbia Basin is monotonously flat, but west of the Tri-Cities, a system of folds topographically expressed as ridges that rise to 2,000

feet (600 m) (Figure 2) (Carson et al., 1987; Miller et al., 2017; Reidel et al., 2013). Megafloods in the late Pleistocene period swept away loess, windblown dust derived from glacial abrasion, but it remained elsewhere to provide fertile soil for agriculture (Carson et al., 1987; Miller et al., 2017; Reidel et al., 2013; Reidel et al., 2003). The shapes and geometry of the folds are different from those typical of fold systems, where the alternating anticlines (a fold with the oldest rock in the core; most have limbs that drop away from the core) and synclines (a fold with the youngest rock in the core; most have limbs that fall toward the core) are regularly spaced and have smoothy rounded shapes (Carson et al., 1987; Miller et al., 2017; Reidel et al., 2013; Reidel et al., 2003). Yakima's anticlines are asymmetrical and broad, with the ridges oriented in a northwest-southeast direction (Carson et al., 1987; Miller et al., 2017; Reidel et al., 2013; Reidel et al., 2003).

Agricultural Land Use Change in Yakima, WA

Land-use change involves converting one land type or ecosystem to another, such as prairies to cropland in North America (DeFries et al., 2004; Field et al., 2020; Meyers et al., 2020). The most significant driver of land-use change is large-scale agriculture with low agrodiversity and high agrochemical inputs (Ellis et al., 2010; Goldewijk et al., 2017; Herrero et al., 2017). In the nineteenth century, the expansion of agriculture began in North America after the industrial revolution (DeFries et al., 2004; Field et al., 2010; Goldewijk et al., 2017). Before 1840, central Washington's lowlands between the Cascade Mountains and the Columbia River were comprised of the Yakama Nation, more than 12 million acres of land used for well-being, fishing, hunting, berry harvesting, and tribe gatherings (Wester, B.L., 2014; Yakima Nation, 2021). In 1855, fourteen separate tribes in eastern Washington were resettled to a 1.3-million-acre reservation now known as the Yakama Indian Reservation as a result of their treaty with the United States (Wester, B.L., 2014; Yakima Nation, 2021). Life in the Columbia Basin changed from rolling foothills that make up the Yakima Fold belt to agricultural hop fields and tree fruit orchards (Wester, B.L., 2014; Yakima Nation, 2021). Central Washington's semi-arid climate receives only 7-9 inches or precipitation a year and the soils in area vary in their water holding capacity, making orchard irrigation management imperative for water pumping costs, loss of nutrients, tree fruit health, erosion, and adverse off-target environmental impacts (WSU Tree Fruit, 2022). Washington's agriculture exports total $6.7 billion, approximately 33% of those exports are apples, and 25% are cherries (WSDA., 2022).

Study Objectives

This project explored the role of changing wind conditions in eastern Washington during the agricultural growing season. The overall objective of this study was to use the dense meteorological data network to forecast drift-prone wind conditions. This study developed a location-specific wind forecasting model to predict changes in wind speed and direction and minimize pesticide drift. We explored the utility of time series methods and wind ramp modeling as appropriate wind prediction to guide pesticide applications.

Aim 1: Determine the necessary inputs for wind ramp modeling in agriculture.

Research Question: How can we apply wind ramp modeling from the wind energy industry to forecast drift-prone wind conditions in agriculture?

Aim 1a: Compare wind speed and wind gust averages, frequency distributions, and variation with wind ramp events. To accomplish this, we utilized historical 15-minute average, 2014-2019 wind data from AWN, and restricted the initial analysis to the Prosser N.E station.

Aim 1b: Determine the amount of historical data required to predict future wind ramping events accurately (i.e., wind speeds greater than 10 or 15 mph) on a short-term timescale (30 minutes to 6 hours) in the following week. To accomplish this, we compared a weekly average of each month in the spraying season to identify cyclic seasonal weather patterns and cyclic daily patterns. We then compared the averages and differences in trend, seasonality, outliers, and discontinuities, if any. We also decomposed the average and evaluated the remaining wind data to identify other trends if present that could predict wind ramp events.

Aim 1c: Determine the best ARIMA model from Aims 1a and 1b to predict future wind ramp events on a daily forecast system.

Aim 1d: Perform descriptive statistics of wind direction. Evaluate the polar coordinates of horizontal wind direction to see if there is a common direction the wind moves during spraying season. If not, determine whether wind direction correlates with increases in wind speed.

Aim 2: Apply the model.
Research Question: How effective are wind ramping models at predicting drift-prone wind conditions in agriculture?

We hypothesized that wind ramp modeling would be an effective tool for predicting wind speed ramp events and providing categorical alerts that inform growers of significant wind ramp events that could impact public health. We tested the model by first replicating the historically plotted 2014 data. We attempted to forecast wind ramp events in real-time for 2.5-hour time intervals. Finally, we compared the model's effectiveness at predicting wind ramp events with different moments in time.

Methods

Study Design

This work was a follow-on from several field studies in the same region where drift events with pesticide-related illnesses have occurred. Previously, the study team used historical wind data from a network of stations throughout Washington state and linked it with pesticide-related illness cases (Kasner et al., 2020, Kasner et al., 2021). We selected an 418 square km study area with dense tree fruit orchards, many weather stations, and frequent drift case reports since 2000 (Kasner et al., 2021).

The study area had five stations that collected 15-minute average wind speed and wind direction data between 2014 and 2020 with a Model 014A Met One Wind Speed Sensor and a Model 024A Met One Wind Direction Sensor. All meteorological data were imported to the RStudio integrated development environment for programming (R version 4.1.1), where they were prepared for descriptive statistics and time series analysis. We compared wind speed to wind gust in the study area to evaluate how wind ramping, a novel concept from the wind power industry, could be applied to short-term wind forecasting to prevent pesticide drift. Current federal and state regulations require that pesticide application cannot occur if wind speeds are greater than 10 mph (4.5 m/s), which was the primary threshold for our analysis.

Emphasis was placed on identifying an appropriate forecasting model to predict wind speed, a nonstationary time series with significant diurnal, meteorological, and seasonal variations. Given that an autoregressive moving average model can only be applied to stationary processes, we utilized built-in decomposition and differencing functions in R to remove any trends and cyclic patterns in the dataset to evaluate the series of residuals to fit a model best. The built-in differencing function in R provided an autoregressive integrated moving average (ARIMA) coefficient that essentially transformed our nonstationary time series into a stationary time series. After differencing our wind speed data, we fit an ARIMA model to the residuals, representing our 'spikes' in wind speed or wind ramps, and produced a 2.5-hour forecast that could potentially alert growers of drift-prone wind conditions. Conveniently, this statistical time series model solely depends on historical wind speed measurements to appropriately predict future values versus weather-based prediction methods that rely on the topology of the land and additional meteorological input metrics.

Study Area

Meteorological Stations

We extracted historical weather data from the Washington State University (WSU) AgWeatherNet (AWN) system. The AWN network assists growers with weather advisories and customized weather alerts to optimize resource use and improve crop quality, crop output, and reduce environmental impact (Kasner et al., 2017; Pierce et al., 2018; WSU, 2015). Each AWN meteorological site provides remote, real-time weather monitoring on its website using continuous updates via cellular telemetry networks and the internet (Kasner et al., 2017; Pierce et al., 2018;

WSU, 2015). To enhance surveillance of pesticide related illness, we retrospectively evaluated specific wind and other weather conditions that could lead to pesticide drift at five specific geolocations between 2014 and 2020. The five locations: *Sunnyside*, *Grandview*, *Prosser N.E.*, *McWhorter*, and *Benton W.* made up an 11 km x 38 km (418 square km) study area, between Yakima and Benton counties, with dense tree fruit orchards, many weather stations, and frequent drift case reports (WSU 2006; WSU 2012; WSU 1989; WSU 2002; WSU 2020; WSU 2015).

The Yakima Valley and Prosser N.E.

Rattlesnake Hills and Horse Heaven Hills form the low ridges near Sunnyside and Grandview (Figures 3, 4, 5, 6, 7). Prosser N.E. was located at the foot of the Horse Heaven Hills and the focus AWN site of this study (Figures 3, 4). The geographical location of Prosser N.E. site was the closest site to where previous drift field studies were completed and was located in a region with frequent drift events and cases involving human illness (Kasner et al., 2020, Kasner et al., 2021). Compared to the other four sites, Prosser N.E was a central point of elevation in the Yakima Valley and our study site (Figures 3, 4, 5, 8). A dense network of AWN stations surrounds Prosser N.E., which helped us determine appropriate distances between the nearest AWN station and a farm or worker location. McWhorter was the highest point of elevation in the study area because it was located on an anticlinal ridge of Horse Heaven Hills (Figures 3, 4, 5, 9). The Benton W. site was on the downward slope of the anticlinal ridge where McWhorter sat atop (Figures 3, 4, 5, 10).

Meteorological Instruments and AWN Meteorological Data Collection

All meteorological variables were recorded every 5 seconds (s) and summarized every 15 minutes (min) by a battery-powered data logger (*Campbell Scientific CR-1000*) that was recharged via solar panel (Kasner et al, 2017; WSU 2006; WSU 2012; WSU 1989; WSU 2002; WSU 2020; WSU 2015). Datasets were sent via cellular data telemetry and the internet to WSU, preprocessed, posted to an online portal, and then made available for download (Kasner et al, 2017, WSU 2006; WSU 2012; WSU 1989; WSU 2002; WSU 2020; WSU 2015). A three-cup anemometer wind speed sensor (*Model 014A Met One*) continuously monitored wind speeds from 0 to 45 m/s with an accuracy of 0.11 m/s (Kasner et al, 2017, WSU 2006; WSU 2012; WSU 1989; WSU 2002; WSU 2020; WSU 2015). A wind vane (*Model 024A Met One*) served as the wind direction sensor that measured 0-360° with 5° accuracy, which was reported as one of eight wind direction categories [4 cardinal (N-E-S-W) and 4 ordinal (NE-SE-SW-NW)] (Kasner et al, 2017, WSU 2006; WSU 2012; WSU 1989; WSU 2002; WSU 2020; WSU 2015). For the weather stations selected in this study, AWN defined a wind gust as the maximum 5-second sampled wind speed over a 15-minute interval measured at a height of 2 meters. Temperature and relative humidity were measured with a probe (*Rotronic HC2S3*) that measured air temperature from -40 to 60°C with a ±0.1°C tolerance and an additional temperature probe (*Model 107*) measured air between 0° and 50°C with a ±0.2°C tolerance (Kasner et al, 2017, WSU 2006; WSU 2012; WSU 1989; WSU 2002; WSU 2020; WSU 2015). Data were provided courtesy of Washington State University AgWeatherNet and are copyright of Washington State University (Kasner et al, 2017, WSU 2006; WSU 2012; WSU 1989; WSU 2002; WSU 2020; WSU 2015).

Scope

Prosser N.E. in the months of April, May, and June 2020

We outlined wind patterns related to wind ramping and forecasting during the heavy tree fruit spraying season in the Yakima Valley between 2014 and 2020. Several field studies were conducted in the same region where drift events have been regularly documented since 2000. We narrowed the scope of forecasting to the months of April 2020, May 2020, and June 2020 at the Prosser N.E. station. In April, growers usually begin to apply pesticides and farmworkers thin budding tree fruit by hand. In June, applicators usually apply insecticides and farmworker activity in tree fruit orchards increases.

Given the descriptive wind statistics in Tables 1, 2, 3, and 4, we trained the forecast models to predict future wind speed values at the Prosser N.E. focus site. This site best represented agricultural tree fruit orchards that also had frequent and sudden wind speed and direction changes (wind ramp events) during the early spraying season. The model was trained to predict wind ramping events for the months of April 2020, May 2020, and June 2020, which required wind data from the months of January, February and March 2020.

Data Analysis

Data Preparation

Statistical analysis and wind forecasting were carried out in R version 4.1.1 with the *stats* package version 4.1.3. Elevation profiles and maps (Figures 3 – 10) of the study site were created in Google Earth Pro 7.3.4.8573. Each software was utilized on a Windows 10 Pro Desktop PC with an Intel(R) Core (TM) i5-6300U CPU 2.40GHz 2.50 GHz Processor.

Exploratory Statistical Data Analysis: Interquartile Ranges and Histograms

We performed basic summary statistics that considered minimums, 25th percentile, means, medians, 75th percentile, and maximums values for the wind speed and wind gust variables at each station. The summary statistics described the center and spread of the wind speed and wind gust variables. Also, the summary statistics helped identify suspected outliers for each site, in this case, wind ramps. Histograms were plotted to reveal distinct features of the wind speed and wind gust distributions at each site. The shape of the distributions helped us determine the best fit for wind forecasting models because not all models can accurately predict future values for unimodal or bimodal patterns (Carta et al., 2009; Ouarda et al., 2015).

Time Plots

To obtain descriptive measures of the main properties for the time series of interest, a time plot was required. By plotting a graph with the observations against time, it revealed important features of the time series such as trend, seasonality, outliers, and discontinuities. Time plots showed gradual or sudden changes in wind speed, wind ramps, an important property of our time series. Alternatively, time plots informed us when a recording device needed to be calibrated or was down and helped us adjust the data before further analysis.

Autocorrelation Function (ACF) and the Correlogram

To predict the future values in a time series and determine if a time series is stationary or not, we identified the relative dependence of each observation (Chatfield et al., 2004, McCullough., 1998; Mizon., 1995). Several statistical R command functions were available, but we utilized the **acf** function in the R *stats* package version 4.1.3. The **acf** function measured the correlation, if any, between observations at different distances and was important for model building (Chatfield et al., 2004, McCullough., 1998; Mizon., 1995). Two important properties of **acf** plots were magnitude, and direction. Correlations ranged in magnitude from -1.00 to 1.00. The larger the absolute value of the coefficient on the y-axis, the greater the magnitude of the relationship (UWOEA, 2019). The direction of the relationship (positive or negative) was indicated by the sign of the coefficient on the y-axis (UWOEA, 2019). A positive correlation implied that increasing the value of one was accompanied by an increase in the other (UWOEA, 2019). A negative correlation implied that increasing the value of one was accompanied by a decrease in the other (UWOEA, 2019). If two values were independent, then the true correlation was zero (Chatfield et al., 2004). For both wind speed and wind gust, we plotted the auto correlation between observations that were k steps apart with the **acf** function in R.

Decomposition and Differencing

When the variation in a time series was dominated by a trend, as is the case for many time series in meteorology, geophysics, marine science, and other physical sciences, it is a common method to decompose the variation in a time series into cyclic trends and residuals components. The residuals sometimes referred to as 'randoms' or 'remainders' are further analyzed or filtered until stationary. The decomposition for the wind speed time series in this thesis was carried out by using the R *stats* package command **stl**, which decomposes a time series into trend (additive or multiplicative), seasonal, and remainder components using moving averages.

Model Identification

ARIMA

After the decomposition of our wind time series data into cyclic trends and residual components, we utilized the **auto.arima** function in the *forecast* package version 8.16 of the statistical R programming software to determine the differencing (d) coefficient required transform our non-stationary wind time series data to a stationary time series (Hyndman et al., 2008, Hyndman et al., 2018). To accomplish this, the **auto.arima** function in R uses a variant of the Hyndman-Khandakar algorithm, which takes the first differences of the data until the data are stationary, then examines the order of the autoregressive (AR) (p) model and the order of the moving average (MA) (q) model through a series of stepwise combination and plots the ACF to evaluate the residuals for remaining non-stationary trends (Hyndman et al., 2008, Hyndman et al., 2018). The **auto.arima** function provides the fitted ARIMA model orders as ARIMA(p, d, q).

We first decomposed five years of historical wind speed data (without gust) that ranged from January 2014 to December 2019. We used five years of historical wind speed data because the **stl** function required a minimum of three years of data (Cleveland et al., 1990). After the

decomposition of our wind speed time series into seasonal and residual components, we ran **auto.arima** function on each component. The ARIMA order values for the seasonal and residual components were ARIMA (2,1,1) and ARIMA (4,1,2), respectively. We then fit or trained both ARIMA (2,1,1) and ARIMA (4,1,2) models to 30-days of historical wind speed data to provide a 2.5-hour forecast of the first day following the end of the 30-days. We repeated this process 800 times and provided the distribution of the root mean square error (RMSE) between the actual wind speed observation and the calculated point forecast values of our ARIMA (2,1,1) and ARIMA (4,1,2) models. The RMSE represents the variability between our ARIMA forecast points and the historical wind speed values in April 2020, May 2020, and June 2020.

Wind Direction Forecasting: Exploratory Analysis

Wind Speed and Direction

Ramp events are wind conditions with sudden change in speed and direction. In the case of pesticide drift, rapid changes in wind speed and direction can significantly impact human exposure. For this thesis, the wind speed forecasting models have assumed a uniform wind direction, however, in practice not all stations in this study experience the same magnitude and variation in wind speed and direction.

The correlation between wind speed and wind direction is important for the prevention of pesticide drift. We first explored prevailing wind directions by taking the wind direction data collected and generated comparative box plots.

Method Figures

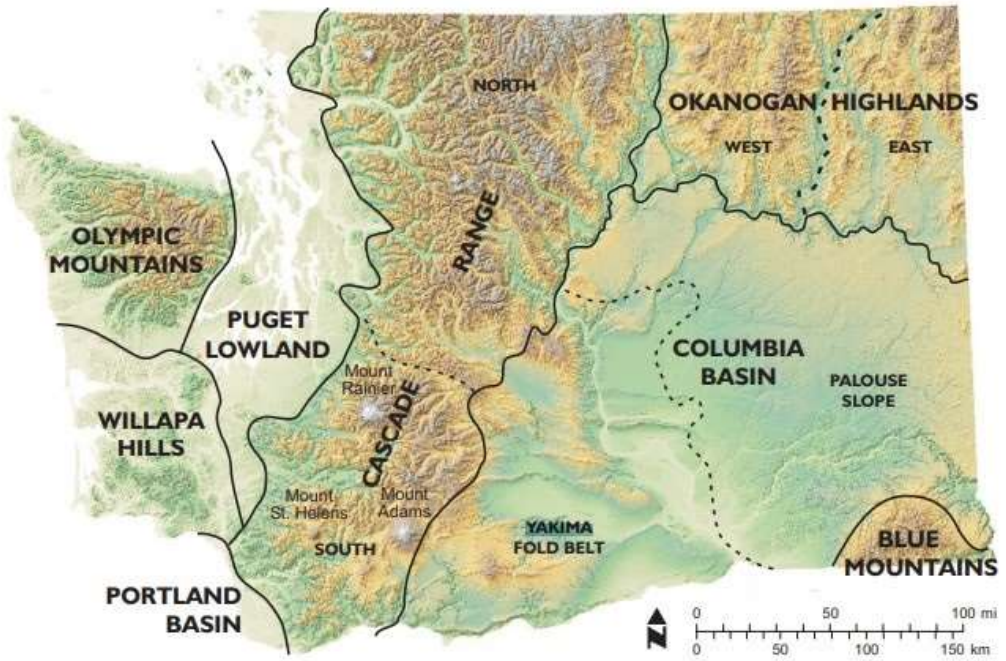

Figure 1:Regions of Washington State.
Image courtesy of Roadside Geology of Washington.

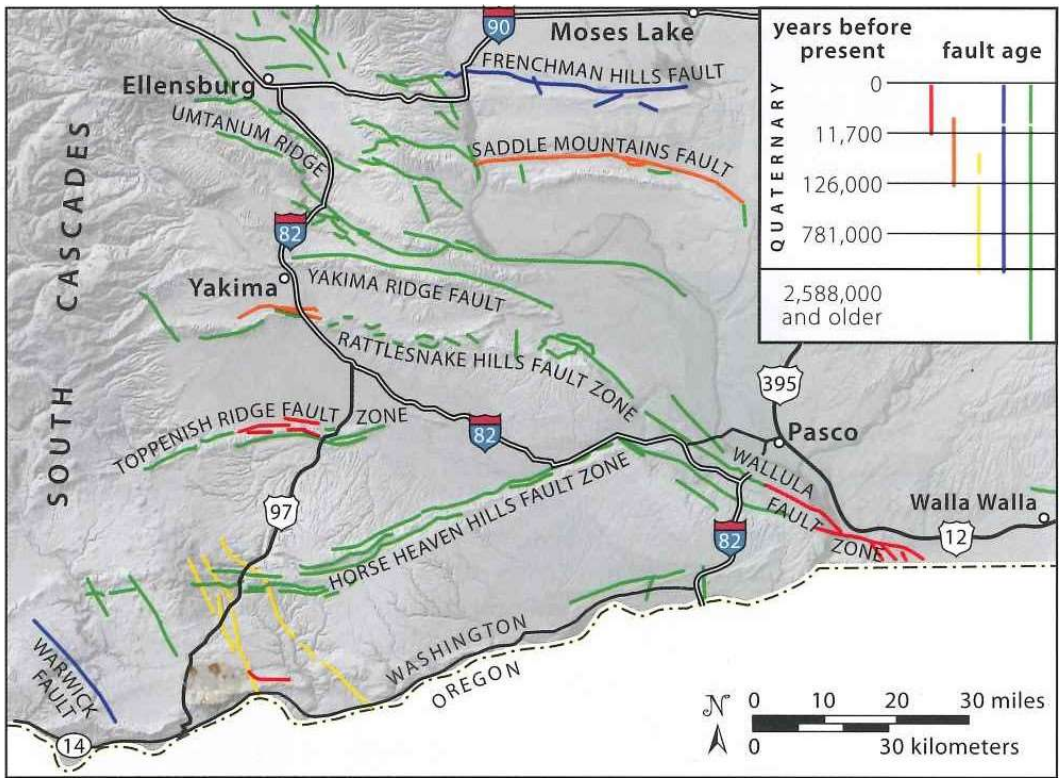

Figure 2: Basalt Ridges of the Yakima Fold Belt.
Image courtesy of Roadside Geology of Washington.

Station Name	Latitude	Longitude	Elevation (ft)
Sunnyside	46.29	-120.01	690
Grandview	46.27	-119.85	972
Prosser N.E.	46.25	-119.74	827
McWhorter	46.32	-119.62	1401
Benton W.	46.30	-119.57	929

Figure 3: AWN Stations in the Yakima Valley, 2022.
Image Courtesy of Google Pro Earth.

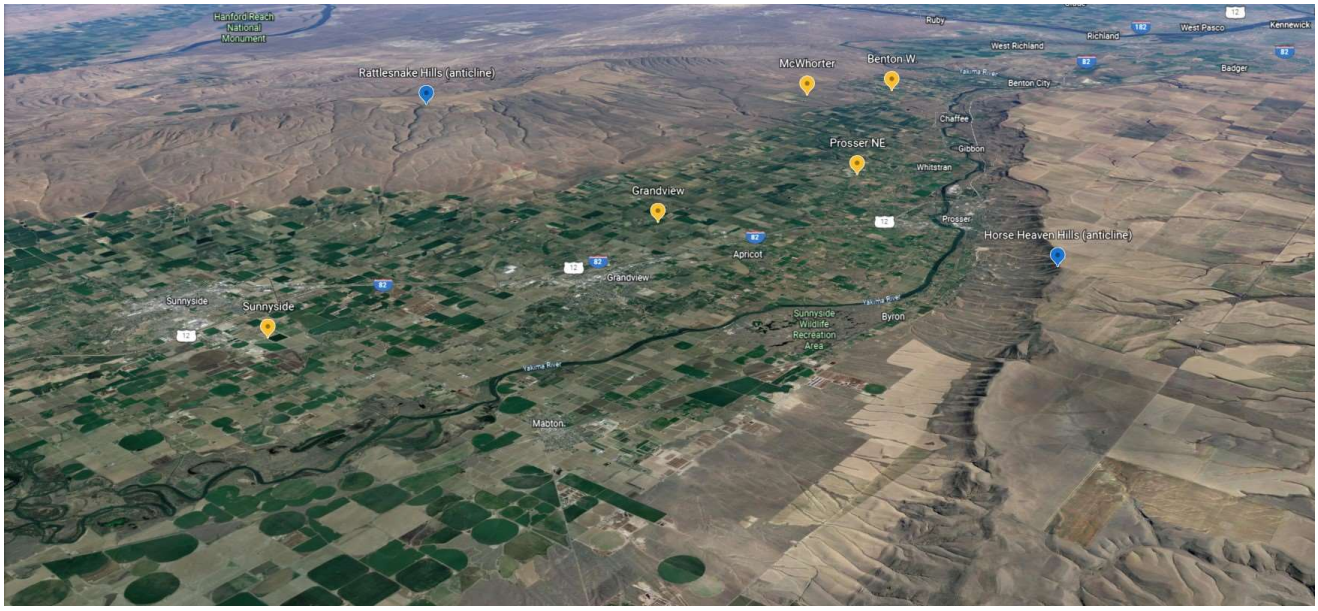

Figure 4: AWN Stations in the Yakima Valley, 2022 (Fan-Shape View).
Image Courtesy of Google Pro Earth.

Figure 5: Elevation Profile of Sunnyside, WA to Benton W., WA.
Image Courtesy of Google Pro Earth.

Figure 6: Elevation Profile of Sunnyside AWN station.
Profile travels from Rattlesnake Hills to Horse Heaven Hills. Latitude: 46.29, Longitude: -120.01, Elevation: 690 ft. Image Courtesy of Google Pro Earth.

Figure 7: Elevation Profile for Grandview AWN station.
Profile travels from Rattlesnake Hills to Horse Heaven Hills. Latitude: 46.27, Longitude -119.85, Elevation: 972 ft. Image Courtesy of Google Pro Earth.

Figure 8: Elevation Profile for Prosser N.E. AWN station.
Profile travels from Rattlesnake Hills to Horse Heaven Hills. Latitude: 46.25, Longitude -119.74, Elevation: 827 ft. Image Courtesy of Google Pro Earth.

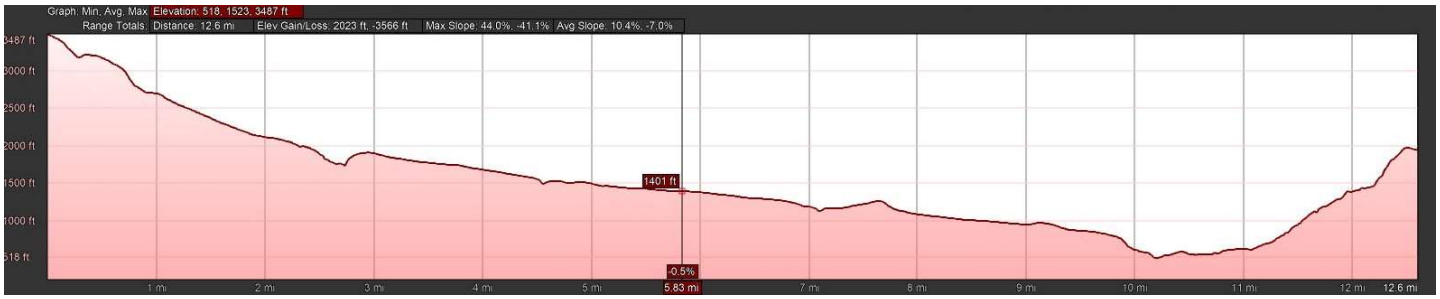

Figure 9: Elevation Profile for McWhorter AWN station.
Profile travels from Rattlesnake Hills to Horse Heaven Hills. Latitude: 46.32, Longitude -119.62, Elevation: 1401 ft. Image Courtesy of Google Pro Earth.

Figure 10: Elevation Profile for Benton W. AWN station.
Profile travels from Rattlesnake Hills to Horse Heaven Hills. Latitude: 46.30, Longitude -119.57, Elevation: 929 ft. Image Courtesy of Google Pro Earth.

Figure 11: Sunnyside AWN station.
Installed August 25th, 2020. Elevation: 690 ft. Photo courtesy of WSU AWN.

Figure 12: Grandview AWN station.
Installed August 30th, 2012. Elevation: 972 ft. Photo courtesy of WSU AWN.

Figure 13: Prosser N.E. AWN station.
Installed July 5th, 2002. Elevation: 827 ft. Photo courtesy of WSU AWN.

Figure 14: McWhorter AWN station.
Installed April 25th, 1989. Elevation: 1401 ft. Photo courtesy of WSU AWN.

Figure 15: Benton W. AWN station.
Installed June 16th, 2006. Elevation: 929 ft. Photo courtesy of WSU AWN.

Results

Sample Size

On average, there were 202,116 observations per meteorological variable at each station for the study period (2014-2020). Each observation was a 15-min average of 5 s readings from each measuring instrument. We reserved 2020 data to serve as the test, removing it from our preliminary analysis. There were 96 15-min observations per day, 672 15-min observations per week, and about 35040 15-min observations per year for each meteorological variable at a station.

Missing Data

The time plots (Figures 17, 18) show missing observations and discontinuities in our time series data from 2014 to 2019. Most of the missing observations and discontinues in the time plots were outside the spraying season (Table 1). Different models were fitted to different parts of the time series data to address this issue. However, the treatment of missing observations and discontinuities was complex and are addressed in the Discussion section.

The Yakima Valley and Prosser N.E.

Rattlesnake Hills and Horse Heaven Hills formed the low ridges near Sunnyside and Grandview (Figures 3, 4, 5, 6, 7). Prosser N.E. was at the foot of the Horse Heaven Hills and was the focus AWN site for this study (Figures 3, 4). The geographical location of Prosser N.E. was close to where previous drift field studies were completed and an area with frequent drift events and cases (Kasner et al., 2020, Kasner et al., 2021). This site was a central point of elevation in the Yakima Valley and our study area (Figures 3, 4, 5, 8). Compared to other stations, Prosser N.E. had less variable wind speeds (Table 1) with moderate to high maximum wind speeds (Table 1).

Aim 1: Determine the necessary inputs for wind ramp modeling in agriculture

Descriptive Statistics

The highest maximum wind speed value and wind speed variability was detected at the McWhorter site, 40.7 mph $\pm$ 4.0 mph (Table 1). The McWhorter station had the highest elevation (1401 ft) with limited surrounding wind breaking barriers or objects (Figures 4, 5, 9, 14). The lowest maximum wind speed value was detected at the Grandview site, 25.8 mph $\pm$ 3.0 mph (Table 1). The Grandview station had second highest elevation (972 ft) and is centered in the lower Yakima valley, surrounded by wind breaking barriers or objects (Figures 4, 7, 12). The Sunnyside station had the lowest elevation (690 ft), second highest maximum wind speed value and second most variable wind speeds; 37.2 mph $\pm$ 3.7 mph (Table 1) (Figures 4, 5, 6, 11). Benton W. had the least variable wind speeds and second lowest maximum wind speed values; 26.4 mph $\pm$ 2.7 mph (Table 1). The Benton W. location had a relatively high elevation (929 ft) and was surrounded by wind breaking barriers (Figures 4, 10, 15). The Prosser N.E. location had a history of relatively high maximum wind speed values and low wind speed variability; 34.3 mph $\pm$ 2.9 mph (Table 1). Prosser N.E. was the center point in our study area with moderate elevation (827 ft), was the nearest site to previous drift field studies, and had a history of frequent drift events and cases (Figures 4, 8, 13).

When comparing the wind gust speeds at each station, we found that Prosser N.E. had the highest maximum wind gust value of 60 mph $\pm$ 5.0 mph (Table 1) and the greatest difference in means between wind gust and wind speed; 4.0 mph $\pm$ 2.1 mph (Table 1). The two stations to the left of Prosser N.E., (Sunnyside and Grandview), had a difference in means of 2.5 mph $\pm$ 1.7 mph between wind gust and wind speed (Table 1). While McWhorter and Benton W. had a difference in means of 3.1 mph $\pm$ 1.7 mph between wind gust and wind speed (Table 1).

The histograms for wind speed and wind gusts (Figure 16) had similar shapes. Both distributions were right skewed with the peaks centered around lower wind speeds (approximately 5 mph) for wind speed alone and (approximately 10 mph) for wind gust (Figure 16). The skewness and center of each distribution indicated that low wind speeds dominated this study area. However, the distribution spreads for wind speed, 0 mph to 40 mph, and 0 mph to 60 mph, for wind gust, indicated that there were "spikes" in wind speed or wind ramps in Sunnyside, Prosser N.E., and McWhorter (Figure 16). The shape of histogram distributions were single-peaked and unimodal for all stations in the study area. This information narrowed our selection of short-term forecasting techniques to models that could accurately estimate these wind speed distributions.

Wind Speed Exceedances

To evaluate how often "spikes" or wind speed exceedances were above the 10-mph federal and state regulations, we stratified the data by station, then limited wind speed and wind gust to speeds greater than 10-mph, 15-mph, and 20-mph (Table 2). We found that McWhorter, the station with the highest elevation (Figures 3, 4), and limited surrounding wind breaking barriers or objects had the highest count and percentage of wind speed exceedances over the five-year period (January 2014 – December 2019) above 10-mph, 15-mph, and 20-mph for the wind speed variable alone (Table 2). Sunnyside, the station with lowest point of elevation (Figures 3, 4), had the second highest count and percentage of wind speed exceedances above 10-mph, 15-mph, and 20-mph for wind speed alone (Table 2). Prosser N.E. had the second highest proportion of wind gust exceedances following only McWhorter (Table 2). Prosser N.E. had 39.1 times more wind speed exceedances for the wind gust variable than wind speed variable (Table 2).

According to Tables 3 and 4, most wind ramp events lasted 30-60 minutes at speeds between 10-15 mph. However, the length of wind exceedances is longer in duration for the wind gust variable when compared to the wind speed variable for all run times. The longest wind ramp events for Prosser N.E. and McWhorter lasted 26.75 hours at wind speeds 20 mph or greater (Table 4).

Time Plots

To analyze the features of the changes in wind speed of the study area we graphed a time plot, observations against time for each station and year, excluding our test year 2020 (Figures 17-18). All time plots for each station and year exhibited similar seasonality and trend. The highest wind speeds were in the winter months during the pruning season, when a limited number of agricultural farmworkers are in the fields and little to no pesticides are normally applied. Wind speeds were variable during the spring months, when early rounds of pesticides are normally applied. The

lowest wind speeds were in the summer months when most farmworkers are in the fields thinning, harvesting various tree fruit, or applying pesticides. Wind speeds were highly variable in the spring and fall months. In the fall, workers were primarily harvesting when little to no pesticides are usually applied.

Overall, wind speed across all stations had significant diurnal, metrological, and seasonal variation, consistent with nonstationary time series (Figures 17, 18). Sunnyside had the most missing data and discontinuities in the winter months in 2019, 2017, and 2016 with approximately 3% of wind speed and gust observations missing (Table 1; Figures 17c, 18a, 18c). McWhorter, Prosser N.E., Benton W., and Grandview had a limited number of missing values scattered throughout each year (Table 1) (Figures 17, 18).

Comparative Box Plots of Wind Direction

Wind from the north was the most prevailing wind direction for lower valley stations (Figure 26) (Table 11). Over the five years between January 2014 and December 2019, 19% of the winds came from the north at Sunnyside, 33% at Grandview, and 28% at Prosser N.E. (Table 11) (Figure 26). West winds were the most prevailing wind direction for the McWhorter and Benton W. stations (Figure 26) (Table 11). Throughout the five-study period 24% of the wind came from the west at McWhorter and 28% at Benton W. (Table 11). South winds were the least prevailing in Sunnyside and Grandview (Figure 26) (Table 11). Whereas winds from the southeast were the least prevailing at Prosser N.E., McWhorter, and Benton W (Table 11) (Figure 26). The outliers represented 'spikes' or wind ramps (Figures 26 and 27). For our focus site at Prosser N.E., most wind ramps were associated with winds from the west over the five-year study period, which were the second most prevailing wind direction (Figure 26) (Table 11). A similar pattern was observed when evaluating the occurrence of wind ramp events from the wind gust variable (Figure 27). Note, all wind directions for the wind gust variable were at or above 15 mph (Figure 27).

Decomposition and Autocorrelation Function (ACF) Correlogram for Prosser N.E.

The correlation between observations was an important property of a time series and guided forecast model building. As expected from the wind forecasting literature, we observed cyclic seasonal and diurnal trends of the wind speed variable for Prosser N.E. in Figures 17, 18. The correlograms in Figure 19 showed that the wind speed time series for Prosser N.E. from January 2104 to March 2020 had many consecutive positive values[e1] (Figure 19). This observation on one side of the overall mean tends to be followed by a large number on the same side of the mean, indicating a trend. The correlogram pattern observed in Figure 19 was a typical non-stationary time series consistent with the wind forecasting literature. The dominant trend in our correlograms indicated that decomposition of the wind speed time series was necessary to understand the correlation between the residuals (Figure 20). We utilized the R stats package command stl to decompose each wind speed data subsets into their seasonal and residual components (Figure 20). The data subsets ranged from January 2014 to March 2020, April 2020, and May 2020 (Figure 20). We can see that the overall trend, seasonal trend, and pattern for the residuals/remainders were the same for all three data subsets. However, the residuals followed a cyclic pattern, indicating that additional filtering (differencing) was required to remove persistent trends. To determine the order

of differencing required to our non-stationary time series into a stationary time series, we used the auto.arima function. To evaluate if the ARIMA (2,1,1) and ARIMA (4,1,2) models achieved stationarity, we used an ACF plot on the residuals (Figure 21). The correlograms in Figure 21 show that the seasonal and cyclic variations have been removed from the residuals through first differencing. We also learned from the seasonal component that the highest wind speed values occurred in the late fall and winter months (Figure 20). Wind speed values then varied in the spring and early summer months (Figure 20). The lowest wind speed values occurred in the summer and then gradually rose in the fall (Figure 20). Also, not all significant 'spikes' in the observed wind time series time plot are isolated in the residual component-time plot (Figure 20). In addition, the highest wind speeds for Prosser N.E. occurred in the fall and winter months and then started to decline in the late winter and early spring months (Figure 20).

ARIMA Model Fitting

To provide a 2.5-hour wind speed forecast for the months of April, May, and June 2020 at the Prosser N.E. station, we fit the ARIMA (2,1,1) and ARIMA (4,1,2) models to three different wind speed data subsets. The first ranged from March 1st – 31st, 2020 to predict the wind speed observations in 1st, April 2020 (Figure 22). The second wind speed data subset ranged from April 1st - 30th, 2020 to predict the wind speed values on May 1st, 2020 (Figure 23). A third wind speed data subset that ranged from May 1st- May 31st, 2020, to predict the observed wind speed values on June 1st, 2020 (Figure 24).

Comparative Box Plots of Wind Direction at Prosser N.E.

The west was the most prominent wind direction for the months of March 2020, April 2020, May 2020, and June 2020 at Prosser N.E. (Table 10) (Figures 26, 27). Southeast winds were the least prominent during the months of April 2020, May 2020, and June 2020. East was the least prominent direction during the month of March 2020.

The outliers represented 'spikes' or wind ramps in Figures 26 and 27. In March and April 2020, wind ramp events occurred more frequently from the north but the highest wind speeds (above 15 mph) were observed from west and southwest direction (Figure 26). In May and June 2020, the highest wind speeds and most wind ramp events occurred from the west (Figure 26). Wind ramp events and maximum wind speeds did not surpass 15 mph in June 2020 (Figure 26).

When wind direction was stratified by the wind gust variable for March 2020, April 2020, May 2020, and June 2020 at Prosser N.E., we observed different patterns (Figure 27). In March and April, wind ramp events occurred more frequently from the north, but the highest wind speeds (above 30 mph) occurred from the northeast, southwest, and west. For May, more wind ramp events were observed from the northwest and the highest wind speeds (above 30 mph) came from the west. In June, the most wind ramp events and highest wind speeds (above 20 mph) came from the southwest.

Aim 2: Apply the model

Prosser N.E. Arima (2,1,1) Wind Speed Forecast for April 1st, 2020

Figure 21 and Table 5 provide a 2.5-hour ARIMA (2,1,1) wind speed forecast for April 1st, 2020, and the forecast's descriptive statistics, respectively. Our ARIMA (2,1,1) model was trained with and fitted to the summarized 15-min averages of 5s readings from the AWN historical wind speed values (Figure 21 black line) at Prosser N.E. in Mach 2020. Each 15-min average counted as one observation, so the wind speed time series for March consisted of 2971 observations, or 2971 15-min averages 5s wind speed data from March 1st, 2020 to March 31st, 2020 (Figure 21 green line). We attempted to forecast the first 10 observations (2.5 hours) of April 1st, 2020 (Figure 21 blue line), which contained a 3.4 mph wind ramp (Figure 21 red line) in the center of the 2.5-hour time interval (Table 5). The wind ramp increased from 2.5 mph to 5.9 mph and gradually tapered back down to 2.7 mph after 30 minutes (Table 5). The ARIMA (2,1,1) model's calculated point forecasts (Figure 21 blue line) are linear and did not respond well to actual observed wind speed values (Figure 21 red line). Also, the forecast appeared as a linear average (Figure 21 blue line) that underestimated the actual observed wind speed values (Figure 21 red line). Our ARIMA (2,1,1) model underestimated the actual speed values of the wind ramp with a predicted value of 2.2 mph with a 95% prediction interval (95-PI) (0, 6.48) and 0.0932 standard error (SE) (Table 5). The variability between our ARIMA (2,1,1) predicted values and the actual observed wind speeds for April 1st, 2020 was 1.44 (Table 5).

Prosser N.E. Arima (2,1,1) Wind Speed Forecast for May 1st, 2020

Figure 22 and Table 6 provide a 2.5-hour ARIMA (2,1,1) wind speed forecast for May 1st, 2020, and the forecast's descriptive statistics, respectively. Our ARIMA (2,1,1) model was trained with and fitted to the summarized 15-min averages of 5s readings from the AWN historical wind speed values (Figure 22 black line) at Prosser N.E. in April 2020. Each 15-min average counts as one observation, this wind speed time series for April consisted of 2880 observations or 2880 15-min averages 5s wind speed data from April 1st, 2020, to April 30th, 2020 (Figure 22 green line). We attempted to forecast the first 10 observations (2.5 hours) of May 1st, 2020 (Figure 22 blue line), which contained a 2.6 mph downward wind ramp (sudden decrease in wind speed) (Figure 22 red line) that lasted for 1 hour and 45 minutes (Table 6). The wind ramp decreased from 3.30 mph to 0.70 mph in the first hour and then increased (upward wind ramp) to 4.60 mph 45 minutes after dropping to 0.70 mph (Table 6). The ARIMA (2,1,1) model's calculated point forecasts (Figure 22 blue line) were linear and had a downward slope, corresponding to the downward wind ramp that occurred over the first hour and 45 minutes (Figure 22 red line). This forecast in May 2020 overestimated the actual observed wind speed values (Figure 22). Our ARIMA (2,1,1) model overestimated the actual speed values of the downward wind ramp with a predicted value of 3.23 mph with a 95-PI (0, 7.37) and 0.0578 SE (Table 6). The variability between our ARIMA (2,1,1) predicted values and the actual observed wind speeds for May 1st, 2020 was 1.64 (Table 6).

Prosser N.E. Arima (2,1,1) Wind Speed Forecast for June 1st, 2020

Figure 23 and Table 7 provide a 2.5-hour ARIMA (2,1,1) wind speed forecast for June 1st, 2020, and the forecast's descriptive statistics, respectively. Our ARIMA (2,1,1) model was trained with

and fitted to the summarized 15-min averages of 5s readings from the AWN historical wind speed values (Figure 23 black line) at Prosser N.E. in May 2020. Each 15-min average counted as one observation, this wind speed time series for March consisted of 2975 observations or 2975 15-min averages 5s wind speed data from May 1st, 2020, to May 31st, 2020 (Figure 23 green line). We attempted to forecast the first 10 observations (2.5 hours) of June 1st, 2020 (Figure 23 blue line), which contained a downward wind ramp and upward wind ramp events (Figure 23 red line). The downward wind ramp decreased from 2.50 mph to 0.70 mph and lasted for 30 minutes in duration (Table 7). Immediately after the wind speed increased from 0.70 mph to 3.00 mph (upward wind ramp) and lasted for 45 minutes in duration (Table 7). The wind speed dropped again for the remainder of the 2.5-hour time interval (Figure 23) (Table 7). The ARIMA (2,1,1) model's calculated point forecasts are non-linear and appear logarithmic (Figure 23 blue line). The logarithmic trend of the predicted values gradually rose from 1.01 mph with a 95-PI (0.00, 3.34) and SE (0.0407) to 1.80 mph with a 95-PI (0.00, 6.50) and SE (0.0407) (Table 7). The continual rise in predicted wind speed values caused the ARIMA (2,1,1) model to overestimate the lowest value of downward wind ramp 0.70 mph versus 1.59 mph with 95-PI (0.00, 5.32) and 0.0407 SE (Table 7). The model underestimated the highest value of the upward wind ramp 3.00 mph versus 1.72 mph with a 95-PI (0.00, 5.86) and 0.0407 SE (Table 7). The variability between our ARIMA (2,1,1) predicted values and the actual observed wind speeds for June 1st, 2020 was 0.81 (Table 7).

800 Additional Forecasts

We ran an additional 800 forecasts by fitting the same ARIMA (2,1,1) and ARIMA (4,2,1) models over sequential 30-day periods or windows. The first training window starts on March 1st, 2020, at12:30 am and ends on March 30th, 2020, at 11:15 pm, forecasting the following 2.5 hours. The second window shifts forward 2.5 hours and starts on March 1st, 2020, at 3:00 am and ends on March 31st at 1:45 am, forecasting the following 2.5 hours. This process repeats for a total of 800 windows. The 800th window starts on May 23rd, 2020 at 6:30 pm and ends on June 23rd at 5:15 pm. Each window provided a 2.5-hours forecast, a training RMSE, (which calculated the variability between our ARIMA (2,1,1) and ARIMA (4,2,1) model with 30-day historical values) a test RMSE, (which calculated the variability between our forecasted points and the observed 2020 values) and an ACF plot of the residuals. Figure 25 shows four additional training windows, their 2.5-hour forecasts, training RMSE value, and test RMSE value, and an ACF plot of residuals. A histogram of the resulting test RMSE values can be found in Appendix 1 Figure 9. Table 9 in the results section provides the summary statistics of the 800 ARIMA (2,1,1) models ran between the months of March 2020, April 2020, May 2020, and June 2020. The lowest variability between our calculated point forecast and actual observed wind speed values was 0.27 (Table 9) (Appendix 1: Figure 9). The greatest variability between our calculated point forecast and actual observed wind speed values was 8.57 (Table 9) (Appendix 1: Figure 9).

Result Tables

Table 1:Descriptive meteorological statistics of Wind Speed (mph) and Wind Gust (mph). This table includes statistics for all stations from 2014 – 2019.

Wind Speed	**Sunnyside**	**Grandview**	**Prosser N.E.**	**McWhorter**	**Benton W.**
n [a]	169618	210538	209434	210465	210527
missing obs. [b]	4252	105	1194	176	50
mean	3.8	2.9	3.8	5.8	5.1
SD [c]	3.7	3.0	2.9	4.0	2.7
min	0	0	0	0	0
25th	1.2	0.2	2	3.5	3.4
Median	3	2.5	3.4	5	4.6
75th	5.1	4.1	4.8	7.6	6.1
Max	37.2	25.8	34.3	40.7	26.4
Wind Gust	**Sunnyside**	**Grandview**	**Prosser N.E.**	**McWhorter**	**Benton W.**
n [a]	205621	210599	210500	210564	210532
missing obs. [b]	4252	48	51	75	50
mean	6.4	5.3	7.8	9.0	8.1
SD [c]	5.3	4.7	5.0	5.8	4.5
min	0	0	0	0	0
25th	3.1	2.1	4.6	5.3	4.9
Median	5.2	4.6	6.4	7.8	7.1
75th	8.5	7.4	9.9	11.7	9.9
Max	51.1	40	60	55	45.7
	Sunnyside	**Grandview**	**Prosser N.E.**	**McWhorter**	**Benton W.**
$\overline{x_2} - \overline{x_1}$ [d]	2.6	2.4	4.0	3.2	3.1
$s_2 - s_1$ [e]	1.7	1.7	2.1	1.8	1.7
% WS missing [f]	3%	0%	1%	0%	0%
% WG missing [g]	2%	0%	0%	0%	0%

a. (n) total number of non-missing observations.
b. (missing observations (obs.)) the total number of missing values.
c. (SD) the standard deviation.
d. ($\overline{x_2} - \overline{x_1}$) difference in means between wind gust and wind speed.
e. ($s_2 - s_1$) difference in variation between wind gust and wind speed.
f. (% WS missing) percentage of missing wind speed values.
g. (% WG missing) percentage of missing wind gust values.

Table 1 contains five-number summaries for the wind speed and wind gust variables. These summaries compare the wind speed distributions for each variable and the wind speed distributions between each site in our study area.

Table 2: Wind Speed Exceedance Counts.
This tables includes wind speed exceedances for all stations from 2014 – 2019.

Wind Speed Alone (mph)	**Sunnyside (n = 169618)**	**Grandview (n = 210538)**	**Prosser N.E. (n = 209434)**	**McWhorter (n = 210465)**	**Benton W. (n = 210527)**
	n (%) [a]	**n (%) [a]**	**n (%) [a]**	**n (%) [a]**	**n (%) [a]**
>10 mph	13996 (8.3)	7052 (3.3)	7999 (3.8)	27230 (12.9)	12070 (5.7)
>15 mph	3349 (2.0)	995 (0.5)	1634 (0.8)	7176 (3.4)	1655 (0.8)
>20 mph	449 (0.3)	96 (0.05)	170 (0.1)	1522 (0.7)	139 (0.1)
Wind Gust (mph)	**Sunnyside (n = 205621)**	**Grandview (n = 210599)**	**Prosser N.E. (n = 210500)**	**McWhorter (n = 210564)**	**Benton W. (n = 210532)**
	n (%) [a]	**n (%) [a]**	**n (%) [a]**	**n (%) [a]**	**n (%) [a]**
>10 mph	35680 (21.0)	25908 (12.3)	36038 (17.1)	69909 (33.2)	49742 (23.6)
>15 mph	15570 (9.2)	9873 (4.7)	17481 (8.3)	30112 (14.3)	17591 (8.4)
>20 mph	5961 (3.5)	2769 (1.3)	6821 (3.2)	11209 (5.3)	5272 (2.5)
Relative Exceedances	**Sunnyside**	**Grandview**	**Prosser N.E.**	**McWhorter**	**Benton W.**
$RE_{(10\ mph)}$ [b]	1.5	2.7	3.5	1.6	3.1
$RE_{(15\ mph)}$ [b]	3.6	8.9	9.7	3.2	9.6
$RE_{(20\ mph)}$ [b]	12.3	27.8	39.1	6.4	36.9

a. n (%) = total number of non-missing observations with its percentage
b. $RE = \frac{x_2 - x_1}{x_1}\ where\ x_1 = wind\ speed, x_2 = wind\ gust$

Table 2 contains the total number of times the wind speed exceeded 10 mph, 15, mph, and 20 mph for wind speed alone and wind gusts. Federal and state regulations require that pesticide application cannot occur if wind speeds are greater than 10 mph (4.5 m/s). When comparing the relative exceedances between the wind gust variable and wind speed variable for each site, we found that Prosser N.E. had 39.1 times as many exceedances using wind gusts than wind speed alone.

Table 3: Run Times (15-minute averages) of Wind Speed Exceedances.
This table includes run times of wind speed exceedances for all stations from 2014 – 2019.

10-mph Run Times (min)	**Sunnyside**	**Grandview**	**Prosser N.E.**	**McWhorter**	**Benton W.**
	n (%)	**n (%)**	**n (%)**	**n (%)**	**n (%)**
30-60	742 (0.39)	444 (0.25)	503 (0.26)	1181 (0.62)	639 (0.33)
75 - 105	250 (0.27)	127 (0.16)	152 (0.20)	399 (0.44)	248 (0.26)
120 - 150	141 (0.23)	63 (0.08)	73 (0.09)	208 (0.41)	125 (0.23)
165 - 195	91 (0.24)	36 (0.10)	41 (0.10)	158 (0.34)	64 (0.20)
210 - 240	54 (0.09)	23 (0.07)	39 (0.09)	102 (0.33)	44 (0.15)
Max (min)	1080 (0.07)	1125 (0.04)	1710 (0.07)	1965 (0.07)	1965 (0.07)
Max (hrs)	18 (0.07)	18.75 (0.04)	28.5 (0.07)	32.75 (0.07)	32.75 (0.07)
15-mph Run Times (min)	**Sunnyside**	**Grandview**	**Prosser N.E.**	**McWhorter**	**Benton W.**
	n (%)	**n (%)**	**n (%)**	**n (%)**	**n (%)**
30-60	295 (0.15)	89 (0.04)	166 (0.09)	416 (0.20)	138 (0.07)
75 - 105	88 (0.10)	17 (0.01)	52 (0.07)	144 (0.17)	31 (0.03)
120 - 150	29 (0.04)	13 (0.02)	18 (0.04)	66 (0.11)	14 (0.04)
165 - 195	18 (0.05)	6 (0.04)	6 (0.04)	35 (0.09)	17 (0.05)
210 - 240	18 (0.05)	4 (0.03)	5 (0.04)	27 (0.07)	7 (0.04)
Max (min)	1020 (0.04)	720 (0.03)	990 (0.03)	1485 (0.06)	975 (0.04)
Max (hrs)	17 (0.04)	12 (0.03)	16.5 (0.03)	24.75 (0.06)	16.25 (0.04)
20-mph Run Times (min)	**Sunnyside**	**Grandview**	**Prosser N.E.**	**McWhorter**	**Benton W.**
	n (%)	**n (%)**	**n (%)**	**n (%)**	**n (%)**
30-60	61 (0.03)	8 (0.01)	19 (0.03)	126 (0.11)	10 (0.02)
75 - 105	10 (0.03)	1 (0.00)	6 (0.02)	33 (0.04)	1 (0.00)
120 - 150	4 (0.02)	3 (0.02)	1 (0.01)	19 (0.03	1 (0.01)
165 - 195	2 (0.01)	2 (0.01)	0 (0.00)	14 (0.03)	2 (0.01)
210 - 240	6 (0.02)	0 (0.00)	2 (0.002)	6 (0.01)	1 (0.01)
Max (min)	225 (0.01)	195 (0.01)	300 (0.01)	990 (0.04)	570 (0.02)
Max (hrs)	3.75 (0.01)	3.25 (0.01)	5 (0.01)	16.5 (0.04)	9.5 (0.02)

a. (Max (hrs.)) = Max (min) / 60 min

Table 3 counts how many of wind speed exceedances from Table 2 lasted 30 minutes to 240 minutes (4 hours) or greater. It is important to note that the meteorological data received from WSU AWN was structured as 15-minute averages of 5 s readings.

Table 4: Run Times (15-minute averages) of Wind Gust Exceedances.
This tables includes run times of wind gust exceedances for all stations from 2014 – 2019.

10-mph Run Times (min)	**Sunnyside**	**Grandview**	**Prosser N.E.**	**McWhorter**	**Benton W.**
	n (%)	**n (%)**	**n (%)**	**n (%)**	**n (%)**
30-60	1869 (0.90)	1386 (0.63)	2114 (0.64)	2484 (0.74)	2403 (0.68)
75 - 105	543 (0.63)	402 (0.43)	586 (0.63)	712 (0.72)	655 (0.68)
120 - 150	280 (0.47)	194 (0.40)	276 (0.54)	384 (0.68)	348 (0.57)
165 - 195	177 (0.39)	123 (0.27)	162 (0.36)	264 (0.60)	208 (0.47)
210 - 240	121 (0.44)	88 (0.17)	109 (0.33)	193 (0.55)	158 (0.38)
Max (min)	1860 (0.07)	2115 (0.08)	2745 (0.10)	4575 (0.17)	2865 (0.11)
Max (hrs)	31 (0.07)	35.25 (0.08)	45.75 (0.10)	76.25 (0.17)	47.75 (0.11)
15-mph Run Times (min)	**Sunnyside**	**Grandview**	**Prosser N.E.**	**McWhorter**	**Benton W.**
	n (%)	**n (%)**	**n (%)**	**n (%)**	**n (%)**
30-60	912 (0.44)	706 (0.36)	1114 (0.49)	1436 (0.67)	1032 (0.46)
75 - 105	267 (0.35)	170 (0.19)	268 (0.27)	315 (0.40)	316 (0.36)
120 - 150	132 (0.16)	94 (0.11)	145 (0.21)	211 (0.38)	157 (0.31)
165 - 195	88 (0.21)	60 (0.14)	80 (0.18)	35 (0.35)	74 (0.16)
210 - 240	48 (0.12)	21 (0.05)	65 (0.19)	108 (0.27)	64 (0.12)
Max (min)	1860 (0.07)	1935 (0.05)	1890 (0.07)	2025 (0.08)	1965 (0.07)
Max (hrs)	31 (0.07)	32.25 (0.07)	31.5 (0.07)	33.75 (0.08)	32.75 (0.07)
20-mph Run Times (min)	**Sunnyside**	**Grandview**	**Prosser N.E.**	**McWhorter**	**Benton W.**
	n (%)	**n (%)**	**n (%)**	**n (%)**	**n (%)**
30-60	457 (0.20)	258 (0.13)	509 (0.25)	680 (0.32)	431 (0.18)
75 - 105	153 (0.14)	61 (0.07)	141 (0.15)	190 (0.24)	111 (0.12)
120 - 150	60 (0.10)	24 (0.06)	71 (0.09)	97 (0.18)	52 (0.08)
165 - 195	34 (0.09)	15 (0.03)	36 (0.10)	54 (0.14)	21 (0.02)
210 - 240	20 (0.07)	9 (0.03)	28 (0.08)	36 (0.09)	18 (0.05)
Max (min)	1050 (0.04)	1095 (0.04)	1605 (0.06)	1605 (0.06)	1095 (0.04)
Max (hrs)	17.5 (0.04)	18.25 (0.04)	26.75 (0.06)	26.75 (0.06)	18.25 (0.04)

a. (Max (hrs.)) = Max (min) / 60 min

Table 4 counts how many of wind gust exceedance averages from Table 2 lasted 30 minutes to 240 minutes (4 hours) or greater. It is important to note that the meteorological data received from WSU AWN was structured as 15-minute averages of 5 s readings. Therefore, these are not the length of the individual wind gusts within a 15-minute time frame.

Table 5: Wind Speed Exceedances Greater than 10 mph for the months March, April, May, June and their percentages, 2014 – 2019.

	2014	2015	2016	2017	2018	2019
WIND SPEED	n (%)	n (%)	n (%)	n (%)	n (%)	n (%)
March	418 (14.0)	215 (7.0)	323 (11.0)	343 (12.0)	197 (7.0)	9 (0.0)
April	228 (8.0)	108 (4.0)	80 (3.0)	166 (6.0)	351 (12.0)	159 (6.0)
May	105 (4.0)	63 (2.0)	53 (2.0)	51 (2.0)	62 (2.0)	55 (2.0)
June	61 (2.0)	19 (1.0)	107 (4.0)	88 (3.0)	66 (2.0)	12 (0.0)
WIND GUST	n (%)	n (%)	n (%)	n (%)	n (%)	n (%)
March	1063 (36.0)	621 (21.0)	949 (32.0)	912 (31.0)	670 (23.0)	231 (8.0)
April	1063 (37.0)	740 (22.0)	678 (33.0)	889 (32.0)	1005 (23.0)	835 (8.0)
May	785 (26.0)	710 (25.0)	805 (23.0)	655 (30.0)	652 (34.0)	711 (28.0)
June	744 (26.0)	436 (25.0)	560 (28.0)	688 (23.0)	817 (23.0)	693 (25.0)

Table 5 provides both the count of wind speed exceedances greater than 10 mph for each month and the precent. The percent was calculated by setting the count of wind speed exceedances greater than 10 mph for each month as the numerator and the total wind speed counts for each month as the denominator. The wind gust variable was calculated the same way. In 2014, 14% of all wind speed observations in March were wind exceedances greater than 10 mph. Also, in March 2014, 36% of all wind gust observations were wind exceedances greater than 10 mph.

Table 6: Prosser N.E. April ARIMA (2,1,1) Wind Speed Forecast Comparison Observed. This table compares the predicted values from the ARIMA (2,1,1) wind speed model to the recorded AWN wind speed values for the first 2.5 hours of first day of April 2020.

April 1st, 2020, ARIMA (2,1,1)							
Forecast Point	**AWN Observed Wind Speed Value (mph)**	**ARIMA (2,1,1) Predicted Wind Speed Value (mph)**	**Low 95% Prediction Interval[a]**	**High 95% Prediction Interval**	**Percent Difference[b]**	**SE[c]**	**RMSE[d]**
1	3.0	2.2	0.00	4.66	73%	0.0932	1.44
2	2.4	2.2	0.00	5.54	93%		
3	2.5	2.2	0.00	6.08	90%		
4	5.9	2.2	0.00	6.48	38%		
5	4.3	2.3	0.00	6.82	52%		
6	2.7	2.3	0.00	7.12	84%		
7	2.8	2.3	0.00	7.41	81%		
8	1.6	2.3	0.00	7.67	141%		
9	2.8	2.3	0.00	7.93	81%		
10	3.4	2.3	0.00	8.17	66%		
	3.1	2.2			80%		

a.) These values have been truncated to zero because we know that these wind speed cannot be less than zero. Software outputted lower bounds are in Appendix 1.

b.) Percent Difference $= \frac{Prediced\ Value}{Observed\ Value} \times 100$

c.) Standard Error that is provided from software output in Appendix 1.

d.) Root Mean Square Error $\sqrt{\frac{\sum_{i=1}^{N}(x_i - \hat{x_i})^2}{N}}$; where x_i is the actual wind speed observation and $\hat{x_i}$ is the predicted wind speed value.

Table 6 contains descriptive statistics of the ARIMA (2,1,1) predicted values (calculated point forecast, the forecast of a single number) and the actual observed values for wind speed on April 1st, 2020. The prediction interval consisted of upper and lower limits between which a future value was expected to lie with a prescribed probability and provided as output from the **Arima** function in the R *forecast* package (See Appendix 1 for R output). The standard error (SE) was also provided from the **Arima** function (See Appendix 1). On average, our model underestimated the wind speed for the first 2.5 hours on April 1st, 2020. The variability between our calculated point forecast values and the actual observed wind speed values was1.44 (RMSE).

Table 7: Prosser N.E. May ARIMA (2,1,1) Wind Speed Forecast Comparison Observed. This table compares the predicted values from the ARIMA (2,1,1) wind speed model to the recorded AWN wind speed values for the first 2.5 hours of first day of May 2020.

May 1st, 2020, ARIMA (2,1,1)							
Forecast Point	**AWN Observed Wind Speed Value (mph)**	**ARIMA (2,1,1) Predicted Wind Speed Value (mph)**	**Low 95% Prediction Interval[a]**	**High 95% Prediction Interval**	**Percent Difference[b]**	**SE[c]**	**RMSE[d]**
1	3.30	3.26	0.81	5.72	99%	0.0578	1.64
2	1.70	3.24	0.00	6.50	191%		
3	1.20	3.23	0.00	7.00	269%		
4	0.70	3.23	0.00	7.37	461%		
5	1.40	3.22	0.00	7.68	230%		
6	2.40	3.22	0.00	7.95	134%		
7	4.60	3.22	0.00	8.19	70%		
8	4.50	3.22	0.00	8.41	71%		
9	5.20	3.22	0.00	8.62	62%		
10	4.80	3.21	0.00	8.82	67%		
	3.0	3.2			165%		

a.) These values have been truncated to zero because we know that these wind speed cannot be less than zero. Software outputted lower bounds are in Appendix 1.

b.) Percent Difference $= \frac{Prediced\ Value}{Observed\ Value} \times 100$

c.) Standard Error that is provided from software output in Appendix 1.

d.) Root Mean Square Error $\sqrt{\frac{\sum_{i=1}^{N}(x_i - \widehat{x_i})^2}{N}}$; where x_i is the actual wind speed observation and $\widehat{x_i}$ is the predicted wind speed value.

Table 7 contains descriptive statistics of the ARIMA (2,1,1) predicted values (calculated point forecast, the forecast of a single number) and the actual observed values for wind speed on May 1st, 2020. The prediction interval consisted of upper and lower limits between which a future value is expected to lie with a prescribed probability and is provided as output from the **Arima** function in the R *forecast* package (See Appendix 1 for R output). The standard error (SE) was also provided from the **Arima** function (See Appendix 1). On average, our model overestimated wind speed for the first 2.5 hours on May 1st, 2020. The variability between our calculated point forecast values and the actual observed wind speed values was 1.64 (RMSE).

Table 8: Prosser N.E. June ARIMA (2,1,1) Wind Speed Forecast Comparison Observed. This table compares the predicted values from the ARIMA (2,1,1) wind speed model to the recorded AWN wind speed values for the first 2.5 hours of first day of June 2020.

June 1st, 2020, ARIMA (2,1,1)							
Forecast Point	**AWN Observed Wind Speed Value (mph)**	**ARIMA (2,1,1) Predicted Wind Speed Value (mph)**	**Low 95% Prediction Interval[a]**	**High 95% Prediction Interval**	**Percent Difference[b]**	**SE[c]**	**RMSE[d]**
1	1.60	1.01	0.00	3.34	63%	0.0407	0.81
2	2.20	1.29	0.00	4.32	59%		
3	2.50	1.47	0.00	4.91	59%		
4	0.70	1.59	0.00	5.32	227%		
5	1.30	1.67	0.00	5.62	128%		
6	3.00	1.72	0.00	5.86	57%		
7	1.60	1.76	0.00	6.05	110%		
8	1.30	1.78	0.00	6.22	137%		
9	1.40	1.79	0.00	6.37	128%		
10	0.60	1.80	0.00	6.50	300%		
	1.6	1.6			127%		

a.) These values have been truncated to zero because we know that these wind speed cannot be less than zero. Software outputted lower bounds are in Appendix 1.

b.) Percent Difference $= \frac{Prediced\ Value}{Observed\ Value} \times 100$

c.) Standard Error that is provided from software output in Appendix 1.

d.) Root Mean Square Error $\sqrt{\frac{\sum_{i=1}^{N}(x_i - \hat{x_i})^2}{N}}$; where x_i is the actual wind speed observation and $\hat{x_i}$ is the predicted wind speed value.

Table 8 contained descriptive statistics of the ARIMA (2,1,1) predicted values (calculated point forecast, the forecast of a single number) and the actual observed values for wind speed on June 1st, 2020. The prediction interval consisted of upper and lower limits between which a future value was expected to lie with a prescribed probability and is provided as output from the **Arima** function in the R *forecast* package (See Appendix 1 for R output). The standard error (SE) was also provided from the **Arima** function (See Appendix 1). On average, our model overestimated the wind speed for the first 2.5 hours on June 1st, 2020. The variability between our calculated point forecast values and the actual observed wind speed values was 0.81 (RMSE).

Table 9: Summary statistics of the 800 ARIMA (2,1,1) training models RMSEs and their 2.5-hour Forecast RMSEs

	Training RMSEs	Forecast RMSEs
Minimum	1.07	0.27
Median	1.23	1.42
Maximum	1.34	8.57
Standard Deviation	0.07	1.11

Table 9 provided the summary statistics of the 800 ARIMA (2,1,1) models ran between the months of March 2020, April 2020, May 2020, and June 2020. The first model of the total 800 models was trained on a 30-day period from March 1st, 2020, to March 30th, 2020, and forecasted ten 15-minute period time points or 2.5-hours. The model was automated to shift forward 2.5-hours from the starting date of March 1st, 2020, and it's end period of March 30th, 2020, to predict a following 2.5-hour time period until it completed 800 forecasts that stayed within the bounds of our time-period of interest (April 2020, May 2020, and June 2020). Examples of the 800 simulations are found in Figure 25 of the Result Figures section. The histogram of the distributions are found in Figures 8 and 9 of Appendix 1.

Table 10: Wind Direction Stratified by Direction and Month for 2020 at Prosser N.E.

Wind Direction	March n (%)	April n(%)	May n(%)	June n(%)
N	791 (27.0)	563 (20.0)	456 (15.0)	396 (14.0)
NE	217 (7.0)	248 (9.0)	335 (11.0)	153 (5.0)
E	159 (5.0)	222 (8.0)	287 (10.0)	119 (4.0)
SE	160 (5.0)	184 (6.0)	191 (6.0)	115 (4.0)
S	267 (9.0)	282 (10.0)	259 (9.0)	192 (7.0)
SW	481 (16.0)	338 (12.0)	375 (13.0)	422 (15.0)
W	515 (17.0)	592 (21.0)	704 (24.0)	940 (33.0)
NW	382 (13.0)	447 (16.0)	369 (12.0)	543 (19.0)
missing	0 (0.0)	4 (0.0)	0 (0.0)	0 (0.0)
Total	2972	2880	2976	2880

Table 10 stratifies the wind direction observations by direction and month for 2020 at Prosser N.E. The west is the most prominent wind direction the months of April 2020, May 2020 and June 2020 for the year 2020 at Prosser N.E. The north is the most prominent wind direction for the month of March and second most prominent for the months of April 2020 and May 2020. The northwest was the second most prominent wind direction for the month of June 2020 at Prosser N.E.

Table 11: Wind Direction Stratified by Direction and Station for 2014 – 2019

Wind Direction	Sunnyside n(%)	Grandview n(%)	Prosser N.E. n(%)	McWhorter n(%)	Benton W. n(%)
N	39448 (19.0)	69722 (33.0)	59322 (28.0)	39884 (19.0)	17052 (8.0)
NE	22390 (11.0)	21016 (10.0)	17400 (8.0)	12533 (6.0)	12186 (6.0)
E	31791 (15.0)	25082 (12.0)	18586 (9.0)	10837 (5.0)	15499 (7.0)
SE	21855 (11.0)	14495 (7.0)	13359 (6.0)	8907 (4.0)	8432 (4.0)
S	14766 (7.0)	11831 (6.0)	13813 (7.0)	12538 (6.0)	12358 (6.0)
SW	19476 (9.0)	14290 (7.0)	19996 (10.0)	42318 (20.0)	48717 (23.0)
W	33845 (16.0)	31006 (15.0)	43136 (21.0)	50980 (24.0)	57922 (28.0)
NW	21586 (11.0)	22853 (11.0)	23791 (11.0)	32172 (15.0)	38126 (18.0)
missing	5179 (3.0)	41 (0.0)	933 (0.0)	167 (0.0)	44 (0.0)
Total	205157	210295	209403	210169	210292

Table 11 stratifies the wind direction observations by direction and station for the years 2014 to 2019. The north was the most prominent wind direction for lower valley stations Sunnyside, Grandviw and Prosser N.E. from the years 2014 to 2019. Southwest was the most prominent wind direction for stations McWhorter and Benton W., both on the edge of Rattlesnake Hills.

Result Figures

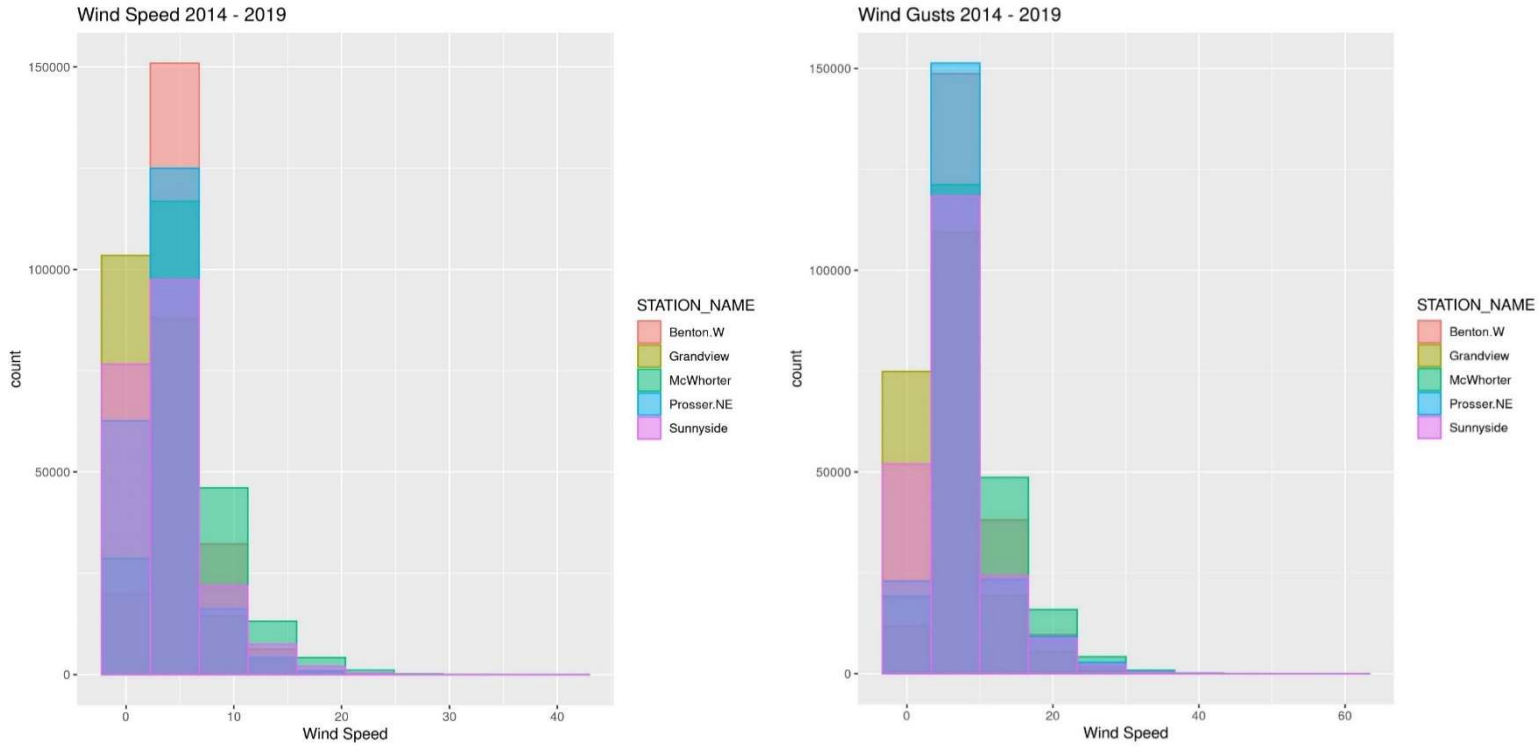

Figure 16: Histograms of Wind Speed and Wind Gust per Station from 2014 – 2019. The histograms are plotted as count over wind speed.

Figure 16a (Left): The wind speed distribution for all stations in this study are unimodal, with the center at 5 mph. The spread of the wind speed distribution is from 0 mph to 40 mph. The stations with the highest wind speeds are Sunnyside, Prosser N.E., and McWhorter; these stations are the lowest, center, and highest points of elevation in this study, respectively.

Figure 16b (Right): Histograms of Wind Gust per Station from 2014 – 2019 – Count Over Wind Speed. The wind speed distribution for all stations in this study are unimodal, with the center at 10 mph. The spread of the wind speed distribution is from 0 mph to 60 mph. The stations with the highest wind gust speeds are Sunnyside, Prosser N.E., and McWhorter; these stations are the lowest, center, and highest points of elevation in this study, respectively.

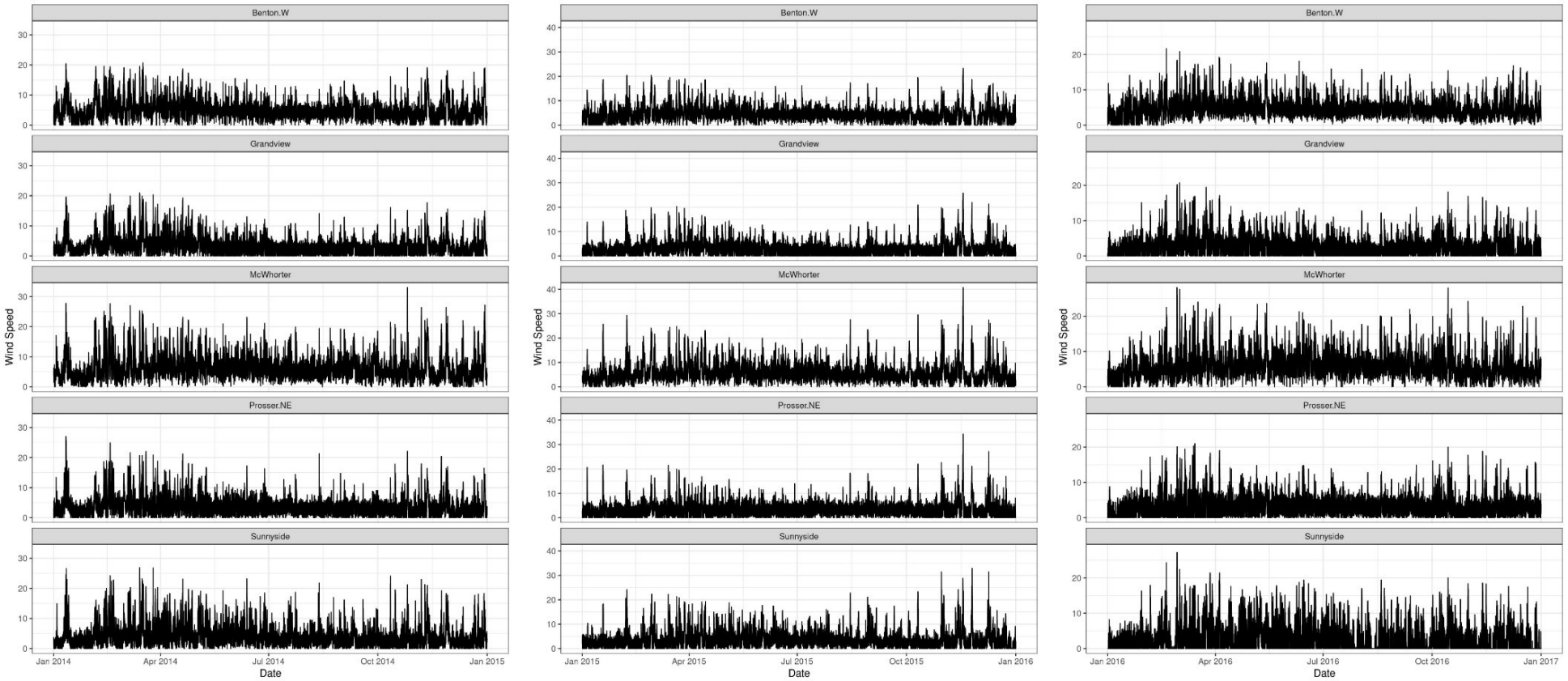

Figure 17: Observed 2014 - 2016 Wind Speed Time Plot Per Station.
These time plots are plotted as wind speed over time.

Figure 17a (Left): Observed 2014 Wind Speed Time Plot Per Station - Wind Speed Over Time. Little to no missing values are observed in 2014.

Figure 17b (Center): Observed 2015 Wind Speed Time Plot Per Station - Wind Speed Over Time. Little to no missing values are observed in 2015.

Figure 17c (Right): Observed 2016 Wind Speed Time Plot Per Station - Wind Speed Over Time. Missing values are observed in the month of January for Sunnyside, Prosser N.E., and McWhorter. Grandview is missing values in February. Sunnyside is missing additional values in March.

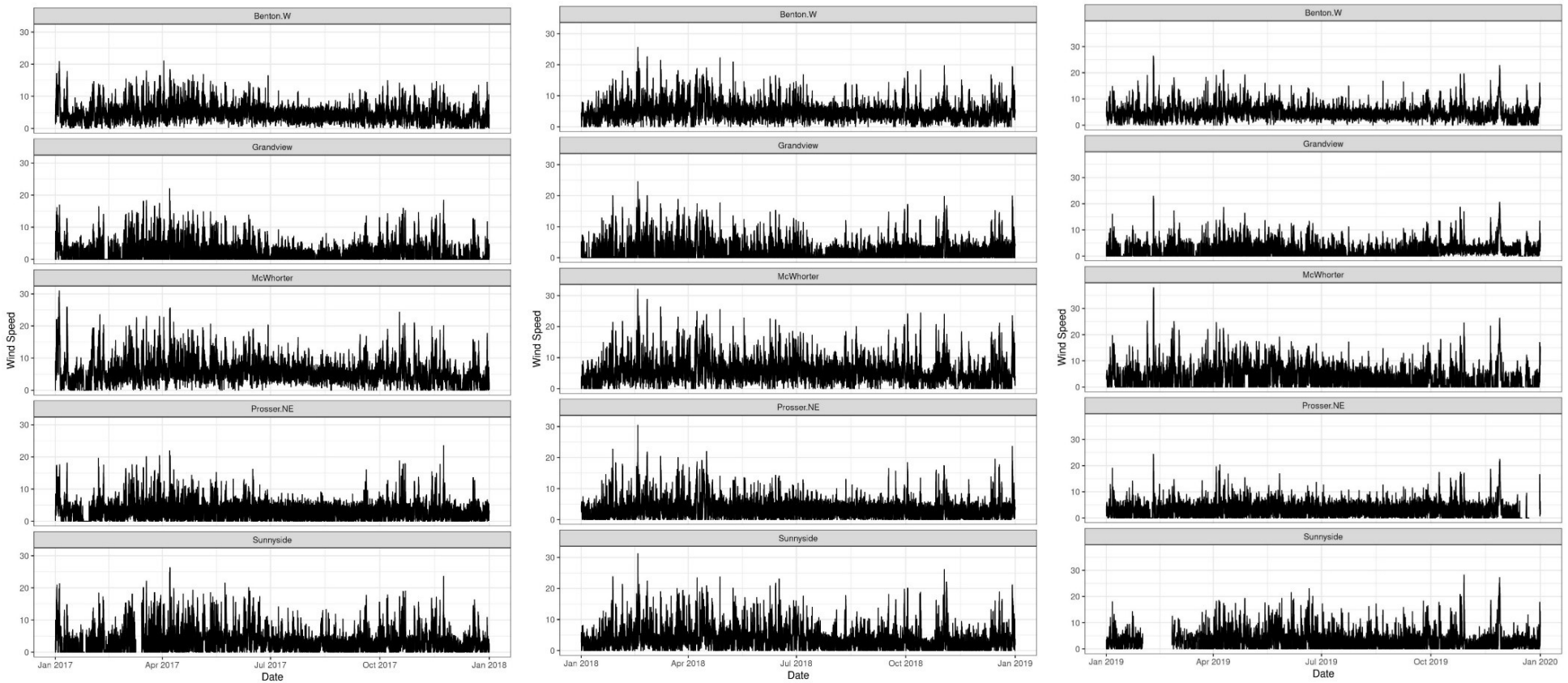

Figure 18: Observed 2017 - 2019 Wind Speed Time Plot Per Station.
These time plots are plotted as wind speed over time.

Figure 18a (Left): Observed 2017 Wind Speed Time Plot Per Station - Wind Speed Over Time. Missing values are observed the month of January for Sunnyside, Prosser N.E., and McWhorter. Grandview is missing values in the month of February, and Sunnyside for the month of March.

Figure 18b (Center): Observed 2018 Wind Speed Time Plot Per Station - Wind Speed Over Time. Little to no missing values are observed in this year.

Figure 18c (Right): Observed 2019 Wind Speed Time Plot Per Station - Wind Speed Over Time. Missing values are observed for Sunnyside in the months of February to March. Grandview, Prosser NE, and McWhorter are also missing values in the month of December.

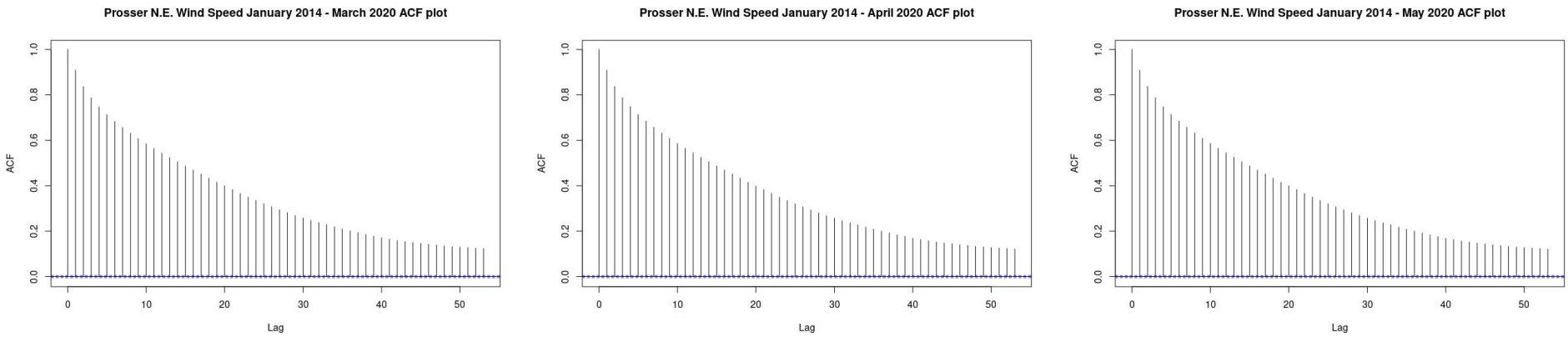

Figure 19: Wind Speed Correlograms at Prosser N.E. from January 2014 – May 2020.
These correlograms show the autocorrelations of the wind speed data (excluding wind gust data).

Figure 19a (Left): A correlogram showing the autocorrelation of the wind speed data (excluding wind gust data) at the Prosser N.E. Site from January 2014 to March 2020.

Figure 19 (Center): A correlogram showing the autocorrelation of the wind speed data (excluding wind gust data) at the Prosser N.E. Site from January 2014 to April 2020.

Figure 19 (Right): A correlogram showing the autocorrelation of the wind speed data (excluding wind gust data) at the Prosser N.E. Site from January 2014 to May 2020.

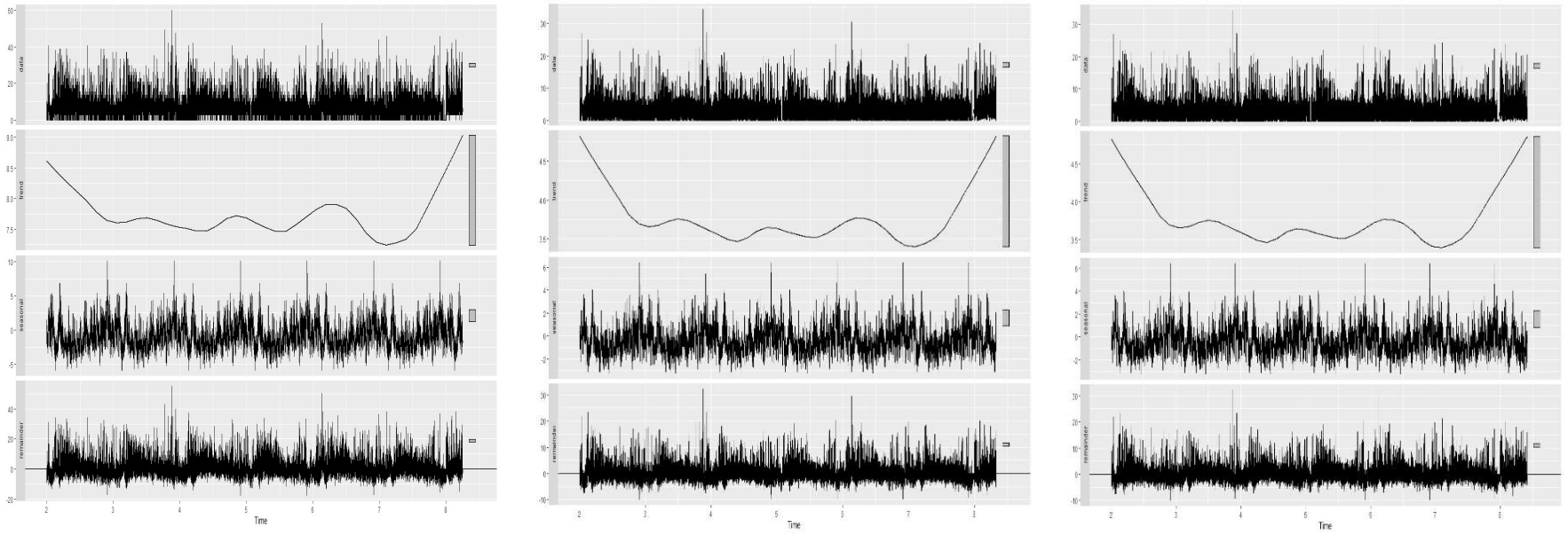

*Figure 20: Decomposition of Wind Speed Data at Prosser N.E. January 2014 to May 2020. These decomposition plots were created using the **stl** function from the R stats package. Note the remainders are the residuals.*

Figure 20a (Left): The wind speed patterns observed at the Prosser N.E. Station from January 2014 to March 2020 and its three additive components obtained from the STL decomposition with annual trend-cycle and seasonal trends.

Figure 20b (Center): The wind speed patterns observed at the Prosser N.E. Station from January 2014 to April 2020 and its three additive components obtained from the STL decomposition with annual trend-cycle and seasonal trends. NOTE: the remainders are the residuals.

Figure 20c (Right): The wind speed patterns observed at the Prosser N.E. Station from January 2014 to May 2020 and its three additive components obtained from the STL decomposition with annual trend-cycle and seasonal trends. NOTE: the remainders are the residuals.

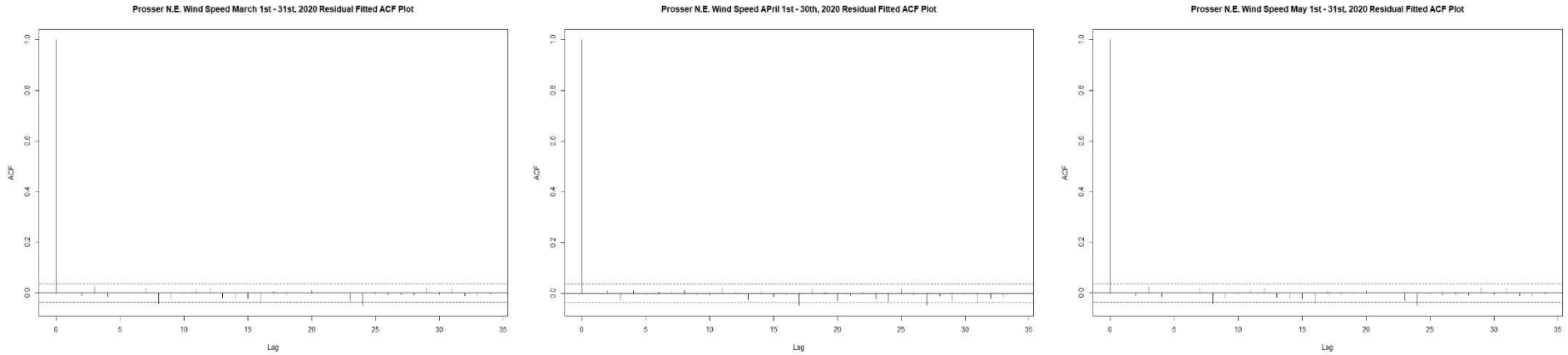

Figure 21: Wind Speed Correlograms at Prosser N.E. from March 1st – May 31st 2020.
These correlograms show the autocorrelations of the wind speed data (excluding wind gust data) after first differencing.

Figure 21a (Left): A correlogram showing the autocorrelation of the wind speed data (excluding wind gust data) at the Prosser N.E. Site from March 1st to March 31st, 2020, after first differencing.

Figure 21 (Center): A correlogram showing the autocorrelation of the wind speed data (excluding wind gust data) at the Prosser N.E. Site from April 1st to April 30th, 2020, after first differencing.

Figure 21 (Right): A correlogram showing the autocorrelation of the wind speed data (excluding wind gust data) at the Prosser N.E. Site from May 1st to May 31st, 2020, after first differencing.

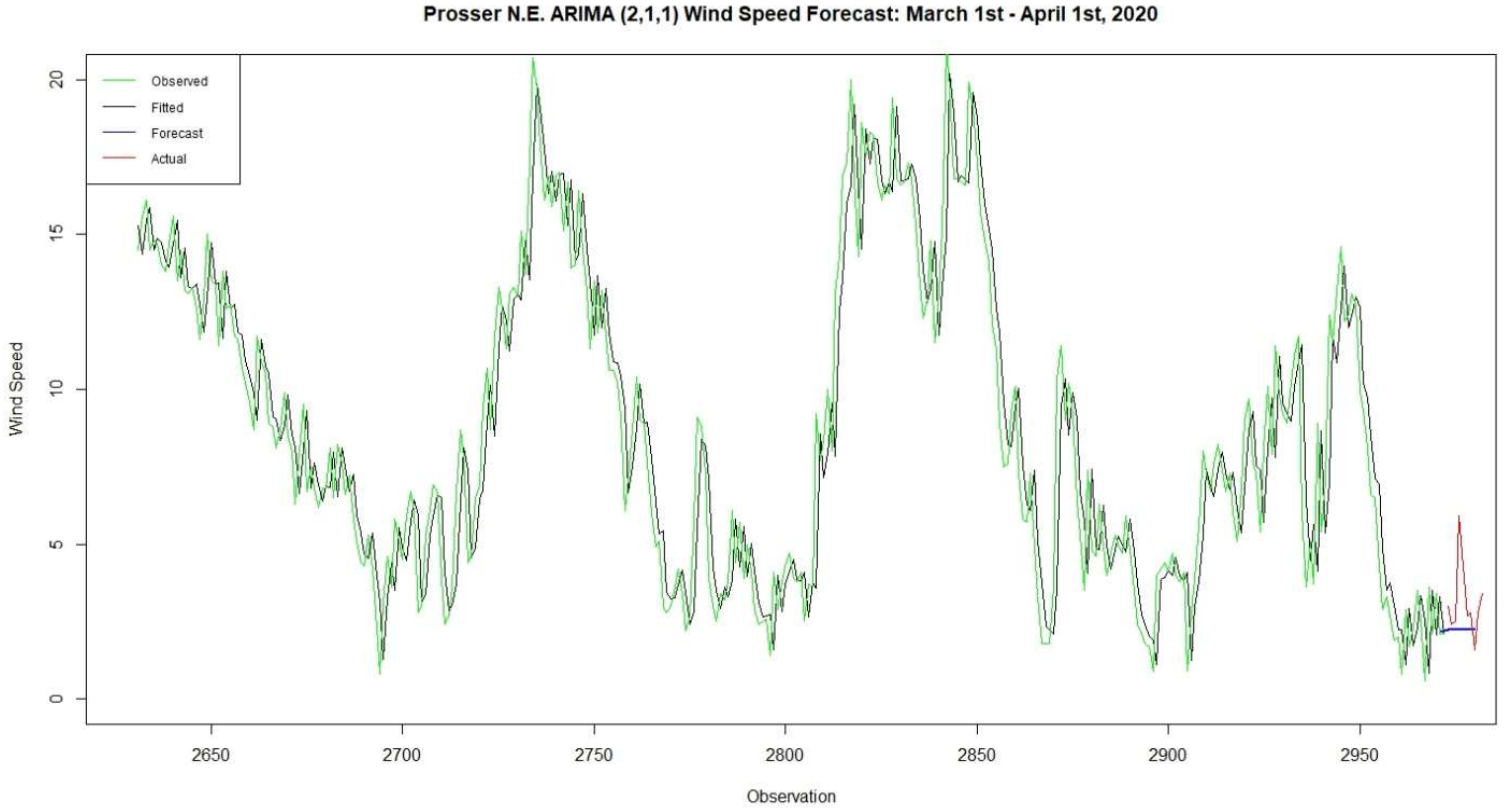

Figure 22: Prosser N.E. ARIMA (2,1,1) Wind Speed Forecast for March 1st - April 1st, 2020.
This ARIMA model was trained with and fitted with summarized 15-min averages of 5s readings from the AWN historical wind speed values (black line) at Prosser N.E. in Mach 2020. Each 15-min average counts as one observation, this time series consisted of 2971 observations or 2971 15-min averages from March 1st, 2020, to March 31st, 2020 (green line). We attempted to forecast the first 10 observations (2.5 hours) of April 1st, 2020 (blue line) and compared the ARIMA (2,1,1) calculated point forecasts to the historical AWN recorded wind speed measurements (red line). Descriptive statistics comparing the point forecasts from our model and the historical April 2020 wind speed measurements are explored in Table 5.

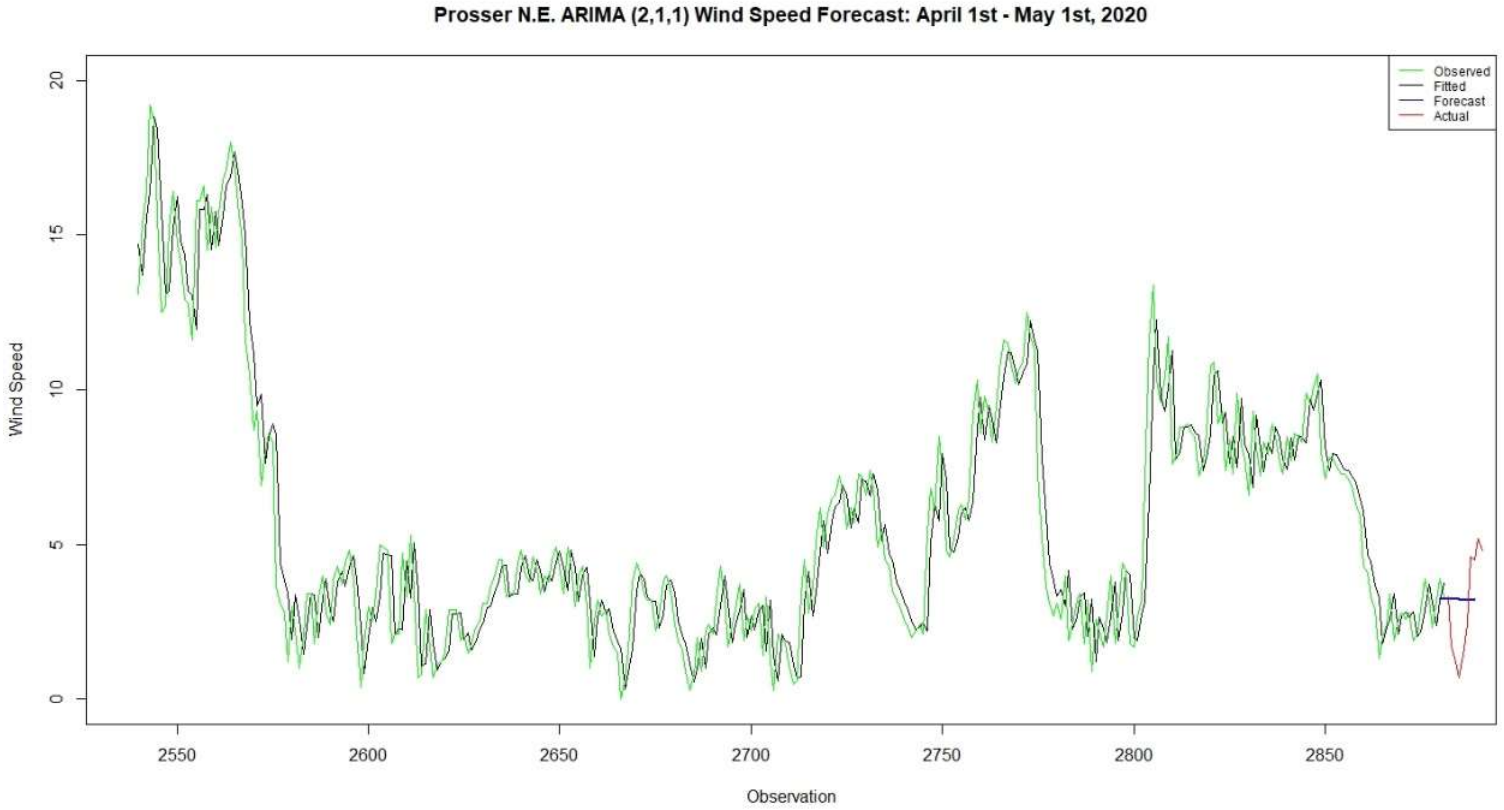

Figure 23: Prosser N.E. ARIMA (2,1,1) Wind Speed Forecast for April 1st - May 1st, 2020.
This ARIMA model was trained with and fitted with summarized 15-min averages of 5s readings from the AWN historical wind speed values (black line) at Prosser N.E. in April 2020. Each 15-min average counts as one observation, this time series consisted of 2880 observations or 2880 15-min averages from April 1st, 2020, to April 30th, 2020 (green line). We attempted to forecast the first 10 observations (2.5 hours) of May 1st, 2020 (blue line) and compared the ARIMA (2,1,1) calculated point forecasts to the historical AWN recorded wind speed measurements (red line). Descriptive statistics comparing the point forecasts from our model and the historical May 2020 wind speed measurements are explored in Table 6.

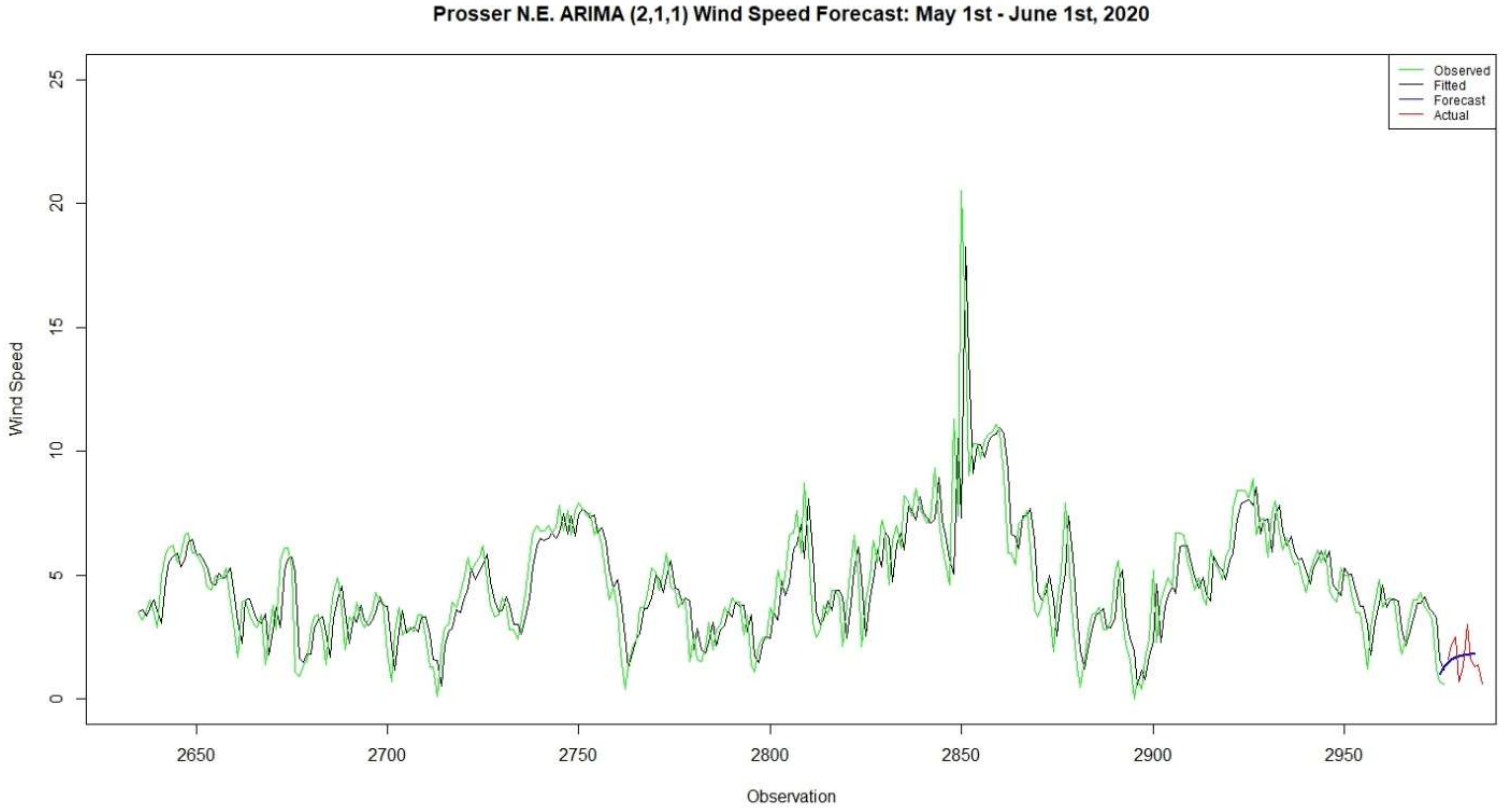

Figure 24: *Prosser N.E. ARIMA (2,1,1) Wind Speed Forecast for May 1st - June 1st, 2020.*
This ARIMA model was trained with and fitted with summarized 15-min averages of 5s readings from the AWN historical wind speed values (black line) at Prosser N.E. in May 2020. Each 15-min average counts as one observation, this time series consisted of 2975 observations or 2975 15-min averages from May 1st, 2020, to May 31st, 2020 (green line). We attempted to forecast the first 10 observations (2.5 hours) of June 1st, 2020 (blue line) and compared the ARIMA (2,1,1) calculated point forecasts to the historical AWN recorded wind speed measurements (red line). Descriptive statistics comparing the point forecasts from our model and the historical June 2020 wind speed measurements are explored in Table 7.

Forecast Window	Forecast Plot	Forecast ACF
Training Window: 500 April 22nd, 2020, 12:30 am – May 22nd, 2020, 11:15 pm **Forecast Window**: 2.5 hours Train RMSE: 1.25 Test RMSE: 0.88	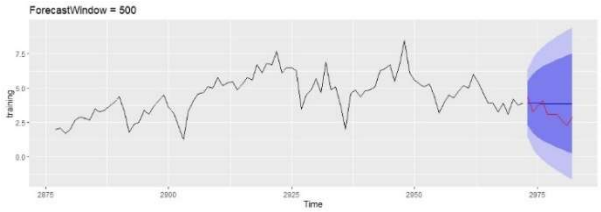	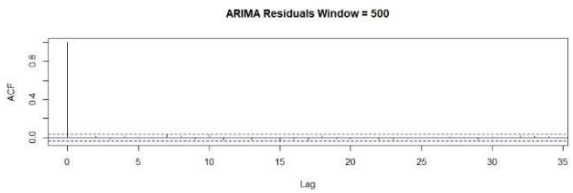
Training Window: 600 May 2nd, 2020, 10:30 am – June 2nd, 2020, 9:15 am **Forecast Window**: 2.5 hours Train RMSE: 1.18 Test RMSE: 1.02	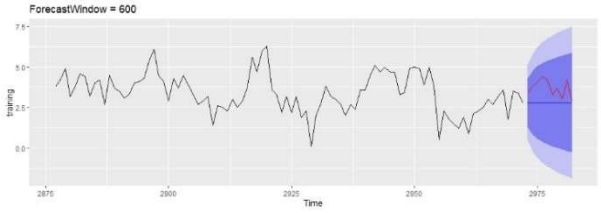	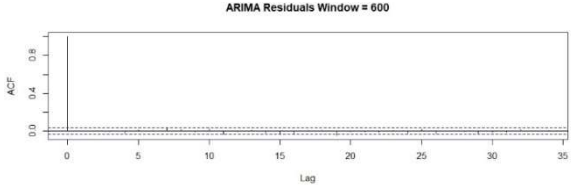
Training Window: 700 May 12th, 2020, 8:30 pm – June 12th, 2020, 7:15 pm **Forecast Window**: 2.5 hours Train RMSE: 1.12 Test RMSE: 0.80	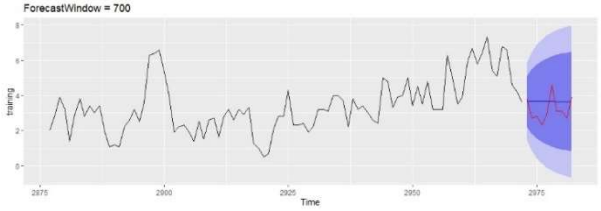	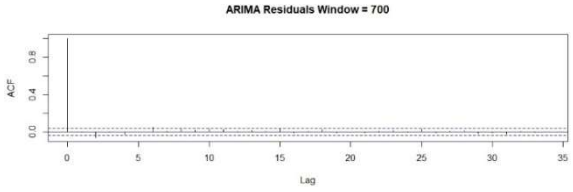
Training Window: 800 May 23rd, 2020, 6:30 am – June 23rd, 2020, 5:15 am **Forecast Window**: 2.5 hours Train RMSE: 1.08 Test RMSE: 0.76	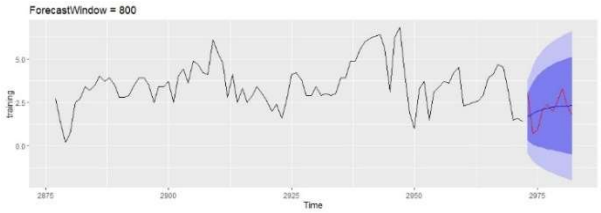	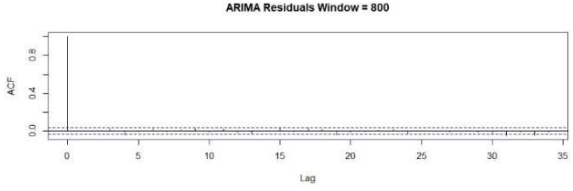

Figure 25: Four ARIMA (2,1,1) Forecast Windows.
Each simulation was trained on 30-days' worth of wind speed data and forecasted 2.5 hours. The dark blue is the 80% prediction interval, and the light purple is the 95% prediction interval. The blue line are the predicted values, and the red line is the observed data. The differenced ACF plot for each model is on the right.

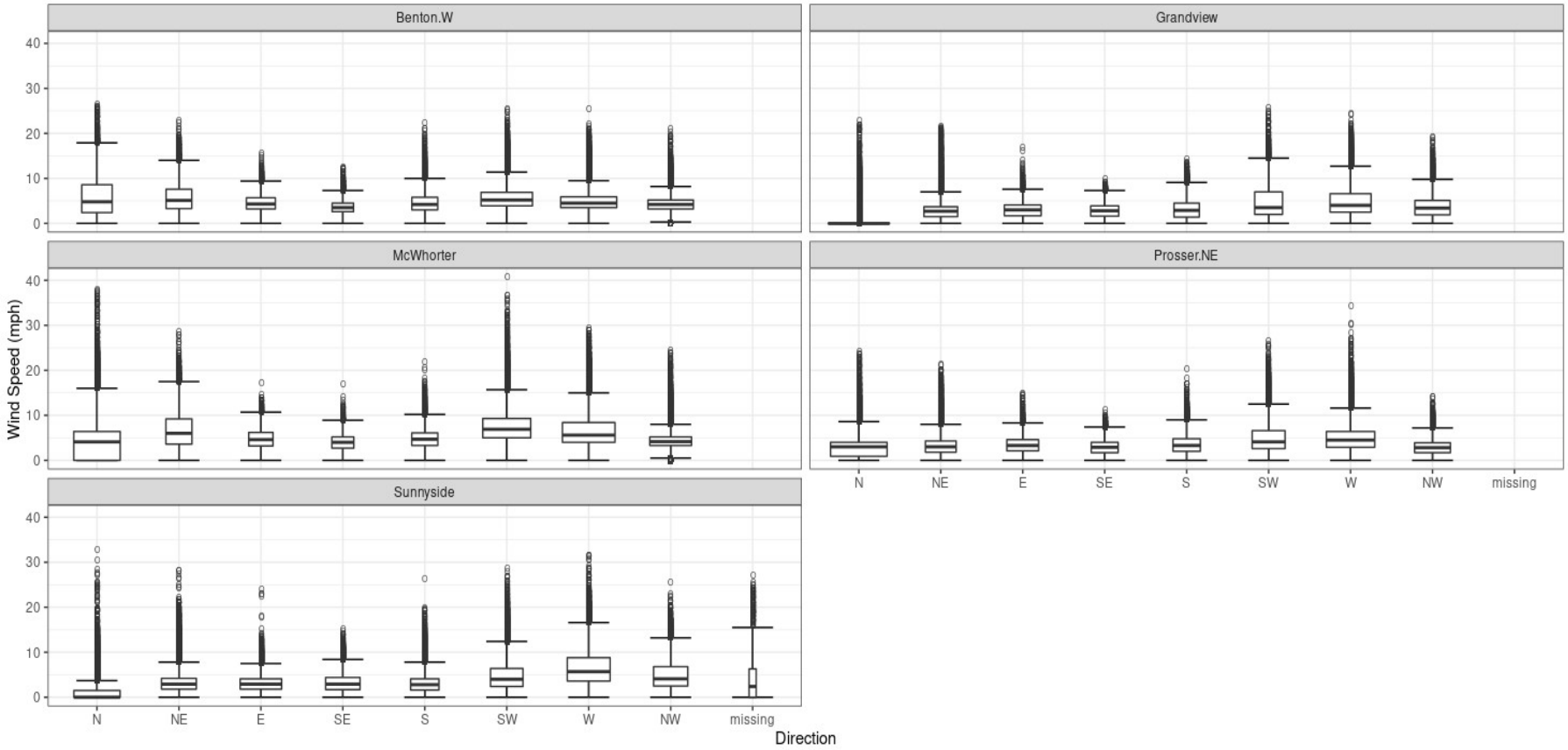

Figure 26: Boxplots comparing the distribution of wind speed directions from 2014 to 2019. The concept of time is detached from this directional analysis. The wind directions were discretized by degrees. North is from 337.5° to 22.5°. Northeast is from 22.5° to 67.5°. East is from 67.5° to 112.5°. Southeast is from 112.5° to 157.5°. South is from 157.5° to 202.5°. Southwest is from 202.5° to 247.5°. West is from 247.5° to 292.5°. Northwest is from 292.5° to 337.5°. The widths of the boxplots are related the number of observations.

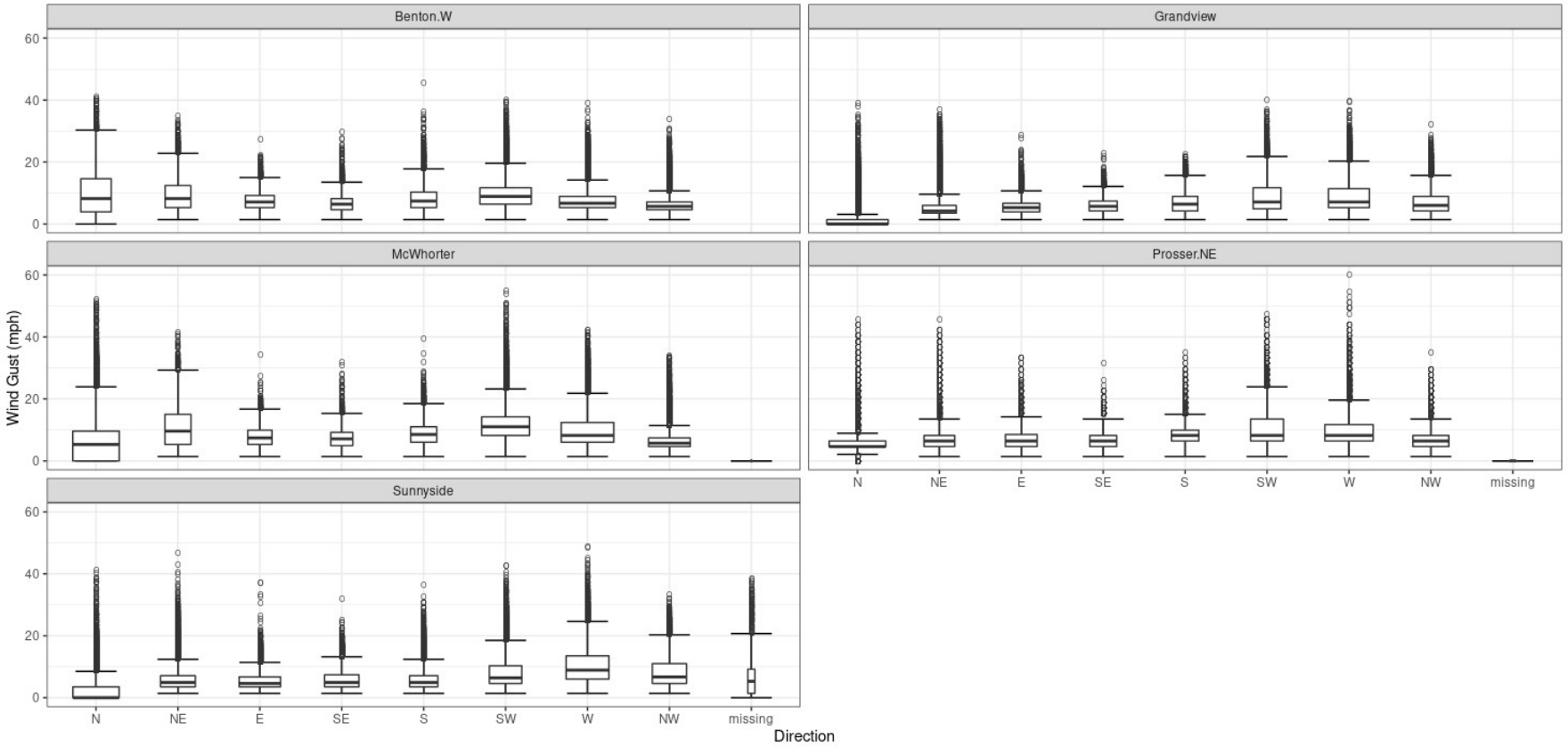

Figure 27: Boxplots comparing the distribution of wind gust directions from 2014 to 2019.
The concept of time is detached from this directional analysis. The wind directions were discretized by degrees. North is from 337.5° to 22.5°. Northeast is from 22.5° to 67.5°. East is from 67.5° to 112.5°. Southeast is from 112.5° to 157.5°. South is from 157.5° to 202.5°. Southwest is from 202.5° to 247.5°. West is from 247.5° to 292.5°. Northwest is from 292.5° to 337.5°. The widths of the boxplots are related the number of observations.

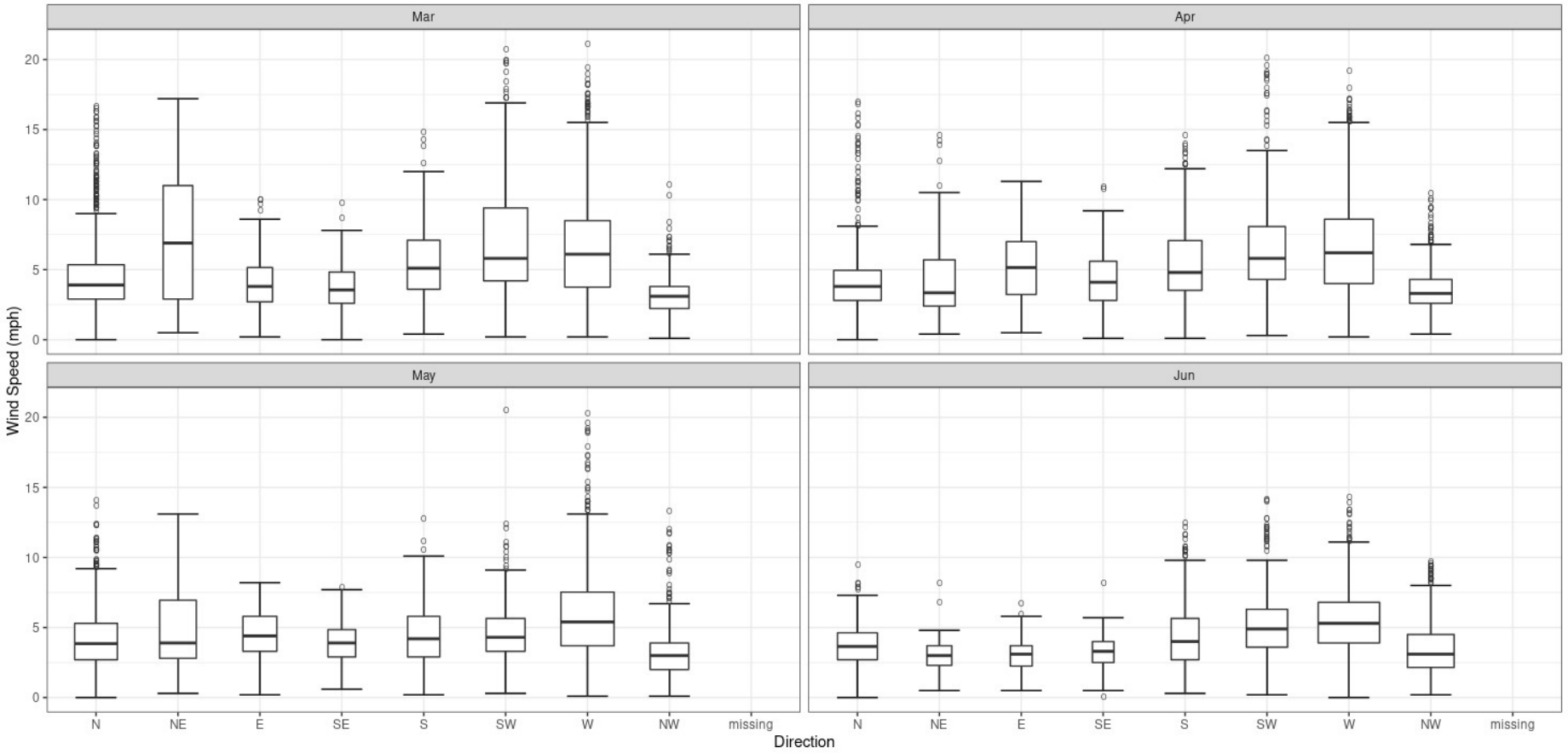

Figure 28: Boxplots comparing the distribution of wind speed directions at Prosser N.E.

We narrowed our scope to the months of spring that we used our ARIMA (2,1,1) model to forecast 2.5-hour wind speed predictions. *The wind directions were discretized by degrees. North is from 337.5° to 22.5°. Northeast is from 22.5° to 67.5°. East is from 67.5° to 112.5°. Southeast is from 112.5° to 157.5°. South is from 157.5° to 202.5°. Southwest is from 202.5° to 247.5°. West is from 247.5° to 292.5°. Northwest is from 292.5° to 337.5°.*

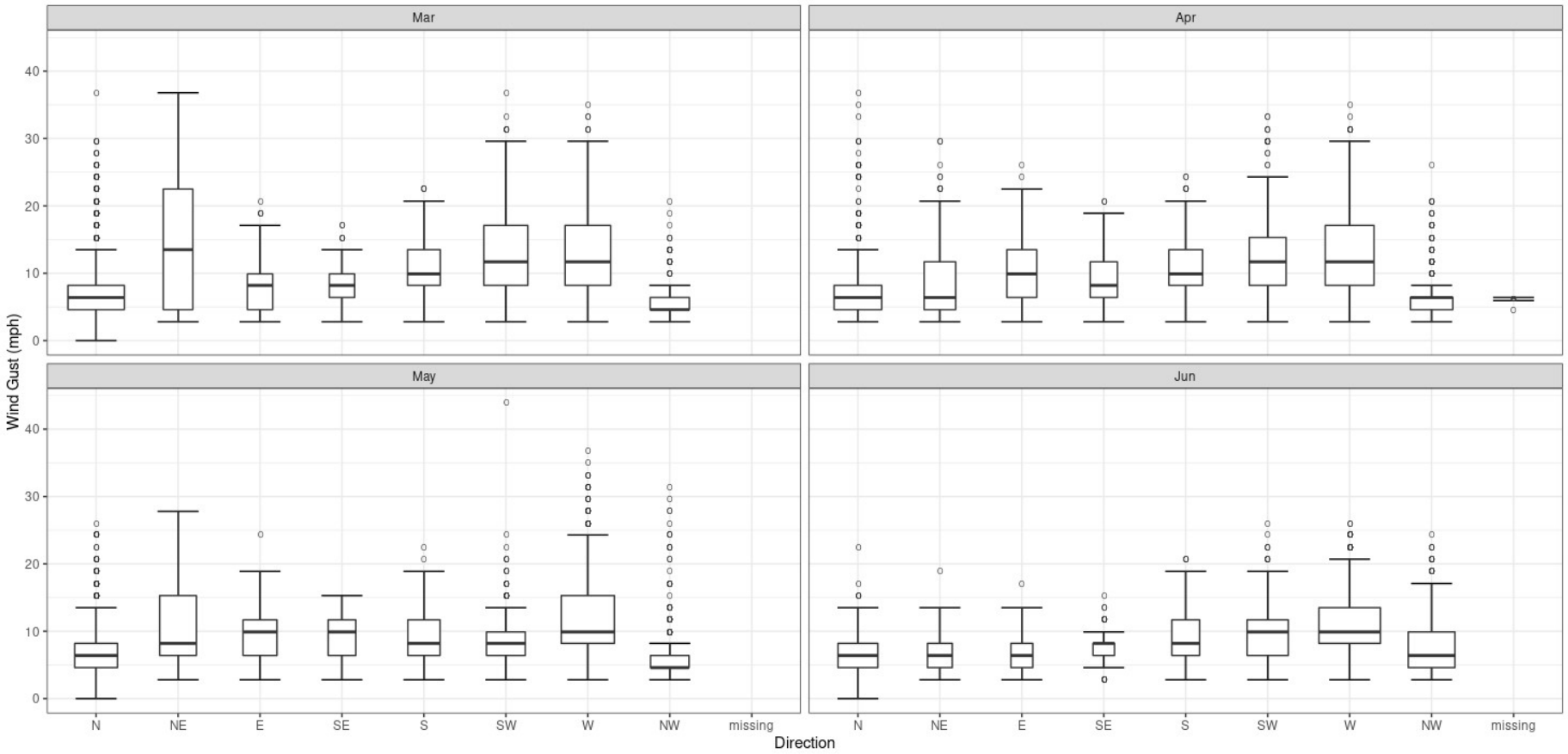

Figure 29: Boxplots comparing the distribution of wind speed directions at Prosser N.E.

We narrowed our scope to the months of spring that we used our ARIMA (2,1,1) model to forecast 2.5-hour wind speed predictions. *The wind directions were discretized by degrees. North is from 337.5° to 22.5°. Northeast is from 22.5° to 67.5°. East is from 67.5° to 112.5°. Southeast is from 112.5° to 157.5°. South is from 157.5° to 202.5°. Southwest is from 202.5° to 247.5°. West is from 247.5° to 292.5°. Northwest is from 292.5° to 337.5°.*

Discussion

Aim 1: Determine the necessary inputs for wind ramp modeling in agriculture

Aim 1a

This thesis applied wind ramp modeling, a concept from the wind energy industry, to forecast drift-prone wind conditions in agriculture. We first completed an exploratory analysis of the wind speed and wind gust in the study area (Tables 1, 2, 3, 4) between the years 2014 and 2019. As expected, the station (McWhorter) with highest elevation (1401 ft) and limited surrounding wind breaking barriers had the highest maximum wind speed and standard deviation values of 40.7 mph $\pm$ 4.0 mph (Table 1). Surprisingly, the station (Sunnyside) with the lowest elevation (690 ft) had the second highest wind speed value of 37.2 mph $\pm$ 3.7 mph (Table 1). The station (Grandview) with second highest elevation (972 ft) had the lowest maximum wind speed value of 25.8 mph $\pm$ 3.0 mph (Table 1). The distance between Sunnyside and Grandview stations was 7.9 miles (mi) with an elevation difference of 282 ft. The distance between Sunnyside and McWhorter was 19.2 mi with an elevation difference of 711 ft. The maximum wind speed difference between Sunnyside and Grandview was 11.4 mph, and the corresponding difference between Sunnyside and McWhorter was 3.5 mph. The larger difference in maximum wind speed alone between Sunnyside and Grandview versus Sunnyside and McWhorter indicated that wind speed profiles could change substantially within small distances.

When comparing wind speed and wind gust at each site, Prosser N.E., a station with moderation maximum wind speed values and moderate elevation had the highest maximum values for wind gust (Table 1). The Prosser N.E. station had an elevation of 827 ft, the center of the 670 square-mile study area with surrounding wind breaking barriers and objects, with an average and maximum wind speed values of 34.3 mph $\pm$ 2.9 mph and 3.8 mph $\pm$ 2.9 mph, respectively (Table 1). However, when stations were compared by their maximum wind gust values, we found that Prosser N.E. had the highest wind gust value of 60 mph $\pm$ 5.0 mph (Table 1). McWhorter and Sunnyside, the two stations with the highest wind speed values, had maximum wind gust values of 55 mph $\pm$ 5.8 mph, and 51.1 mph $\pm$ 5.3 mph (Table 1).

As expected, Table 2 showed more exceedances for wind gust than wind speed at each station. After setting wind speed thresholds of 10 mph, 15 mph, and 20 mph (Table 2), the relative exceedances (RE) (ratio of wind gust to wind speed count) for each station showed a non-linear increase (Table 2). Prosser N.E. had the highest RE values for each speed threshold (Table 2). At the federal and state regulation threshold of 10 mph, Prosser N.E. had 3.5 times as many exceedances using wind gusts than wind speed alone (Table 2). For a threshold of 15 mph, Prosser N.E. had 9.7 as many exceedances using wind gusts than wind speed alone and for a threshold of 20 mph, Prosser N.E. had 39.1 times as many exceedances with wind gust than wind speed alone (Table 2). A similar trend in the RE values is observed for Benton W. and Grandview (Table 2). While McWhorter and Sunnyside had the two lowest RE values for each speed threshold, which may indicate that sites with high maximum wind speed variable values will also have high

maximum wind gust values (Table 2). We believe the frequency of gusts can be linked to wind ramping. These trends can be further explored in a future study with a larger region.

Tables 3 and 4 investigate the duration of the exceedances for each threshold in Table 2. It is important to note that the meteorological data received from WSU AWN was structured as 15-minute averages of 5 s readings and therefore generated equal-length time intervals that ranged from 30 minutes to 240 minutes (4 hours) and or greater. Also, the wind energy industry defines wind gust as a brief (less than 20 seconds) increase in speeds that reach at least 18.4 mph and vary in 10 mph between the peak and lulls. However, WSU AWN researchers define wind gust as the maximum 5-second sampled wind speed over a 15-minute interval measured at a height of 2 meters. Given the 15-minute time intervals that structured our data we could not compare wind gusts to wind ramps that lasted longer than 20 seconds and less than 15 minutes in duration. However, we were able to evaluate wind exceedances or wind ramp events that occurred sequentially within 15-minute time intervals. This is important because this data structure can allow us to explore the prediction of wind ramp events using the frequency of wind gust exceedances.

Wind speed exceedances above 10 mph are frequent and can last from 18 hours to 32 hours in duration for the wind speed variable and from 31 hours to approximately 3 days for the wind gust variable across all stations (Tables 2, 3, 4). Wind speed exceedances above 20 mph do occur but not as often and did not last as long in duration when compared to 10 mph exceedances (Tables 2, 3, 4). The 20 mph exceedances ranged from 3.25 hours to 16.5 hours for the wind speed variable and 17.5 hours to approximately 27 hours for the wind gust variable across all stations (Tables 2, 3, 4). We found that wind speed exceedances centered around 15 mph were not as frequent as the exceedances above 10 mph but occurred more often than 20 mph exceedances (Table 2). Fifteen mile per hour exceedances had a duration of 12 hours to 1 day in duration across all stations for the wind speed variable (Tables 3, 4). While 15 mph exceedances for the wind gust variable lasted from 31 hours to 33.75 hours for all stations (Tables 3, 4). This information can guide WSU AWN and DEOHS researchers on which speed threshold is best to alert tree fruit growers and develop a binary notification system for spray applicators to follow.

Scope: Prosser N.E. and Wind Speed Variable

We were able to forecast future wind speed values on a short-term timescale to alert growers 2.5-hours ahead of drift-prone wind conditions. The Prosser N.E. site has less variable wind speeds, moderate to high maximal wind speeds that represents farms with high pesticide cases and a high RE value for each wind exceedance threshold and moderate run times (Tables 1, 2, 3, 4). We narrowed the scope of forecasting to the months of April 2020, May 2020, and June 2020 at the Prosser N.E. station to best represent spray application timelines, farmworker activity, and historical pesticide illness cases in the Yakima Valley.

Aim 1b and 1 c

When we began this analysis, we were unaware of how much historical data was required to predict future wind speed values. The wind ramping literature informed us that wind speed is a known non-stationary time series and recommended the decomposition of our wind speed time series. The decomposition components allowed us to visualize the cyclic and seasonal trends at our five stations but required a minimum of three years of historical wind speed data. Moving forward researchers could run the **auto.arima** function on a month of less time of historical values and will likely get a differencing order of zero, indicating stationarity. An ACF plot should be used to verify this assumption.

Aim 1d

From the wind direction analysis, we learned that the most prevailing wind direction is not associated with most wind ramps. The most prevailing wind direction came from the north at Prosser N.E. (Tables 11) (Figures 26). Winds from west had the most wind exceedances and maximum wind speeds at Prosser N.E. (Table 11) (Figure 26). Less than 10 miles away at the Grandview station the most prevailing wind direction and most observed wind ramps came from the north (Table 11) (Figure 26). However, the maximal wind speeds were from the southwest at the Grandview station (Table 11) (Figure 26). This information is important because we now know that the most prevailing wind direction is not associated with the most wind ramps, which varies per station that are less than 10 miles apart in distance. Indicating that wind ramp models should be specific to each site. Also, when pesticide applicators are deciding whether to spray pesticides on a given day, they should use wind data that is most specific to their tree-fruit orchard and should not rely on distance alone.

Aim 2: Apply the model

We hypothesized that wind ramp modeling would be an effective tool for predicting wind ramps events and provide critical binary alerts, (yes, it is okay to spray pesticides, or no, it is not okay to spray pesticides), that inform growers of significant wind ramp events that will impact public health. To evaluate our ARIMA (2,1,1) and ARIMA (4,1,2) model we ran 800 forecasts and plotted a distribution of their RMSEs (Results Figure 25, Appendix 1: Figure 9). The lowest variability between our calculated point forecast and actual observed wind speed values was 0.27 (Table 9) (Appendix 1: Figure 9). The greatest variability between our calculated point forecast and actual observed wind speed values was 8.57 (Table 9) (Appendix 1: Figure 9). The fit of our ARIMA (2,1,1) and ARIMA (4,1,2) varies per moment in time, possibly indicating that an effective prediction tool of wind ramps is not only specific to geographical location but also to time of year.

Limitations

Missing Values

Our data selection had limitations. When performing time series analysis, one needs to consider the following to reduce uncertainty in forecasting: the choice of model for the historical data and the continuation of the historical data. Statistical time series concerned with random or sudden changes in observations rely on statistical theories that observations are usually not independent, and the analysis must consider the time order of the observations. Wind speed is a known stochastic

time series, the future is only partly determined by past values. Stochastic time series predictions rely on the idea that future values have a probability distribution, which is conditioned on the knowledge of past values. There are no algebraic solutions for long periods of missing historical data from sensors that were frozen in cold and wet weather. However, our model was able to provide 2.5-hour forecasts with single-months' worth of data.

Data Structure

The meteorological data received from WSU AWN was structured as 15-minute averages of 5 s readings. This limited our evaluation of wind ramp events that lasted greater than 20 seconds and less than 15 minutes. Also, it would be of interest to evaluate the difference in ARIMA forecasting that occurs when training a model with un-summarized data versus the 15-minute averaged data we received from AWN.

Future Research

Data Collection

Future Research should aim to replicate and improve on our study. For one, selecting data that is not convoluted into 15-min averaged time periods will allow for the comparison of wind gusts to wind ramp events greater than 20 seconds and less than 15-minutes. Also, deconvoluted data may provide may improve accuracy of the single point calculated forecast values because the ARIMA model will be trained on un-averaged time intervals. The ARIMA (2,1,1) model used in this study predicts an average that either overestimated or underestimated decreases and increases in wind speed, respectively. Forecasting a mean is acceptable for our application however, we would rather overestimate the mean of drift-prone wind conditions to prevent pesticide drift exposure in farmworkers. A follow-up study should also consider the use of multiple or more robust meteorological measurement recording devices that withstand cold and wet environmental conditions to reduce the missingness of week to months long periods of data to improve forecast model training and prediction accuracy.

Future Directions

Future studies should bypass the decomposition step outlined in our methods and focus on determining the order of ARIMA coefficients (p, d, q) with days to one month worth of data. Variant ARIMA models coupled machine learning or GARCH models should be considered to improve daily and sub-daily forecasting. These ARIMA variants are known as seasonal ARIMA (SARIMA) and fractional-ARIMA (f-ARIMA), respectively (Chatfield et al., 2004; Dhiman et al., 2020). Another model to consider is a Generalized Auto-Regressive Conditional Heteroskedascticinty (GARCH) model. A GARCH model is also a statistical model used to analyze and forecast volatility. University of Washington biostatical researchers have used GARCH models to capture and forecast large spikes in atmospheric data from rain to wind (Cardoso et al., 2007, Hamer et al., 2021).

Public Health Implications

The statistics of this thesis can inform growers, pesticide applicators and farmworkers of important wind patterns throughout the agricultural growing season. Pesticide spraying schedules and farmworker activity can be guided by AWN-powered forecast that are specific to each orchard to prevent pesticide related illness. The Washington State Pesticide Application Safety Committee can explore methods to improve current practices by utilizing AWN platform to get geo-specific wind data and accurate short-term forecasts. The EPA should also consider updating pesticide labels on how and where to get wind information.

Conclusion

Accurate short-term wind forecasting techniques are necessary to minimize the adverse health and environmental outcomes associated with pesticide drift. To our knowledge, this was the first study that utilized historic wind data to build a wind forecast model tailored to specific times and locations of pesticide applications. We demonstrated that wind speed profiles could change substantially within short distances. Also, prior to this work we did not know that most prevailing wind direction was not associated with the most wind ramps. We anticipate that these findings will inform best practices for pesticide applicator training, provide evidence for state policy discussions, and contribute to administrative and engineering controls using the precision agriculture framework.

References

Aicher L., Wilks M.F. (2021b). *Chapter 1 - From risk assessment to regulation*. Exposure and Risk Assessment of Pesticide Use in Agriculture. Academic Press, 3-23.

Ali, S., Cooper, R., Cylinder, Mia., Driggers, P.E., Graham, L.S., Ha, J., Hernandez, B., Nonato, Y.V., Oriel, M.S., Pabla, J., Richmond, D. (2019). *Summary Results from the California Pesticide Illness Surveillance Program – 2016*. California Environmental Protection Agency, Department of Pesticide Regulation, Worker Health and Safety Branch. https://www.cdpr.ca.gov/docs/whs/pisp/2016/2016summary_complete.pdf

Bailey, H., Fritschi, L., Infante-Rivard, C., Glass, D., Miligi, L., Dockerty, J., . . . Schüz, J. (2014). Parental occupational pesticide exposure and the risk of childhood leukemia in the offspring: Findings from the childhood leukemia international consortium. International Journal of Cancer, 135(9), 2157-2172.

Baldi, I., Lebailly, P., Bouvier, G., Rondeau, V., Kientz-Bouchart, V., Canal-Raffin, M., & Garrigou, A. (2014). Levels and determinants of pesticide exposure in vineyards: Results of the PESTEXPO study. Environmental Research, 132, 360-369.

Bassil, K., Vakil, C., Sanborn, M., Cole, D., Kaur, J., & Kerr, K. (2007). Cancer health effects of pesticides - Systematic review. Canadian Family Physician, 53, 1705-1711.

Brown, B., Katz, R., & Murphy, A. (1984). *Time Series Models to Simulate and Forecast Wind Speed and Wind Power*. Journal of Climate and Applied Meteorology, 23(8), 1184-1195.

Butler Ellis, M., Kennedy, M., Kuster, C., Alanis, R., & Tuck, C. (2018). *Improvements in Modelling Bystander and Resident Exposure to Pesticide Spray Drift: Investigations into New Approaches for Characterizing the 'Collection Efficiency' of the Human Body*. Annals of Work Exposures and Health, 62(5), 622-632.

Calvert, G., Rodriguez, L., & Prado, J. (2015). *Worker Illness Related to Newly Marketed Pesticides —*
Douglas County, Washington, 2014. MMWR. Morbidity and Mortality Weekly Report, 64(2), 42-44.

Cardoso P. T., Guttorp P. 2007. *A Hierarchical Bayes Model for Combing Precipitation Measurements from Different Sources*. Technical Report Series no. 082.

Carson, R. J., Tolan, I. L., and S. Reidel. 1987. Geology of the Vantage area, south-central Washington: An introduction to the Miocene flood basalts, Yakima fold belt, and the Channeled Scabland. In GSA Centennial Field Guide: Cordilleran Section, ed. M. Hill, p. 357-62.

Carta, J.A., Ramirez, P. & Velazquez, S., 2009. A review of wind speed probability distributions used in wind energy analysis Case studies in the Canary Islands. Renewable & sustainable energy reviews, 13(5), pp.933–955.

Chaplin-Kramer, R., Dombeck, E., Gerber, J., Knuth, K.A., Mueller, N.D., Mueller, M., Ziv, G., Klein, A.-M., 2014. *Global malnutrition overlaps with pollinator-dependent micronutrient production*. 20141799–20141799 Proc. Roy. Soc. B 281. https://doi.org/10.1098/rspb.2014.1799.

Chatfield, C., Haipeng, X. 2004. The Analysis of Time Series: an introduction 6th ed., Boca Raton, FL: CRC Press. Kindle Edition.

Chen, J., Shi, H., Sivakumar, B., & Peart, M. (2016). *Population, water, food, energy and dams*. Renewable & Sustainable Energy Reviews, 56, 18-28.

Centner, T., Colson, G., & Lawrence, A. (2014). *Assigning liability for pesticide spray drift*. Land Use Policy, 36, 83-88.

Cleveland, R. B., Cleveland, W. S., McRae, J. E., & Terpenning, I. J. (1990). STL: A seasonal-trend decomposition procedure based on loess. Journal of Official Statistics, 6(1), 3–33.

Costa L.G. (2021). *Chapter 22: Toxic effects of pesticides*. Klaassen C.D., & Watkins J.B., III(Eds.), Casarett & Doull's Essentials of Toxicology, 4e. McGraw Hill.

Courshee, R. (1959). *Drift Spraying for Vegetation Baiting*. Bulletin of Entomological Research, 50(2), 355-370.

Dai, M., Euling, S., Phillips, L., & Rice, G. (2021). *ExpoKids: An R-based tool for characterizing aggregate chemical exposure during childhood*. Journal of Exposure Science & Environmental Epidemiology, 31(2), 233-247.

DeFries, R.S., Foley, J.A. & Asner, G.P., 2004. Land-Use Choices: Balancing Human Needs and Ecosystem Function. Frontiers in ecology and the environment, 2(5), pp.249–257.

Desmarteau, D., Ritter, A., Hendley, P., & Guevara, M. (2020). Impact of Wind Speed and Direction and Key Meteorological Parameters on Potential Pesticide Drift Mass Loadings from Sequential Aerial Applications. Integrated Environmental Assessment and Management, 16(2), 197-210.

Dhiman, H., Deb, Dipankar, & Balas, Valentina Emilia. (2020). *Supervised machine learning in wind forecasting and ramp event prediction* (Wind energy engineering series). London, United Kingdom: Academic Press.

Eilers, E.J., Kremen, C., Smith Greenleaf, S., Garber, A.K., Klein, A.-M., 2011. *Contribution of*

pollinator-mediated crops to nutrients in the human food supply. PLoS ONE 6, e21363. https://doi.org/10.1371/journal.pone.0021363.

Ellis, E.C. et al., 2010. Anthropogenic transformation of the biomes, 1700 to 2000. Global ecology and biogeography, p.no.

Ellis, E., Klein Goldewijk, K., Siebert, S., Lightman, D., & Ramankutty, N. (2010). *Anthropogenic transformation of the biomes, 1700 to 2000*. Global Ecology and Biogeography, 19(5), 589-606.

Ellis, A.M., Myers, S.S., Ricketts, T.H., 2015. *Do pollinators contribute to nutritional health?* PLoS ONE 10. https://doi.org/10.1371/journal.pone.0114805 e114805–e114805.

Fenske, R., & Risk Reduction Engineering Laboratory. (1993). *Fluorescent tracer evaluation of protective clothing performance*. Cincinnati, OH: Risk Reduction Engineering Laboratory, Office of Research and Development, U.S. Environmental Protection Agency.

Field, C., Tilman, D., DeFries, R., Montgomery, D.R., Gleick, P., Frumkin, H., Landrigan, P. (2020). *Chapter 4: A Changing Planet*. Planetary health: Protecting nature to protect ourselves. Island Press.

Finnigan, J.J., Brunet, Y., Coutts, M., Grace, J. (1995). *Chapter 1 – Turbulent Airflow in Forests on Flat and Hilly Terrian*. Wind and trees. Cambridge; New York, NY, USA: Cambridge University Press.

Food and Agriculture Organization of the United Nations (FAO). (2020a). *Guidelines for personal protection when handling and applying pesticides*. Retrieved December 19, 2021, from https://www.fao.org/documents/card/en/c/ca7430en/

Food and Agriculture Organization of the United Nations (FAO). (2020b). *Main Topics*. Food and Agriculture Organization of the United Nations. Retrieved December 7, 2021, from https://www.fao.org/home/en

Food and Agriculture Organization of the United Nations (FAO). (2021). *Worker Hazard Assessment*. Pesticide Registration Toolkit. Retrieved December 19, 2021, from https://www.fao.org/pesticide-registration-toolkit/registration-tools/assessment-methods/method-detail/en/c/1187108/

Frumkin, H., Haines, A. (2020). *Chapter 7: Global Environmental Change and*

Noncommunicable Disease Risks. Planetary health: Protecting nature to protect ourselves. Island Press.

Garcia-Santos, G. (2021). *Chapter 12 - Review: Use of tracers to assess pesticide drift exposure in soil and human*. Exposure and Risk Assessment of Pesticide Use in Agriculture, Academic Press, 283-327.

Goldewijk, K.K. et al., 2017. Anthropogenic land use estimates for the Holocene - HYDE 3.2. Earth system science data, 9(2), pp.927–953.

Gore, A., Chappell, V., Fenton, S., Flaws, J., Nadal, A., Prins, G., . . . Zoeller, R. (2015). *EDC-2: The Endocrine Society's Second Scientific Statement on Endocrine-Disrupting Chemicals*. Endocrine Reviews, 36(6), E1-E150.

Goumenou, M., Renieri E.A., Petrakis D., Nathanail A.V., Kokaraki V., Tsatsakis A. (2021). *Chapter 14 - Methods for environmental monitoring of pesticide exposure*. Exposure and Risk Assessment of Pesticide Use in Agriculture. Academic Press, 347-387.

Greaves, B., Collins, J., Parkes, J., & Tindal, A. (2009). *Temporal Forecast Uncertainty for Ramp Events*. Wind Engineering, 33(4), 309-319.

Graphical.weather.gov. (n.d.). *Wind Gust Definition*. Retrieved December 19, 2021, from https://graphical.weather.gov/definitions/defineWindGust.html.

Hamer, T.E. et al., 2021. Influence of local weather on collision risk for nocturnal migrants near an electric power transmission line crossing Kittatinny Ridge, New Jersey. The Wilson journal of ornithology, 133(2), pp.190–201.

Hannah, P., Palutikof, J.P., Quine, C.P., Coutts, M., Grace, J. (1995). *Chapter 6 – Predicting Windspeeds for Forest Areas in Complex Terrain*. Wind and trees. Cambridge; New York, NY, USA: Cambridge University Press.

Haslett, J. 1997. On the sample variogram and the sample autocovariance for non-stationary time series. The Statistician, 46, 475-485. [13.7.8]

Herrero, M. et al., 2017. Farming and the geography of nutrient production for human use: a transdisciplinary analysis. The Lancet. Planetary health, 1(1), pp.e33–e42.

Herrington P, Mapother H, Stringer A. (1981) Spray retention and distribution on apple trees. Pestic Sci; 12: 515–20.

Hope, J. (2013) *What is CERCLA and why is it Important?* HAZARDOUS WASTE EXPERTS

Retrieved December 16, 2021, from http://www.hazardouswasteexperts.com/what-is-cercla-and-why-is-it-important-2.

Hu H, Wang L, Tao R (2021) *Wind speed forecasting based on variational mode decomposition and improved echo state network*. Renew Energy 164:729–751.

Hyndman, R.J. & Athanasopoulos, G., 2018. Foreacsting: Principles and Practice, 2nd Edition. OTexts: Melbourne, Australia.

Hyndman, R.J. & Khandakar, Y., 2008. Automatic time series forecasting: The forecast package for R. Journal of statistical software, 27(3), pp.1–22.

Intergovernmental Science-Policy Platform on Biodiversity and Ecosystem Services (IPBES). (2016). *The assessment report of the Intergovernmental Science-Policy Platform on Biodiversity and Ecosystem Services on pollinators, pollination, and food production*. Secretariat of the Intergovernmental Science-Policy Platform on Biodiversity and Ecosystem Services, Bonn, Germany. https://ipbes.net/sites/default/files/downloads/pdf/2017_pollination_full_report_book_v12_pages.pdf

Jiao-jun, Z., Xiu-fen, L., Yutaka, G., & Takeshi, M. (2004). *Wind profiles in and over trees*. Journal of Forestry Research, 15(4), 305-312.

Kasner, E.J. & Fenske, Richard A., 2017. On preventing farmworker exposure to pesticide drift in Washington orchards, Seattle]: University of Washington.

Kasner, E., Fenske, R., Hoheisel, G., Galvin, K., Blanco, M., Seto, E., & Yost, M. (2020). *Spray Drift from Three Airblast Sprayer Technologies in a Modern Orchard Work Environment*. Annals of Work Exposures and Health, 64(1), 25-37.

Kasner, E., Prado, J., Yost, M., & Fenske, R. (2021). *Examining the role of wind in human illness due to pesticide drift in Washington state, 2000-2015*. Environmental Health, 20(1), 26-15.

Khan, M., Costa, F., Fenton, O., Jordan, P., Fennell, C., & Mellander, P. (2020). *Using a multi-dimensional approach for catchment scale herbicide pollution assessments*. The Science of the Total Environment, 747, 141232.

Klaassen, C., & Watkins, John B. (2021). *Casarett & Doull's essentials of toxicology* (Fourth ed.). New York: McGraw Hill.

Klass, A. (2005). Bees, Trees, Preemption, and Nuisance: A New Path to Resolving Pesticide

Land Use Disputes. Ecology Law Quarterly, 32(4), 763-820.

Kuster, C., Hewitt, N., Butler Ellis, C., Timmermann, C., & Anft, T. (2021). *Measurements of the dermal exposure to bystanders from direct off-crop drift during the application of plant protection products*. Annals of Applied Biology, 179(1), 123-133.

Langenbach, T., Mager, A., Campos, M., De Falco, A., Aucélio, R., Campos, T., & Caldas, L. (2021). *The use of hedgerows to mitigate pesticide exposure of a population living in a rural area*. Integrated Environmental Assessment and Management, Integrated environmental assessment and management, 2021-06-14.

Lee, J., Hwang, I., Kim, J., Moon, H., Kim, K., Park, S., . . . Hong, S. (2015). *Common Pesticides Used in Suicide Attempts Following the 2012 Paraquat Ban in Korea*. Journal of Korean Medical Science, 30(10), 1517-1521.

Lee, S., Mehler, L., Moraga-Mchaley, S., Gergely, R., Calvert, G., Beckman, J., . . . Mitchell, Y. (2011). *Acute Pesticide Illnesses Associated with Off-Target Pesticide Drift from Agricultural Applications: 11 States, 1998-2006*. Environmental Health Perspectives, 119(8), 1162-1169.

Lehman-McKeeman, L. D. (2010). *Chapter 5. Absorption, Distribution, and Excretion of Toxicants*. In C. D. Klaassen & J. B. Watkins (Eds.), Casarett & Doull's Essentials of Toxicology, 2e (Vols. 1–Book, Section). New York, NY: The McGraw-Hill Companies.

Lesmes-Fabian, C., García-Santos, G., Leuenberger, F., Nuyttens, D., & Binder, C. (2012). *Dermal exposure assessment of pesticide use: The case of sprayers in potato farms in the Colombian highlands*. The Science of the Total Environment, 430, 202-208.

Lu, Y., Song, S., Wang, R., Liu, Z., Meng, J., Sweetman, A., . . . Wang, T. (2015). *Impacts of soil and water pollution on food safety and health risks in China*. Environment International, 77, 5-15.

Luo, W., Taylor, M., & Parker, S. (2008). *A comparison of spatial interpolation methods to estimate continuous wind speed surfaces using irregularly distributed data from England and Wales*. International Journal of Climatology, 28(7), 947-959.

Mammedov, Y., Olugu, E., & Farah, G. (2021). *Weather forecasting based on data-driven and physics-informed reservoir computing models*. Environmental Science and Pollution Research International, Environmental science and pollution research international, 2021-11-25.

Mandic-Rajcevic, S., Rubino, F., Ariano, E., Cottica, D., Neri, S., & Colosio, C. (2018).

Environmental and biological monitoring for the identification of main exposure determinants in vineyard mancozeb applicators. Journal of Exposure Science & Environmental Epidemiology, 28(3), 289-296.

Mandic-Rajcevic, S., Rubino, F., Ariano, E., Cottica, D., Negri, S., & Colosio, C. (2019). *Exposure duration and absorbed dose assessment in pesticide-exposed agricultural workers: Implications for risk assessment and modeling*. International Journal of Hygiene and Environmental Health, 222(3), 494-502.

Mandić-Rajčević S., Rubino F.M., Colosio C. (2021). *Chapter 9 - Exposure and risk profiles: From field studies to typical exposure and risk scenarios*. Exposure and Risk Assessment of Pesticide Use in Agriculture. Academic Press, 199-224

Maroufpoor, S., Bozorg-Haddad, O., Maroufpoor, E., Gerbens-Leenes, P., Loáiciga, H., Savic, G., & Singh, V. (2021). *Optimal virtual water flows for improved food security in water-scarce countries*. Scientific Reports, 11(1), 21027.

Marrs, T., & Ballantyne, B. (2004). *Pesticide toxicology and international regulation* (Current toxicology series). John Wiley & Sons.

Matthews, G., Bateman, Roy, Miller, Paul, & Thompson, Steve. (2014). Pesticide application methods (Fourth ed.). Chichester, England: Wiley-Blackwell.

Matthews, G., Hislop, E. C, & C.A.B. International. (1993). Application technology for crop protection. Wallingford: CAB International.

McCullough, B.D. 1998. Algorithms for (partial) autocorrelation coefficients. J. Economic Soc. Meas., 24, 265-278. [4.2.2, 14.2]

Menegaux, F., Baruchel, A., Bertrand, Y., Lescoeur, B., Leverger, G., Nelken, B., . . . Clavel, J. (2006). *Household exposure to pesticides and risk of childhood acute leukemia*. Occupational and Environmental Medicine (London, England), 63(2), 131-134.

Metruccio F., Tosti L., Moretto A. (2021). *Chapter 2 - Models used in the world (European Union, United States, other countries)*. Exposure and Risk Assessment of Pesticide Use in Agriculture. Academic Press, 25-67.

Miller, M.B. & Cowan, Darrel S., 2017. Roadside geology of Washington Second., Missoula, Montana: Mountain Press Publishing Company.

Mizon, G.E. 1995. A simple message for autocorrelation correctors: Don't. J. Econometrics, 69, 267-288. [5.3.1]

Moeller, D. (2019). *Superfund, Pesticide Regulation, and Spray Drift: Rethinking the Federal Pesticide Regulatory Framework to Provide Alternative Remedies for Pesticide Damage*. Iowa Law Review, 104(3), 1523-1550.

Myers, S. (2020). *Chapter 5: Food and Nutrition on a Rapidly Changing Planet*. Planetary health: Protecting nature to protect ourselves. Island Press.

Myers, S., & Frumkin, H. (2020). *Planetary health: Protecting nature to protect ourselves*. Island Press.

Natarajan N, Vasudevan M, Rehman S (2021) *Evaluation of suitability of wind speed probability distribution models: a case study from Tamil Nadu, India*. Environ Sci Pollut Res 1–14.

Ouarda, T.B.M.J. et al., 2015. Probability distributions of wind speed in the UAE. Energy conversion and management, 93, pp.414–434.

Palardy, N., & Centner, T. (2017). *Improvements in pesticide drift reduction technology (DRT) call for improving liability provisions to offer incentives for adoption*. Land Use Policy, 69, 439-444.

Pathak, N., & McKinney, A. (2021). Planetary Health, Climate Change, and Lifestyle Medicine: Threats and Opportunities. American Journal of Lifestyle Medicine, 15(5), 541-552.

Peña, A., Gryning, S., & Hasager, C. (2008). *Measurements and Modelling of the Wind Speed Profile in the Marine Atmospheric Boundary Layer*. Boundary-layer Meteorology, 129(3), 479-495.

Phillips, L., Johnson, M., Deener, K., & Bonanni, C. (2015). EPA's Exposure Assessment Toolbox (EPA-Expo-Box). Journal of Environmental Informatics, 25(2), 81-84.

Pierce, F.J. & Elliott, T.V., 2008. Regional and on-farm wireless sensor networks for agricultural systems in Eastern Washington. Computers and electronics in agriculture, 61(1), pp.32–43.

Postel, S., Daily, G., & Ehrlich, P. (1996). *Human appropriation of renewable fresh water*. Science (American Association for the Advancement of Science), 271(5250), 785-788.

Priestley, M.B. 1988. Non-linear and Non-stationary Time Series Analysis. London: Academic Press. [11.1.1, 11.2.4, 11.7, 13.2]

Raisigl U., Felber H., Siegried et al. (1991) Comparison of different mist blowers and volume rates for orchard spraying. BCPC Monograph No. 46. Basil, Switzerland: British Crop Protection. pp. 185–96

Reidel, S. P., Camp, V. E., Tolan, I. L., and B. S. Martin. 2013. The Columbia River flood basalt province: Stratigraphy, areal extent, volume, and physical volcanology. In The Columbia River Basalt Province, GSA Special Paper 497, eds. S. P. Reidel, V. E. Camp, M. E. Ross, et al., P. 1-44.

Reidel, S. P., Martin, B. S, and H. I. Petcovic. 2003. The Columbia River food basalts and the Yakima fold belt. In Western Cordillera and Adjacent Areas, GA Field Guide 4, ed. T. W. Swanson, p. 87-105.

Sanchez-Bayo, F., Goulson, D., Pennacchio, F., Nazzi, F., Goka, K., Desneux, N., 2016. Are bee diseases linked to pesticides? — A brief review. Env. Internat. 89–90, 7–11. https://doi.org/10.1016/j.envint.2016.01.009.

Sapcanin, A., Cakal, M., Imamovic, B., Salihovic, M., Pehlic, E., Jacimovic, Z., & Jancan, G. (2016). Herbicide and pesticide occurrence in the soils of children's playgrounds in Sarajevo, Bosnia and Herzegovina. Environmental Monitoring and Assessment, 188(8), 1-6.

Schwaier A., Ackerman-Leist P. (2017). *Playground Contamination Study in South Tyrol*. Suedtirol: Dachverband fuer Natur- und Umweltschutz in Suedtirol

Simpson, R. (1990). *A model to control emissions which avoid violations of PM10 health standards for both short- and long-term exposures*. Atmospheric Environment. Part A, General Topics, 24(4), 917-924.

Slitt A.L. (2021). *Chapter 5: Absorption, Distribution, and Excretion of Toxicants*. Klaassen C.D., & Watkins J.B., III(Eds.), Casarett

Smith, Matthew R, PhD, Singh, Gitanjali M, PhD, Mozaffarian, Dariush, Prof, & Myers, Samuel S, Dr. (2015). Effects of decreases of animal pollinators on human nutrition and global health: A modelling analysis. The Lancet (British Edition), 386(10007), 1964-1972.

Snoun H, Bellakhal G, Kanfoudi H, Zhang X, Chahed J (2019) *One way coupling of WRF with a Gaussian dispersion model: a focused fine-scale air pollution assessment on southern Mediterranean*. Environ Sci Pollut Res 26:22892–22906.

Spaan, S., Glass, R., Goede, H., Ruiter, S., & Gerritsen-Ebben, R. (2020). Performance of a Single Layer of Clothing or Gloves to Prevent Dermal Exposure to Pesticides. Annals of Work Exposures and Health, 64(3), 311-330.

Springmann, M., Clark, M., Mason-D'Croz, D., Wiebe, K., Bodirsky, B., Lassaletta, L., . . .

Willett, W. (2018). *Options for keeping the food system within environmental limits*. Nature (London), 562(7728), 519-525.

Steiner P. (1969) *The distribution of spray material between target and non-target areas of a mature apple orchard by airblast equipment*. MS Thesis. Ithaca, New York: Cornell University.

Teysseire, R., Manangama Duki, G., Baldi, I., Carles, C., Brochard, P., Bedos, C., & Delva, F. (2021). *Determinants of non-dietary exposure to agricultural pesticides in populations living close to fields: A systematic review*. The Science of the Total Environment, 761, 143294.

Tilman, D., Balzer, C., Hill, J., & Befort, B. (2011). *Global food demand and the sustainable intensification of agriculture*. Proceedings of the National Academy of Sciences - PNAS, 108(50), 20260-20264.

University of Washington Office of Educational Assessment (UWOEA). (2019). Understanding Correlations. Retrieved April 20, 2022, from: https://www.washington.edu/assessment/scanningscoring/scoring/reports/correlations/

US Code. (2006). *Title 7, sections 136-136y*. Retrieved December 17, 2021, from https://www.govinfo.gov/app/details/USCODE-2011-title7/USCODE-2011-title7-chap6-subchapII-sec136/context

US Court for the District of Puerto Rico. (2000). *United States v. Tropical Fruit, S.E., 96 F*. Supp. 2d 71, 83–84. Retrieved December 18, 2021, from https://law.justia.com/cases/federal/district-courts/FSupp2/96/71/2420954/

US Court of Appeals, Eleventh Circuit. (1996). South Florida Water Mgmt. Dist. V. Montalvo. 84 F. 3d 402. Nos. 93-5113, 94-4397. Retrieved December 18, 2021, from https://casetext.com/case/south-florida-water-mgmt-dist-v-montalvo

US EPA. (1966). *The Food Quality Protection Act (FQPA*. United States Environmental Protection Agency. Retrieved May 10, 2022, from https://archive.epa.gov/pesticides/regulating/laws/fqpa/web/html/backgrnd.html

US EPA. (2001). PRN 2001-X Draft: Spray and Dust Drift Label Statements for Pesticide Products. Retrieved December 16, 2021, from https://www.epa.gov/pesticide-registration/prn-2001-x-draft-spray-and-dust-drift-label-statements-pesticide-products

US EPA. (2007). *Spray drift workshop – final report to PPDC*. Retrieved December 17, 2021,

from https://archive.epa.gov/pesticides/ppdc/web/pdf/session1-spraydrift-rpt.pdf

US EPA. (2011). *Chapter 7 – Dermal Exposure Factors*. Exposure Factors Handbook: 2011 Edition (EPA/600/R-09/052F). https://www.epa.gov/sites/default/files/2015-09/documents/efh-chapter07.pdf

US EPA. (2014a). *Consideration of Spray Drift in Pesticide Risk Assessment*. Notice of Availability and Request for Comment. Vol. 79. Federal Register. No. 19. 4691-4693. Retrieved December 16, 2021, from http://www.gpo.gov/fdsys/pkg/

US EPA. (2014b). *Consideration of Volatilization in Pesticide Risk Assessment*. Notice of Availability and Request for Comment. Vol. 79. Federal Register. No. 58. 16791-16793. Retrieved December 16, 2021, from http://www.gpo.gov/fdsys/pkg/

US EPA. (2015). *In Case of Pesticide Poisoning*. United States Environmental Protection Agency. Retrieved May 10, 2022, from https://www.epa.gov/pesticide-worker-safety/case-pesticide-poisoning.

US EPA. (2016a). *About the Drift Reduction Technology Program*. United States Environmental Protection Agency (US EPA). Retrieved December 16, 2021, from https://19january2017snapshot.epa.gov/reducing-pesticide-drift/about-drift-reduction-technology-program_.html

US EPA. (2021a). *Exposure Assessment Tools by Routes*. EPA. Retrieved December 16, 2021, from https://www.epa.gov/expobox/exposure-assessment-tools-chemical-classes-pesticides

US EPA. (2021b). *Exposure Assessment Tools by Chemical Classes - Pesticides*. EPA. Retrieved December 16, 2021, from https://www.epa.gov/expobox/exposure-assessment-tools-chemical-classes-pesticides

US EPA. (2021c). *Land Use: What are the trends in land use and their effects on human health and the environment?* EPA. Retrieved December 16, 2021, from https://www.epa.gov/report-environment/land-use

US Supreme Court. (1984). *Ruckelshaus v. Monsanto Co.,* 467 U.S. 986. Retrieved December 18, 2021, from https://supreme.justia.com/cases/federal/us/467/986/

US Supreme Court. (1991). *Wisconsin Pub. Intervenor v. Mortier*, 501 U.S. 597, 613. Retrieved December 18, 2021, from https://supreme.justia.com/cases/federal/us/501/597/

Van Maele-Fabry, G., Gamet-Payrastre, L., & Lison, D. (2017). Residential exposure to pesticides as risk factor for childhood and young adult brain tumors: A systematic review and meta-analysis. Environment International, 106, 69-90.

Vercruysse F. Steurbaut W, Drieghe S et al. (1999) *Off target ground deposits from spraying a semi-dwarf orchard*. Crop Prot; 18: 565–70.

Venäläinen, A., & Heikinheimo, M. (2002). *Meteorological data for agricultural applications*. Physics and Chemistry of the Earth. Parts A/B/C, 27(23), 1045-1050.

Vryzas, Z. (2018). *Pesticide fate in soil-sediment-water environment in relation to contamination preventing actions*. Current Opinion in Environmental Science & Health, 4, 5-9.

Washington State Department of Health (WADOH). (2013). *Pesticide Data Report Washington State: 2010–2011Agency Data – A report to the governor, agency directors, the legislature, and the public*. Chapter 380, Laws of 1989, and RCW 70. 104. http://www.doh.wa.gov/Portals/1/Documents/Pubs/334-319.pdf.

Washington State Department of Agriculture (WSDA), 2022. Export Statistics – 2020 Washington-Grown or Processed Food and Agriculture Exports. Retrieved April 4, 2022, from https://agr.wa.gov/departments/business-and-marketing-support/international/statistics

Washington State University (WSU), 2017. AgWeatherNet Standard Instruments. Retrieved April 4, 2022, from http://weather.wsu.edu/?p=92550

Washington State University (WSU), 2006. WSU Benton W AgWeatherNet Station. Retrieved April 4, 2022, from https://weather.wsu.edu/

Washington State University (WSU), 2012. WSU Grandview AgWeatherNet Station. Retrieved April 4, 2022, from https://weather.wsu.edu/

Washington State University (WSU), 1989. WSU McWhorter AgWeatherNet Station. Retrieved April 4, 2022, from https://weather.wsu.edu/

Washington State University (WSU), 2002. WSU Prosser NE AgWeatherNet Station. Retrieved April 4, 2022, from https://weather.wsu.edu/

Washington State University (WSU), 2020. WSU Sunnyside AgWeatherNet Station. Retrieved April 4, 2022, from https://weather.wsu.edu/

Washington State University (WSU), 2015. The Washington Agricultural Weather Network, Washington State University (WSU) Prosser–AgWeatherNet. (2022). Retrieved April 4, 2022, from http://weather.wsu.edu/awn.php

Washington State University (WSU) Tree Fruit. *Irrigation*. Retrieved May 10, 2022, from

http://treefruit.wsu.edu/web-article/irrigation/

West Group. (2003). American jurisprudence proof of facts, 3d series: Fact book. Eagan, MN: West.

Wester, B.L., 2014. Land divided by law : the Yakama Indian Nation as environmental history, 1840-1933, New Orleans, Louisiana: Quid Pro Books.

Wilfert, L., Brown, M., & Doublet, V. (2021). OneHealth implications of infectious diseases of wild and managed bees. Journal of Invertebrate Pathology, 186, 107506.

Xue, S., Xi, X., Lan, Z., Wen, R., & Ma, X. (2021). *Longitudinal drift behaviors and spatial transport efficiency for spraying pesticide droplets*. International Journal of Heat and Mass Transfer, 177, 121516.

Yakama Nation., 2021. Yakama Nation History. Retrieved April 4, 2022, from https://www.yakama.com/about/.

Yaglom, A.M. 1962. An Introduction to the Theory of Stationary Random Functions. Englewood Cliffs, NJ: Prentice-Hall. [Exercise 3.14, 5.6]

Yu, S. (2014). *The Toxicology and Biochemistry of Insecticides, Second Edition*. (2nd ed.). Hoboken: CRC Press.

Zaidon, S.Z., Ho, Y.B., Hashim, Z., Saari, N., Praveena, S.M. (2020). *Physicochemical properties and water quality parameter of paddy soil and water and their relationship with pesticides concentration*. Malaysian Journal of Medicine and Health Sciences, 16(2).

Zhang Y, Zhang C, Gao S, Wang P, Xie F, Cheng P, Lei S (2018) *Wind Speed Prediction Using Wavelet Decomposition Based on Lorenz Disturbance Model*. IETE J Res 66:635–642.

Zhang Y, Pan G (2020) *A hybrid prediction model for forecasting wind energy resources*. Environ Sci Pollut Res 27:19428–19446.

Appendices

Appendix 1: R output

Appendix 1 Figure 1: Arima function from forecast package help documentation in R version 4.1.1

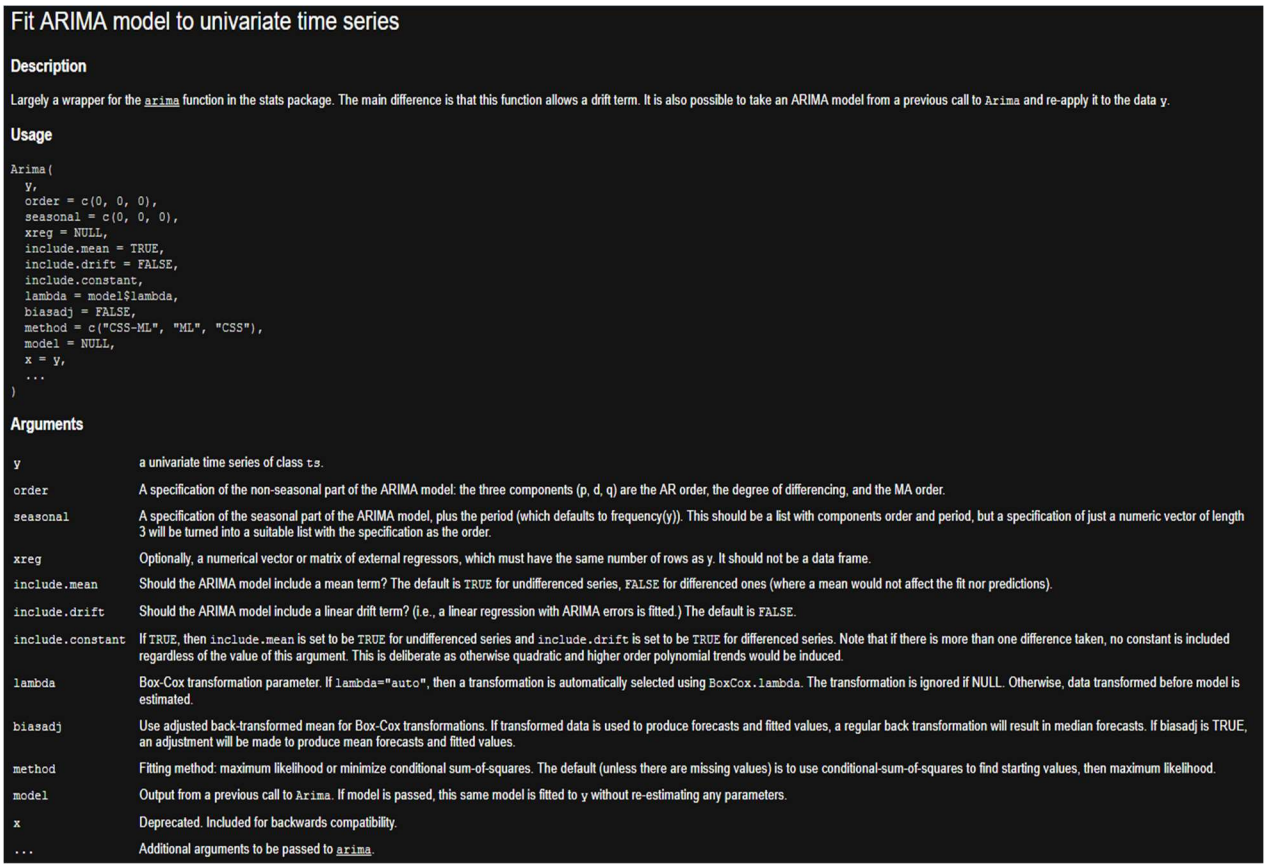

Fit ARIMA model to univariate time series

Description

Largely a wrapper for the `arima` function in the stats package. The main difference is that this function allows a drift term. It is also possible to take an ARIMA model from a previous call to `Arima` and re-apply it to the data `y`.

Usage

```
Arima(
  y,
  order = c(0, 0, 0),
  seasonal = c(0, 0, 0),
  xreg = NULL,
  include.mean = TRUE,
  include.drift = FALSE,
  include.constant,
  lambda = model$lambda,
  biasadj = FALSE,
  method = c("CSS-ML", "ML", "CSS"),
  model = NULL,
  x = y,
  ...
)
```

Arguments

`y`	a univariate time series of class `ts`.
`order`	A specification of the non-seasonal part of the ARIMA model: the three components (p, d, q) are the AR order, the degree of differencing, and the MA order.
`seasonal`	A specification of the seasonal part of the ARIMA model, plus the period (which defaults to frequency(y)). This should be a list with components order and period, but a specification of just a numeric vector of length 3 will be turned into a suitable list with the specification as the order.
`xreg`	Optionally, a numerical vector or matrix of external regressors, which must have the same number of rows as y. It should not be a data frame.
`include.mean`	Should the ARIMA model include a mean term? The default is `TRUE` for undifferenced series, `FALSE` for differenced ones (where a mean would not affect the fit nor predictions).
`include.drift`	Should the ARIMA model include a linear drift term? (i.e., a linear regression with ARIMA errors is fitted.) The default is `FALSE`.
`include.constant`	If `TRUE`, then `include.mean` is set to be `TRUE` for undifferenced series and `include.drift` is set to be `TRUE` for differenced series. Note that if there is more than one difference taken, no constant is included regardless of the value of this argument. This is deliberate as otherwise quadratic and higher order polynomial trends would be induced.
`lambda`	Box-Cox transformation parameter. If `lambda="auto"`, then a transformation is automatically selected using `BoxCox.lambda`. The transformation is ignored if NULL. Otherwise, data transformed before model is estimated.
`biasadj`	Use adjusted back-transformed mean for Box-Cox transformations. If transformed data is used to produce forecasts and fitted values, a regular back transformation will result in median forecasts. If biasadj is TRUE, an adjustment will be made to produce mean forecasts and fitted values.
`method`	Fitting method: maximum likelihood or minimize conditional sum-of-squares. The default (unless there are missing values) is to use conditional-sum-of-squares to find starting values, then maximum likelihood.
`model`	Output from a previous call to `Arima`. If model is passed, this same model is fitted to `y` without re-estimating any parameters.
`x`	Deprecated. Included for backwards compatibility.
`...`	Additional arguments to be passed to `arima`.

Appendix 1 Figure 2: Raw R Output for Prosser N.E. April 1st, 2020, ARIMA (2,1,1) Wind Speed Forecast

```
> print(WS.train)
Series: training
ARIMA(2,1,1)

Coefficients:
          ar1      ar2      ma1
      0.5430  -0.0542  -0.6550
s.e.  0.0932   0.0266   0.0924

sigma^2 = 1.606:  log likelihood = -4917.95
AIC=9843.9   AICc=9843.92   BIC=9867.89
> View(fit)
> fit
     Point Forecast       Lo 80    Hi 80      Lo 95    Hi 95
2973       2.179525  0.55543833 3.803612 -0.3043013 4.663352
2974       2.222710  0.05066353 4.394757 -1.0991486 5.544569
2975       2.241849 -0.26692636 4.750624 -1.5949916 6.078689
2976       2.249900 -0.51570048 5.015500 -1.9797207 6.479520
2977       2.253234 -0.73215043 5.238618 -2.3125173 6.818984
2978       2.254607 -0.92966267 5.438878 -2.6153135 7.124528
2979       2.255173 -1.11403221 5.624378 -2.8975816 7.407927
2980       2.255405 -1.28822568 5.799036 -3.1641106 7.674921
2981       2.255501 -1.45402167 5.965023 -3.4177242 7.928726
2982       2.255540 -1.61263131 6.123711 -3.6603175 8.171398
>
```

Appendix 1 Figure 3: : Raw R Output for Prosser N.E. April 1st, 2020, ARIMA (4,1,2) Wind Speed Forecast

```
> WS.train
Series: training
ARIMA(4,1,2)

Coefficients:
         ar1     ar2     ar3     ar4      ma1      ma2
      0.2824  0.4925  0.0825  0.0575  -0.4049  -0.5934
s.e.     NaN     NaN  0.0189     NaN      NaN      NaN

sigma^2 = 1.584:  log likelihood = -4897.11
AIC=9808.22   AICc=9808.25   BIC=9850.19
Warning message:
In sqrt(diag(x$var.coef)) : NaNs produced
> fit
     Point Forecast       Lo 80    Hi 80       Lo 95    Hi 95
2973       2.439022  0.82612995 4.051914 -0.02768341 4.905727
2974       2.601741  0.45596195 4.747519 -0.67994466 5.883426
2975       2.739933  0.28305799 5.196807 -1.01753287 6.497398
2976       2.887067  0.16554794 5.608586 -1.27513712 7.049271
2977       3.029580  0.08201183 5.977148 -1.47833648 7.537496
2978       3.163036  0.02420315 6.301868 -1.63739446 7.963466
2979       3.290987 -0.01259085 6.594565 -1.76139924 8.343373
2980       3.413056 -0.03442343 6.860535 -1.85940863 8.685520
2981       3.529740 -0.04424134 7.103721 -1.93619256 8.995672
2982       3.641031 -0.04482957 7.326892 -1.99600649 9.278069
```

Appendix 1 Figure 4: Raw R Output for Prosser N.E. May 1st, 2020, ARIMA (2,1,1) Wind Speed Forecast

```
> WS.train
Series: training
ARIMA(2,1,1)

Coefficients:
         ar1      ar2      ma1
      0.6613  -0.0123  -0.7914
s.e.  0.0578   0.0243   0.0549

sigma^2 = 1.568:  log likelihood = -4733.02
AIC=9474.03   AICc=9474.05   BIC=9497.9
> View(fit)
> fit
     Point Forecast       Lo 80    Hi 80        Lo 95    Hi 95
2882       3.262306  1.65742945 4.867183  0.807859132 5.716753
2883       3.244757  1.11767211 5.371841 -0.008338513 6.497852
2884       3.233616  0.77240342 5.694828 -0.530483614 6.997715
2885       3.226464  0.51557911 5.937349 -0.919476752 7.372405
2886       3.221872  0.30709723 6.136647 -1.235891407 7.679636
2887       3.218924  0.12784500 6.310002 -1.508473147 7.946320
2888       3.217030 -0.03241115 6.466472 -1.752561508 8.186622
2889       3.215814 -0.17956201 6.611191 -1.976965750 8.408595
2890       3.215034 -0.31717895 6.747247 -2.187019459 8.617087
2891       3.214533 -0.44751966 6.876585 -2.386093008 8.815158
>
```

Appendix 1 Figure 5: Raw R Output for Prosser N.E. May 1st, 2020, ARIMA (4,1,2) Wind Speed Forecast

```
> WS.train
Series: training
ARIMA(4,1,2)

Coefficients:
         ar1      ar2      ar3     ar4      ma1     ma2
      1.2924  -0.3527  -0.0253  0.0501  -1.4431  0.4431
s.e.  0.1503   0.1311   0.0304  0.0225   0.1501  0.1501

sigma^2 = 1.537:  log likelihood = -4704.49
AIC=9422.97   AICc=9423.01   BIC=9464.73
> fit
     Point Forecast     Lo 80    Hi 80      Lo 95    Hi 95
2882       3.385780 1.7968027 4.974757  0.9556492 5.815910
2883       3.454948 1.3698812 5.540016  0.2661134 6.643783
2884       3.564360 1.1662708 5.962449 -0.1032009 7.231921
2885       3.649108 1.0451047 6.253112 -0.3333715 7.631588
2886       3.722595 0.9542574 6.490932 -0.5112119 7.956401
2887       3.788375 0.8791474 6.697603 -0.6609048 8.237655
2888       3.850810 0.8175613 6.884059 -0.7881436 8.489764
2889       3.910688 0.7681798 7.053196 -0.8953634 8.716739
2890       3.968071 0.7293413 7.206800 -0.9851385 8.921280
2891       4.022830 0.6992087 7.346451 -1.0602101 9.105870
```

Appendix 1 Figure 6: Raw R Output for Prosser N.E. June 1st, 2020, ARIMA (2,1,1) Wind Speed Forecast

```
> WS.train
Series: training
ARIMA(2,1,1)

Coefficients:
         ar1      ar2      ma1
      0.6766  -0.0136  -0.8476
s.e.  0.0407   0.0237   0.0365

sigma^2 = 1.418:  log likelihood = -4739.36
AIC=9486.72   AICc=9486.73   BIC=9510.71
> View(fit)
> fit
     Point Forecast      Lo 80    Hi 80     Lo 95    Hi 95
2977       1.009933 -0.5160918 2.535958 -1.323920 3.343786
2978       1.288634 -0.6935104 3.270779 -1.742794 4.320063
2979       1.471627 -0.7797584 3.723013 -1.971570 4.914824
2980       1.591649 -0.8471941 4.030492 -2.138240 5.321538
2981       1.670367 -0.9131522 4.253886 -2.280785 5.621518
2982       1.721995 -0.9815195 4.425509 -2.412674 5.856663
2983       1.755856 -1.0524066 4.564118 -2.539011 6.050722
2984       1.778063 -1.1249887 4.681116 -2.661772 6.217899
2985       1.792629 -1.1983784 4.783636 -2.781722 6.366980
2986       1.802182 -1.2718622 4.876225 -2.899163 6.503526
>
```

Appendix 1 Figure 7: Raw R Output for Prosser N.E. June 1st, 2020, ARIMA (4,1,2) Wind Speed Forecast

```
> WS.train
Series: training
ARIMA(4,1,2)

Coefficients:
          ar1     ar2      ar3      ar4      ma1      ma2
      0.0329  0.3491  -0.0173  -0.0358  -0.2037  -0.4709
s.e.  0.2306  0.1730   0.0289   0.0274   0.2302   0.2066

sigma^2 = 1.418:  log likelihood = -4738.33
AIC=9490.66   AICc=9490.7   BIC=9532.64
> fit
     Point Forecast      Lo 80    Hi 80     Lo 95    Hi 95
2977       1.010304 -0.5159653 2.536574 -1.323924 3.344532
2978       1.327467 -0.6553351 3.310269 -1.704967 4.359902
2979       1.500787 -0.7528226 3.754397 -1.945812 4.947386
2980       1.613669 -0.8309284 4.058267 -2.125020 5.352359
2981       1.657678 -0.9223995 4.237756 -2.288210 5.603567
2982       1.684156 -1.0143153 4.382627 -2.442800 5.811111
2983       1.692219 -1.1101164 4.494555 -2.593583 5.978022
2984       1.696918 -1.2038463 4.597682 -2.739418 6.133254
2985       1.697851 -1.2962828 4.691984 -2.881281 6.276983
2986       1.698433 -1.3860721 4.782938 -3.018910 6.415776
```

Appendix 1 Figure 8: Distribution of 800 ARIMA (2,1,1) Training RMSEs

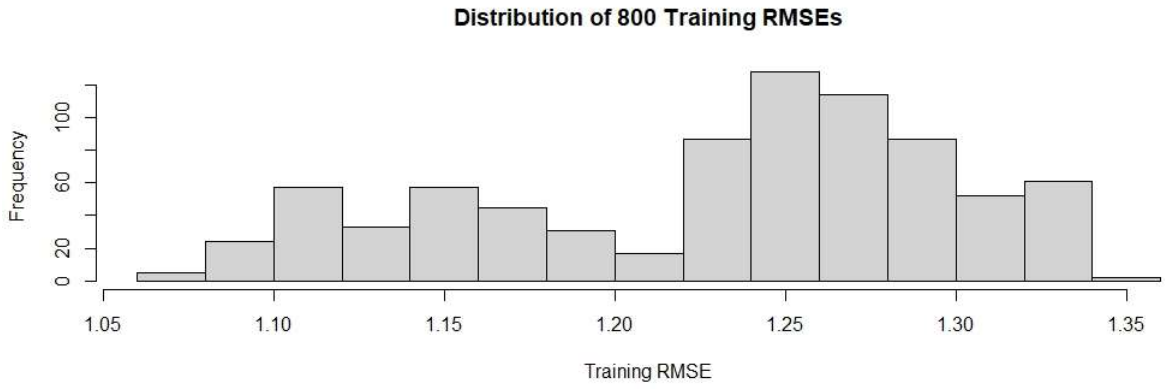

Appendix 1 Figure 8: shows the distribution of the training RMSE values for all of the 800 ARIMA (2,1,1) models fitted on the 4 months (March, April, May, June) of historical wind data in 2020. The mean of this distribution is 1.23. The lowest value of this distribution is 1.07 and the maximum value of this distribution is 1.34.

Appendix 1 Figure 9: Distribution of 800 ARIMA (2,1,1) Forecast RMSEs

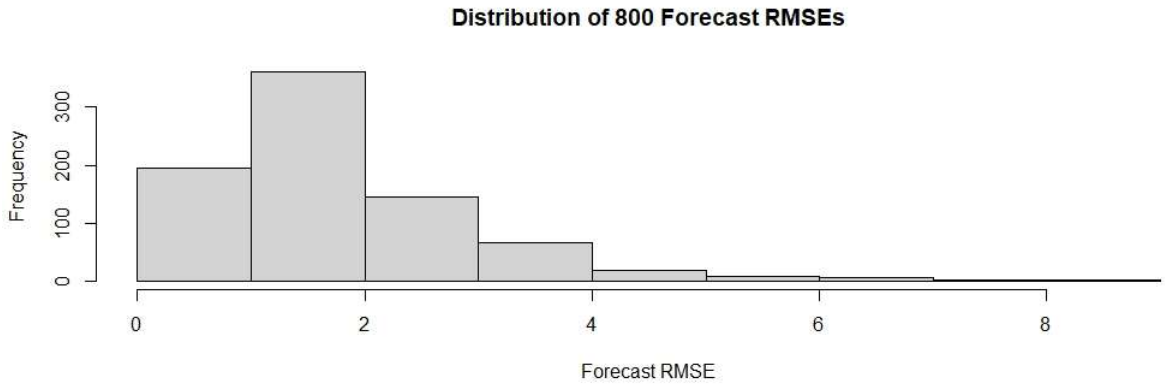

Appendix 1 Figure 9 shows the distribution of the 800 ARIMA (2,1,1) forecasted RMSEs. The RMSEs show the variability between our calculated point forecast values and the actual observed wind speed values in April 2020, May 2020, and June 2020. The mean of this distribution is 1.76. The lowest value of this distribution is 0.27 and the maximum value of this distribution is 8.57.

s

Appendix 2: Supplementary Meteorological Statistic Tables

Appendix 2 Table 1: Descriptive meteorological statistics for Sunnyside, WA; Grandview, WA; Prosser N.E., WA; McWhorter, WA; and Benton W., WA; from 2014 – 2019.

Wind Direction	Stations	n	Mean	SD	Min	25th	Median	75th	Max
	Sunnyside	210336	155	111	0	60	139	262	360
	Grandview	210336	134	121	0	1	102	263	360
	Prosser N.E.	210336	197	121	0	84	235	297	360
	McWhorter	210336	213	107	0	147	244	290	360
	Benton W.	210336	221	91	0	188	246	287	360
Temperature	**Stations**	**n**	**Mean**	**SD**	**Min**	**25th**	**Median**	**75th**	**Max**
	Sunnyside	210336	53.0	18.3	-6.3	38.3	52.7	65.9	108.6
	Grandview	210336	52.5	17.9	-1	38.8	51.7	64.7	105.6
	Prosser N.E.	210336	53.4	18.3	-1.9	39.1	52.8	66	107
	McWhorter	210336	52.8	18.5	-2	38.625	52.1	66.2	106.4
	Benton W.	210336	53.9	18.3	-1.9	39.8	53.3	67.1	108.3
Dewpoint	**Stations**	**n**	**Mean**	**SD**	**Min**	**25th**	**Median**	**75th**	**Max**
	Sunnyside	210336	40.1	12.0	-13.4	32.3	40.5	48.9	76.3
	Grandview	210336	39.3	11.8	-18.6	31.6	39.8	47.9	77.8
	Prosser N.E.	210336	38.6	11.0	-11.2	31.8	39.3	46.7	76.1
	McWhorter	210336	36.7	10.3	-14.3	30.7	37.6	43.9	70.4
	Benton W.	210336	38.0	10.7	-12.9	31.6	38.8	45.5	72.3
Humidity	**Stations**	**n**	**Mean**	**SD**	**Min**	**25th**	**Median**	**75th**	**Max**

Sunnyside	21033 6	68.2	25. 3	9	46	70	93	100
Grandview	21033 6	67.6	25. 7	8	45	70	93	100
Prosser N.E.	21033 6	63.7	24. 0	8	44	65	84	100
McWhorter	21033 6	62.1	26. 7	6	39	60	88	100
Benton W.	21033 6	61.4	24. 6	7	41	60	83	100

Appendix 2 Table 2: Descriptive meteorological statistics for Prosser N.E., WA in 2019.

Wind Direction	Quarter 1	n	Mean	SD	Min	25th	Median	75th	Max
		297		11					
	January	6	168	3	0	70	176	270	360
		268		12				255.2	
	February	8	132	0	0	0	99	5	360
		297		12					
	March	2	196	2	0	91	236	306	360
	Quarter 1	863		12					
	Summary	6	167	1	0	48	164	271	360
	Quarter 2	**n**	**Mean**	**SD**	**Min**	**25th**	**Median**	**75th**	**Max**
		288		11					
	April	0	198	0	0	96	239	277	360
		297		12					
	May	6	190	0	0	65	211	282	360
		288		10				308.2	
	June	0	229	9	0	179	262	5	360
	Quarter 2	873		11					
	Summary	6	205	4	0	102	246	289	360
	Quarter 3	**n**	**Mean**	**SD**	**Min**	**25th**	**Median**	**75th**	**Max**
		297		11		153.7			
	July	6	228	8	0	5	267	332	360
		297		12					
	August	6	211	4	0	86	255	331	360
		288		12				308.2	
	September	0	195	7	0	54.75	228	5	360
	Quarter 3	883		12					
	Summary	2	211	4	0	90	257	325	360
	Quarter 4	**n**	**Mean**	**SD**	**Min**	**25th**	**Median**	**75th**	**Max**
		297		12					
	October	6	198	4	0	75	231	316	360
		288		12					
	November	4	168	8	0	47	133	312	360
		297		11					
	December	6	88	6	0	0	0	206	359
	Quarter 4	883		13					
	Summary	6	159	1	0	18	137	273	360

Temperature	Quarter 1	n	Mean	SD	Min	25th	Median	75th	Max
	January	2976	35.1	5.4	22	31.3	33.5	38.4	52.8
	February	2688	25.2	6.7	0.9	21	25.1	30.6	41.9
	March	2976	36.8	13.1	7.8	26.7	36.6	46.6	67.3
	Quarter 1 Summary	8636	32.6	10.4	0.9	25.7	31.8	38.2	67.3
	Quarter 2	**n**	**Mean**	**SD**	**Min**	**25th**	**Median**	**75th**	**Max**
	April	2880	54.0	8.6	33.6	47.6	53.3	59.8	79.1
	May	2976	63.2	10.7	35.7	55.4	63	70.5	87.8
	June	2880	68.2	11.9	39.5	59.075	67.6	77.125	96
	Quarter 2 Summary	8736	61.8	12.0	33.6	52.9	60.4	69.8	96
	Quarter 3	**n**	**Mean**	**SD**	**Min**	**25th**	**Median**	**75th**	**Max**
	July	2976	71.7	11.2	47.7	62.5	71.5	80.925	97.4
	August	2976	73.3	11.1	50.6	64.6	72.5	82	102.2
	September	2880	62.7	11.6	35.8	54.3	62.2	70.9	90.4
	Quarter 3 Summary	8832	69.3	12.2	35.8	60.2	68.5	79	102.2
	Quarter 4	**n**	**Mean**	**SD**	**Min**	**25th**	**Median**	**75th**	**Max**
	October	2976	47.2	11.1	16.2	39.8	47.25	55.1	74.7
	November	2880	39.6	7.7	20.5	33.5	40.3	44.9	65.8
	December	2976	34.8	6.9	24.4	29.6	33.6	37.5	60.7
	Quarter 4 Summary	8832	40.7	10.4	16.2	32.7	39.1	47.5	74.7

Dewpoint	Quarter 1	n	Mean	SD	Min	25th	Median	75th	Max
	January	2976	32.1	4.5	18.5	29.2	32.1	35.2	43.4
	February	2688	21.2	8.3	-4.9	16.2	21	27	41.7

	March	2972	28.4	10.8	-1.3	22.3	30.8	36.8	46.8
	Quarter 1 Summary	8636	27.5	9.4	-4.9	21.5	29.5	34.2	46.8
	Quarter 2	**n**	**Mean**	**SD**	**Min**	**25th**	**Median**	**75th**	**Max**
	April	2880	36.9	8.3	8.9	32.3	38	42.4	52.5
	May	2976	42.0	7.8	12.5	37.1	41.2	48.4	58.7
	June	2880	42.9	5.9	19.1	39.2	43.4	47.2	57.4
	Quarter 2 Summary	8736	40.6	7.9	8.9	36.2	40.9	46.4	58.7
	Quarter 3	**n**	**Mean**	**SD**	**Min**	**25th**	**Median**	**75th**	**Max**
	July	2976	47.6	4.9	28.2	44.7	48	51.2	59
	August	2976	51.7	5.1	35.2	48.3	51.5	55.1	62.8
	September	2880	47.1	6.2	28.8	44.4	48.4	51.1	59.5
	Quarter 3 Summary	8832	48.8	5.8	28.2	45.7	49.25	52.3	62.8
	Quarter 4	**n**	**Mean**	**SD**	**Min**	**25th**	**Median**	**75th**	**Max**
	October	2976	31.0	10.8	-3.7	24.7	33.5	38	52
	November	2884	32.0	7.6	12.7	26.3	32.3	38.2	47.4
	December	2976	33.1	4.9	23.2	29	33.2	36.8	48.6
	Quarter 4 Summary	8836	32.0	8.3	-3.7	27.4	33.1	37.6	52
Humidity	**Quarter 1**	**n**	**Mean**	**SD**	**Min**	**25th**	**Median**	**75th**	**Max**
	January	2976	90.0	12.1	37	84	96	99	100
	February	2688	88.9	12.4	44	83	94	99	100
	March	2972	75.8	18.8	24	62	79	93	99
	Quarter 1 Summary	8636	84.8	16.2	24	75	90	99	100
	Quarter 2	**n**	**Mean**	**SD**	**Min**	**25th**	**Median**	**75th**	**Max**
	April	2880	56.5	20.8	11	40	56	72	99
	May	2976	50.9	21.5	11	33	49	66	99
	June	2880	44.2	18.7	8	28	42	59	90
	Quarter 2 Summary	8736	50.6	21.0	8	34	49	66	99
	Quarter 3	**n**	**Mean**	**SD**	**Min**	**25th**	**Median**	**75th**	**Max**
	July	2976	46.6	19.0	11	30	45	63	88
	August	2976	51.4	20.3	14	34	50	67	96
	September	2880	60.2	18.4	16	45	62	76	94
	Quarter 3 Summary	8832	52.6	20.1	11	36	52	70	96
	Quarter 4	**n**	**Mean**	**SD**	**Min**	**25th**	**Median**	**75th**	**Max**
	October	2976	56.5	18.0	16	41	58	72	94
	November	2884	74.5	19.8	27	61	76.5	92	99
	December	2976	95.5	10.5	46	99	100	100	100
	Quarter 4 Summary	8836	75.5	23.0	16	58	79	99	100